SYNTHESIS OF ACTIVATED CARBON FROM FLY ASH AND ITS APPLICATION FOR THE REMOVAL OF ACIDIC GAS AND OTPHER POLLUTANTS

BY

H M Zaheer Aslam

A Dissertation Presented to the

DEANSHIP OF GRADUATE STUDIES

KING FAHD UNIVERSITY OF PETROLEUM & MINERALS

DHAHRAN, SAUDI ARABIA

In Partial Fulfillment of the

Requirements for the Degree of

DOCTOR OF PHILOSOPHY

In

CHEMICAL ENGINEERING

May, 2015

KING FAHD UNIVERSITY OF PETROLEUM & MINERALS

DHAHRAN- 31261, SAUDI ARABIA

DEANSHIP OF GRADUATE STUDIES

This thesis, written by **H M Zaheer Aslam** under the direction his thesis advisor and approved by his thesis committee, has been presented and accepted by the Dean of Graduate Studies, in partial fulfillment of the requirements for the degree of **DOCTOR OF PHILOSOPHY IN CHEMICAL ENGINEERING.**

Dr. Reyad A. Shawabkeh
(Advisor)

Dr. Mohammded Ba-Shammakh
Department Chairman

Dr. Ibnelwaleed Ali Hussein
(Co-Advisor)

Dr. Salam A. Zummo
Dean of Graduate Studies

Dr. Muhammad B. Amin
(Member)

22/6/15
Date

Dr. Mohammad Ba-Shammakh
(Member)

Dr.Mohammad Mozahar Hossain
(Member)

Dedicated to my beloved parents

Mr. & Mrs. Aslam

To my wife

ACKNOWLEDGMENTS

All thanks are due to God Almighty who enabled me to complete this thesis. The thesis has been an inspiring, very challenging, but always interesting and exciting experience. I am very grateful to my adviser Prof. Dr. Reyad A. Shawabkeh for the patience, encouragement, many fruitful discussions, and excellent advice throughout this study. I would also like to express my sincere thanks to my co-advisor Dr Ibnelwaleed Hussein for his valuable suggestions in science discussion and reviewing the manuscripts. His understanding to the topic and personal guidance has provided a good basis for the present thesis.

I am highly thankful to Department of chemical Engineering, King Fahd University of Petroleum and Minerals (KFUPM), Saudi Arabia for awarding me scholarship to pursue my PhD. Special thanks to the support of King Abdul Aziz City for Science and Technology (KACST) through the science and technology unit at King Fahd University of Petroleum & Minerals (KFUPM) for funding this research through project #11-ENV1645-as part of the National Science, Technology and Innovation Plan (NSTIP).

My hearties thanks to my committee members: Dr. Mohammad B. Amin, Dr. Mohammed Ba-Shammakh and Dr. M. Mozahar Hossain for their useful comments and suggestion.

Last but not least, thanks to my parents, my wife and friends; those prayed for my success.

TABLE OF CONTENTS

LIST OF TABLES

LIST OF FIGURES

LIST OF ABBREVIATIONS

OFA	:	Oil Fly Ash
AC	:	Activated Carbon
MB	:	Methylene Blue
MO	:	Methyl Orange
Rh	:	Rhodamine 6G
BJH	:	Barrett-Joyner-Halenda
BET	:	Brunauer-Emmett-Teller
FTIR	:	Fourier Transform Infra-red Spectroscopy
SEM	:	Scanning Electron Microscope

ABSTRACT

Full Name : H M Zaheer Aslam

Thesis Title : Synthesis of Activated Carbon from Oil fly ash (OFA) and its application for the removal of acidic gas and other dyes

Major Field : Chemical Engineering

Date of Degree : May 2015

This OFA (oil fly ash) is by product of many industrial and power generation plant operations. OFA usually causes environmental and health problems and requires safe disposal. OFA is pozzolanic in nature; it contains mainly unburned carbon (~80%) with some inorganic oxides like SiO_2, Fe_2O_3, Al_2O_3, and CaO and traces of heavy metals. Exploiting the use of fly ash as a precursor of activated carbon is advantageous due to its cheap source, availability, and one step activation procedure as compared to conventional production of activated carbon by two step activation. Acid mixture comprising of HNO_3, H_2SO_4, and H_3PO_4 was used to leach out the mineral contents from ash and increases the porosity of raw material. After acid treatment, mico porosity was further increased by physically activating it with CO_2 at elevated temperatures. The specimens treated with 20 vol. % H_2SO_4, 40 vol. % HNO_3 and 40 vol. % H_3PO_4 and activated at 990^oC have a BET surface area of 375.7m^2/g when compared to 2.8 m^2/g for the original OFA. The synthesized high surface area activated carbon were characterized by Scanning Electron microscopy (SEM), Fourier Transform spectroscopy (FTIR), ASAP 2020 surface area analyzer, X-ray diffraction, thermo-gravimetric analysis (TGA). The AC was further treated with $HNO_3$and NH_4OH solutions in order to attach the carboxylic and amine groups on the surface, respectively. FTIR characterization was used to confirm the

presence of the functional groups on the surface of AC at different stages of its development. The performance of functionalized AC samples is tested for the removal of H_2S from a synthetic natural gas by carrying out breakthrough experiments. The results from these tests have shown maximum adsorption capacity of 0.3mg/g for NH_4OHfunctionalized activated carbon with 86.43% regeneration efficiency. The ammonium hydroxide treated AC is found to be more effective for H_2S removal than acid treated AC as confirmed by breakthrough experiments. The results indicate that the presence of more acidic functionalities on the surface reduces the H_2S adsorption efficiency from the gas mixture. Another sample that was treated with acid mixture (20% HNO_3 and 80% H_3PO_4) followed by 2M KOH to improve surface area as well as surface affinity to adsorb H_2S. Adsorption of H_2S onto activated OFA were studied using kinetic and breakthrough modeling using well-known Langmuir, Freundlich, Sips and dual site Langmuir (DSL) model. Equilibrium isotherm modeling showed that OFA has dual site with higher and lower affinity for H_2S adsorption. The effect flow rates and inlets concentrations have been explain through Yoon-Nelson model, Thomas model and Clark model. Maximum uptake capacity of 8.5mg/g was obtained for 0.2L/min flow rate with 100 ppm inlet concentration.

Dyes removal tests were also done by impregnating the acid activated fly ash with NH_4OH and tested it to remove the dyes from an aqueous solution by batch experiments. The adsorption capacity of activated ash were tested with three different dyes namely Methylene blue, Methyl-orange and Rhodamine 6G. The adsorption experiments were performed with both single and binary dye aqueous solutions. As single component adsorption, both Methylene blue and Rhodamine 6G have 19mg/g uptake capacity while

methyl orange have 12mg/g adsorption capacity. Adsorption experiments with binary solution comprise of cationic and anionic combinations of dyes shows synergistic effect. Solution comprises of only cationic dyes (Methylene Blue and Rhodamine 6G exhibits a constant uptake for all concentration tested. Kinetic data shows the endothermic adsorption of all three dyes as single component adsorption. During binary component adsorption some combination (like methylene blue / methyl orange and methylene blue / Rhodamine 6G) exhibits exothermic adsorption while the solution comprises of Rhodamine 6G and Methyl orange presents endothermic adsorption.

ملخص الرسالة

الاسم الكامل: حفيظ محمد ظهير اسلم

عنوان الرسالة: تحضير الكربون النشط من رماد النفط المتطاير (OFA) واسنخدامه في ازالة الغازات الحمضية واصباغ اخرى

التخصص: هندسة الكيميائية

تاريخ لدرجة العلمية: مايو 2015

رماد النفط المتطاير (OFA) عبارة عن منتج جانبي من عديد من الصناعات ومصانع انتاج الكهرباء.ان (OFA) يتسبب بمخاطر صحية وبيئية ويتطلب تخلص آمن. رماد النفط المتطاير (OFA) بوز ولاني/pozzolanic في الطبيعة, ويتكون اساسا من 80% من كربون غير محترق مع اكاسيد معدنية مثل $CaO- Al_2O_3- Fe_2O_3-SiO_2$ وآثار من المعادن الثقيلة. استغلال رماد النفط المتطاير (OFA) مصدر للكربون النشط يعد ذا فائدة وذلك لانخفاض سعره وتوفره وخطوة واحدة للتنشيط مقارنة للطرق التقليدية لتحضير الكربون النشط بخطوتين. خليط من الاحماض $H_3PO_4- H_2SO_4-HNO_3$ تم استعماله لاستخلاص المعادن من رماد النفط المتطاير وزيادة مسامية المادة الخام. بعد المعالجة الحمضية, المسام الدقيقة تم زيادتها فيزيائيا بثاني اكسيد الكربون في درجات حرارة مرتفعة. العينات تم معالجتها 40. % H_3PO_4 ,40 % HNO_3 ,20 % H_2SO_4 حجميا تنشط عند 990 ^oC تتحصل مساحة سطح قدرها $375.7m^2/g$ عند مقارنتها بالرماد النفط المتطاير (OFA) الاصلي $2.8\ m^2/g$. مساحة السطح العالية تم اختبارها بواسطة .(TGA)- (XRD) - (FTIR)-(SEM). الكربون النشط تم معالجته بمحاليل $NH_4OH\ HNO_3$ - لاضافة الزمرات الكربوكسيلية والامينية للسطح. تم استخدام FTIR لتأكيد وجود الزمر الوظيفية عبى سطح الكربون النشط في مراحل مختلفة من تطويره. اداء الكربون النشط جربت لازالة H_2S من غاز طبيعي محضر عن طريق ...../ Breakthrough experiment. نتائج هذه التجارب اوضح سعة الادمصاص 0.3 mg/g عند الكربون النشط بـ NH_4OH مع 86.43% كفاءة تجديد. الكربون النشط المعالج هيدروكسيد الامونيوم اكثر كفاءة في ارالة H_2S من العالج بالحمض مثل ما تم تأكيده بـ ...../Breakthrough experiment . النتائج اشارت الى وجود كثير من الزمرات الحمضية يقلل من كفاءة ادمصاص H_2S من خليط الغاز. عينة اخرى تم معالجتها 80% - 20% HNO_3 H_3PO_4 وايضا 2M KOH لتحسين مساحة السطح وايضا ألفة السطح لادمصاص H_2S.تم دراسة ادمصاص H_2S

الى رماد النفط المتطاير (OFA) النشط عن طريق حركية التفاعل و..../breakthrough experiment باستعمال نماذج الادمصاص التماثلية مثل Langmuir, Freundlich, Sips , dual site Langmuir (DSL). نماذج الادمصاص الاتزانية اوضحت ان OFA لديه مواقع مزدوجة ذات ألفة عالية ومنخفضة لادصاص H_2S. تأثير معدل التدفق وتركيز التغذية درس عن طريق نموذج Yoon-Nelson و نموذج Thomas و نموذج Clark. اقصى سعة 8.5 mg/g تحصلت عند معدل تدفق 0.2L/min وتركيز 100 ppm.

ازالة الاصباغ تم دراسته بتقنية تحميل التنشيط الحمضي NH_4OH لرماد النفط المتطاير النشط وتجربتها لازالة الاصباغ من المحاليل المائية. سعة الادصاص للكربون النشط تم اختبارها لثلاث اصباغ Methylene blue, Mthyl orange Rhodamine 6G. تجربة الادمصاص تم اجراؤها للاصباغ احاديا وثنائيا في المحاليل المائية. الادمصاص الاحادي, كل من Methylene blue , Rhodamine 6G سعة 19 mg/g بينما methyl orange سعته 12 mg/g. الادمصاص الثنائي يتكون من أيوني وكاتيوني من الاصباغ نتج عنه تأثير تآزري/synergistic . محلول المتكون من اصباغ كاتيونية (Methylene Blue , Rhodamine 6G) نتج عنه سعة ثابتة لكل التراكيز المدروسة. البيانات الحركية التفاعلية اوضحت الادمصاص ماص للحرارة لكل الاصباغ عند الادمصاص الاحادي. ولكن عند الادمصاص الثنائي بعض نتج عنه مثل (methylene blue / methyl orange _ methylene blue / Rhodamine 6G) ادمصاص طارد للحرارة بينما المحلول المتكون من Rhodamine 6G , Methyl orange نتج عنه ادمصاص ماص للحرارة.

CHAPTER 1

INTRODUCTION

1.1 Introduction

Most of the local power generation plants of the Saudi electricity company use heavy fuel oil combustion for power generation, which results in large quantities of oil fly ash. There are 70 power plants consuming 22 million metric tons of diesel fuel, crude oil and heavy fuel oil. Fly ash is a by-product of the fuel combustion process, including combustion of coal and fuel oil. Oil fly ash (OFA) is typically a black powder type of waste material that results from the use of crude and residual oil for power generation. The OFA contains mainly elemental carbon (92-95 wt %); the remaining are sulfur (4-6wt%) , very small amount of metals (vanadium , magnesium) and silicon[1,2]. OFA is collected in the electrostatic precipitators (ESP) which are installed on the smoke stacks of boilers burning oil of air pollution control. These quantities must be disposed of properly.

Based on the type of fuel used, fly ash is divided into ‘’coal fly ash’’ (CFA) and ‘’Oil Fly Ash’’ (OFA). According to a 2009 survey of American chemical society, more than 71 million tons of fly ash is produced annually in USA by coal-fired plants and 45% of this quantity is reused in different applications. It is mainly used as a replacement of Portland cement; as a filler in polymers, asphalt and cementitious material; stabilizing agent and also for adsorption of solutes and solidification for waste and sludge[3–6]. The ministry of water and electricity in Saudi Arabia owns 70 power plants across the country. In

2006, these plants consumed 9,285,832 metric tons of diesel fuel, 7,210,998 metric tons of crude oil, 5,436,897 metric tons of heavy fuel oil and 22,913 million m^3 of gas. A number of local power generation plants of the Saudi electricity and water desalination companies use heavy fuel oil combustion for power generation, which results in large quantities of OFA. The total amount of disposed OFA in 2008 was about 240,000m^3. This amount is expected to increase to 440,000m^3 by 2013. The disposal of these quantities is an expensive process as it requires strict disposal procedure to ensure limited environmental pollution[2,6,7].

Analysis of OFA have shown that OFA produced in the Kingdom is mainly composed of around 90% unburned carbon in addition to some inorganic substances such as SiO2, Fe2O3 , Al2O3 and CaO and traces of heavy metals. Because of carbonaceous contents and morphology of oil fly ash has gained much attention as a low-cost adsorbent[6]. It is expected that with some chemical treatment activated, the OFA can be utilized to remove toxic gases from the mixture. OFA has gained a particular attention as a cheap adsorbent due to its ability to leach objectionable metals from wastewater and to remove pollutant gases from flue gas[8]. Md. Azhar Uddin et al. prepared an activated carbon for adsorption applications by the pyrolysis of mixture of fly ash with road paving asphalt dissolved in kerosene at 650oC in N2 atmosphere. They showed macropore diameter of the sample increased by an asphalt ratio[9]. Yang et al studied the surface modification of fly ash by heating it isothermally and investigated its impact on the properties of polymer composites[10]. Shawabkeh et al. reported the increase in a BET surface area of OFA by treating it with acid mixture. They used the combination of sulfuric and nitric acid to attach the COOH group to the surface of fly ash. Functionalizing the OFA made it more

compatible with non-polar polymers[1]. Kulkarni et al. Performed adhesion experiments to modify the surface properties of fly ash and study its effect on the polymer composite[11]. SalvatroAndidi et al were used oil fly ash to adsorbed 2-chlorophenol (CP), 2-chloroaniline (CA) and methylene blue (MB) from aqueous solutions. Adsorption was highest for 2-chlorophenol (CP) and quite low for other two organics [12]. Ali L-yaumi et al activated the fly ash with 30% NH4OH and recorded its adsorption capacity around 250 mg/g for the selective adsorption of CO2 from a mixture of CO2-N2[5]. Bada et al. investigated the adsorption capabilities of chemically treated and heat treated fly ash samples. They used Hydrochloric acid for chemical treatment and found relatively higher specific surface area as compared to heat treated fly ash. This increased surface area was achieved due to the corrosion of the outer layer of the fly ash to ash to disintegrate its stable glassy layer [13].

Keeping in view the adsorption abilities of fly ash, the present study is aimed to activate the raw OFA collected from power plant by treating it with suitable activating agent and then use the modified oil fly ash for selective removal of acidic gases from a gas mixture. The physic-chemical treatment adopted in this research is intended to increase the surface area of OFA as well as the adsorption capacity at elevated temperatures. The success of this work will steer us to utilize the one pollutant (i.e. OFA) to remove another pollutants (i.e. H_2S and CO_2) from an industrial gas. The raw ash was also modified to access the capability of ash to remove the dyes from aqueous solution.

1.2 Thesis Summary

This section will highlight the summary of each chapter. Each chapter will be discussed in the manuscript format.

Chapter 2

This chapter outlines the literature regarding the application of fly ash carbon as adsorbent to remove objectionable compounds from either gas stream or from aqueous solution.

Chapter 3

This chapter describes about the mesoporous activated carbon is produced from oil fly ash (OFA) using chemical and thermal treatment at different activation conditions. The ash samples were refluxed with a range of compositions of sulfuric, nitric and phosphoric acids followed by thermal activation in a tubular reactor. The composition of the acids and the reaction temperature were optimized to yield mesoporous activated carbon with a high surface area and yield. Several characterization methods were used to study the surface characteristics, morphology, functional groups, phase transition, and adsorption. FTIR spectra show the existence of carboxylic and amine functional groups, which increases with increasing percentage of nitric acid. SEM spot analysis and EDX demonstrate that the carbon content increases from 77.4 to 95.7% upon chemical treatment. Specimens treated with 20 vol. % H_2SO_4, 40 vol. % HNO_3 and 40 vol. % H_3PO_4 and activated at 990^oC have a BET surface area of 375.7m^2/g when compared to 4 m^2/g for the original OFA. The BJH adsorption pore distribution indicates an average pore size of 50 Å with a total mesopore volume of 0.22cm^3/g (73.6% of the total pore volume). Thus, waste OFA is a suitable raw material for the production of activated carbon.

Chapter 4

This chapter describes that Activated carbon (AC) is made from waste oil fly ash (OFA) which is produced in large quantities from power generation plants through combustion of heavy fuel oil. OFA contains ~ 80% carbon that makes it suitable for producing AC by physicochemical treatments using a mixture of HNO_3, H_2SO_4, and H_3PO_4 acids to remove non-carbonaceous impurities. The acid treated OFA is then activated by CO_2 at 990°C.Thephysico-chemical treatments of OFA have increased the surface area from 4 to 375 m^2/g. Surface morphology and pore volume of AC are characterized by combined SEM and EDX techniques. Elemental analysis shows that sulfur content is reduced from 7.1 wt% in untreated OFA to 0.51 wt% for the treated OFA. The AC is further treated with HNO_3 and NH_4OH solutions in order to attach the carboxylic and amine groups on the surface, respectively. FTIR characterization is used to confirm the presence of the functional groups on the surface of AC at different stages of its development. The performance of functionalized AC samples is tested for the removal of H_2S from a synthetic natural gas by carrying out breakthrough experiments. The results from these tests have shown maximum adsorption capacity of 0.3mg/g for NH_4OH functionalized activated carbon with 86.43% regeneration efficiency. The ammonium hydroxide treated AC is found to be more effective for H_2S removal than acid treated AC as confirmed by breakthrough experiments. The results indicate that the presence of more acidic functionalities on the surface reduces the H_2S adsorption efficiency from the gas mixture.

Chapter 5

This chapter describes that Waste oil fly ash (OFA) collected from power generation plants disposal was treated by physico-chemical treatments to improve the surface properties of OFA for potential H2S adsorption from synthetic natural gas. As-received OFA was treated with acid mixture (20% HNO_3 and 80% H_3PO_4) followed by 2M KOH to improve surface area as well as surface affinity to adsorb H_2S. Surface morphology and pore volume of activated were characterized using combined SEM-EDX, XRD analysis. FTIR characterization was used to confirm the presence of the functional groups on the surface of activated carbon at different stages of its development. Adsorption of H_2S onto activated OFA were studied using kinetic and breakthrough modeling using well-known Langmuir, Freundlich, Sips and dual site Langmuir (DSL) model. Equilibrium isotherm modeling showed that OFA has dual site with higher and lower affinity for H_2S adsorption. The effect flow rates and inlets concentrations have been explain through Yoon-Nelson model, Thomas model and Clark model. Maximum uptake capacity of 8.5mg/g was obtained for 0.2L/min flow rate with 100 ppm inlet concentration.

Chapter 6

This chapter describes that Oil fly ash (OFA) is treated by different mixtures of oxidizing agents followed by either steam or CO_2 activation. A setup is designed where steam generated at 8bar and 300^oC is injected through a long coil tubing which is kept with the OFA sample in an oven. The oven temperature is maintained at three different temperatures namely 330, 660, and 990^oC. The activated samples were characterized for their surface area, pore size distribution and morphology. The treatment with 40 wt.%

(16M) HNO_3, 40 wt.% (18 M) H_3PO_4 and 20 wt.% (18 M) H_2SO_4 followed by CO_2 activation at 990^oC has shown the highest surface area of 375 m^2/g. SEM images have shown more micro-pores and well developed particle size and porous structure resulting from steam activation at high temperature. Acid activation provided -OH- functional group which is also confirmed by FTIR analysis. The maximum adsorption capacity for H2S from natural gas, obtained at ambient conditions and a flow rate of 0.4L/min, is found to be 4.9mg/g. The sorption kinetics has shown chemisorption of H_2S on the surface. The sorption isotherm shows a multilayer adsorption which fits BET equation.

Chapter 7

This chapter summarizes the results of the removal of dyes from a binary solution of different combinations of methylene blue, Methyl orange and Rhodamine 6G.

Chapter 8

This chapter summarizes the results of adsorption of CO_2 onto prepared activated carbon

Chapter 9

The content of this chapter includes conclusions and recommendations.

1.3 References

[1] M. J. Khan, A. A. Al-juhani, A. Ul-hamid, R. Shawabkeh, and I. A. Hussein, "Effect of Chemical Modification of Oil Fly Ash and Compatibilization on the Rheological and Morphological Properties of Low-Density Polyethylene Composites," 2011.

[2] M. a. Al-Ghouti, Y. S. Al-Degs, A. Ghrair, H. Khoury, and M. Ziedan, "Extraction and separation of vanadium and nickel from fly ash produced in heavy fuel power plants," *Chem. Eng. J.*, vol. 173, no. 1, pp. 191–197, Sep. 2011.

[3] a. Mofarrah, T. Husain, and C. Bottaro, "Characterization of activated carbon obtained from Saudi Arabian fly ash," *Int. J. Environ. Sci. Technol.*, Sep. 2013.

[4] S. Arabia, "Characteristics of Fly ash Produced at Power and Water Desalination Plants Firing Fuel Oil," vol. 7, no. 2, pp. 455–466, 2013.

[5] A. L. Yaumi, I. a. Hussien, and R. a. Shawabkeh, “Surface modification of oil fly ash and its application in selective capturing of carbon dioxide,” *Appl. Surf. Sci.*, vol. 266, pp. 118–125, Feb. 2013.
[6] M. Ahmaruzzaman, “A review on the utilization of fly ash,” *Prog. Energy Combust. Sci.*, vol. 36, no. 3, pp. 327–363, Jun. 2010.
[7] B. Rubio and M. T. Izquierdo, “Coal fly ash based carbons for SO2 removal from flue gases.,” *Waste Manag.*, vol. 30, no. 7, pp. 1341–7, Jul. 2010.
[8] C. Wang, J. Li, L. Wang, X. Sun, and J. Huang, “Adsorption of Dye from Wastewater by Zeolites Synthesized from Fly Ash: Kinetic and Equilibrium Studies,” *Chinese J. Chem. Eng.*, vol. 17, no. 3, pp. 513–521, Jun. 2009.
[9] M. Visa and A. Duta, “TiO2/fly ash novel substrate for simultaneous removal of heavy metals and surfactants,” *Chem. Eng. J.*, vol. 223, pp. 860–868, May 2013.
[10] S. Guo, J. Peng, W. Li, K. Yang, L. Zhang, S. Zhang, and H. Xia, “Effects of CO2 activation on porous structures of coconut shell-based activated carbons,” *Appl. Surf. Sci.*, vol. 255, no. 20, pp. 8443–8449, Jul. 2009.
[11] S. Kulkarni, D. Sunil, and S. Sharathchandra, “Effect of surface treatment on the impact behaviour of fly-ash filled polymer composites,” *Polym. Int.*, vol. 51, no. 12, pp. 1378–1384, Dec. 2002.
[12] S. Andini, R. Cioffi, F. Colangelo, F. Montagnaro, and L. Santoro, “Adsorption of chlorophenol, chloroaniline and methylene blue on fuel oil fly ash.,” *J. Hazard. Mater.*, vol. 157, no. 2–3, pp. 599–604, Sep. 2008.
[13] S. O. Bada and S. Potgieter-vermaak, “Evaluation and Treatment of Coal Fly Ash for Adsorption Application,” no. 12, pp. 37–48, 2008.

CHAPTER 2

LITERATURE REVIEW

Fly ash is a by-product of fuel combustion process which is typically black powder type waste material that results from the use of crude and residual oil in power generation plants. This material has no economic value and is considered as one of the major wastes in the Kingdom that requires disposal. The ministry of water and electricity owns 70 power plants across the country. In 2006, these plants consumed 9.3, 7.2, and 5.5 million metric tons of diesel, crude oil and heavy fuel, respectively, where 240,000 cubic meter of fly ash was produced.

On the other hand, emission of toxic gases into the Kingdom atmosphere is another primary source of air pollution. Combustion of this heavy oil, refineries by-products, smelting operation, sulfuric acid manufacturing and metallurgical processes are the main source for discharging of these gases into atmosphere. For example, in 2006, the power plants have used 22,913 million cubic meter of natural gas that contains 3-8 vol.% of H2S which is discharged directly into atmosphere [1]. Once these gases enter into troposphere, they react with water and oxygen molecules to form acid rain. The presence of these gases in natural gas is the root for many major problems in gas processing industry. Hydrogen sulfide, for example, is certainly highly hazardous material as it is flammable and poisonous to humans and animals, which can be lethal at 350 ppm level.

Therefore, it is required to treat sour gases from such pollutant and decrease its concentration in the downstream product. Consequently, several attempts were made to

treat the discharge of acidic gases, into atmosphere. The most widely used removal technique is chemical absorption and neutralization by amine solution. Although this technique is the most commonly used as gas separation process in the petrochemical industries, it suffers from numerous problems including: high-energy requirements, corrosion, and susceptibility to foaming. Alternatively, adsorption process is used with an efficient manner. Numerous adsorbents were used to clean up these toxicants from sour gases. Activated ash is intensively used in treatment of sulfur dioxide, carbon dioxide, and hydrogen sulfide in upstream gases [2]. Other adsorbents such as fly ash [3], titanium dioxide and synthetic and natural zeolite are also used [4, 5].

2.1 Fly ash as an Adsorbent

Several studies have been reported on the utilization of fly ash for the adsorption of individual toxicant in an aqueous solution or from flue gas. Salvatro Andidi et al were used oil fly ash to adsorbed 2-chlorophenol (CP), 2-chloroaniline (CA) and methylene blue (MB) from aqueous solutions. Adsorption was highest for 2-chlorophenol (CP) and quite low for other two organics[6]. Bada et al. investigated the adsorption capabilities of chemically treated and heat treated fly ash samples. They used Hydrochloric acid for chemical treatment and found relatively higher specific surface area as compared to heat treated fly ash. This increased surface area was achieved due to the corrosion of the outer layer of the fly ash to ash to disintegrate its stable glassy layer[7]. Md. Azhar Uddin et al. prepared an activated carbon for adsorption applications by the pyrolysis of mixture of fly ash with road paving asphalt dissolved in kerosene at 650^{o}C in N_2 atmosphere. They showed macropore diameter of the sample increased by an asphalt ratio [8]. A. Al-Shawabkeh et al. prepared Calcium hydroxide treated fly ash adsorbent and tested it for

SO_2 adsorption. SO_2 was chemically adsorbed and showed first order kinetics [9]. Bagreeve et al studied the NaOH modified activated carbon for the adsorption of H_2S and concluded that adsorption capacity was increased with loading of NaOH and insensitive to pore structure and surface area [10]. Prezeprioski et al also reported a significant improvement in adsorption capacity of H_2S after treating activated carbon with K_2CO_3[11] . It is concluded that the presence of alkali metals on the activated carbon surface helps to dissociate the H_2S molecule and hence increases the uptake capacity. From the literature, it is revealed that not only the porosity but also the surface chemistry is important to enhance the adsorption capacity of AC. Higher surface area and very fine micropores exerts strong interactions between adsorbate gas molecules and carbon structure and results physical adsorption but on the other hand the presence of OH functional group or the cations dissociates the H_2S and promote chemisorption.

Yaumi et al. modified OFA using ammonium hydroxide and studied the adsorption of CO_2 under various flow conditions. They noticed the increase in adsorption capacity with higher concentration of CO_2 and flow rate [12]. Rubio and Izquierdo obtained promising results for SO_2 removal using activated carbon produced from oil agglomerated fly ash [13]. Wang et al. used fly ash to synthesize zeolite adsorbent for the treatment of waste water containing cationic dyes [14]. Visa and Duta synthesized a substrate by hydrothermal processing of fly ash and TiO_2 nano-powder. They reported an efficient and simultaneous removal of surfactant and heavy metals in a single step process [15]. It is evident that fly ash has a great potential in the environmental applications. Fly ash is an interesting alternative to replace activated carbon or zeolites for adsorption in the water

pollution treatment. Despite the number of published laboratory data, fly ash adsorbent has not been applied at an industrial scale.

2.2 Adsorption of H_2S

Environmental pollution is one of the burning issue that this world facing today since the start of industrial revolution. Exponential rise of pollutants in the air and aquatic streams make this environmental issue more severe with regard to its direct and indirect effect on the inhabitants of this world [16]. Toxic acidic gases (like CO_2 and H_2S) are considered one of the pollutants that have direct effect on human. Natural gas contains these acidic gases as an impurity in addition to light and heavier hydrocarbons. The gas quality is highly dependent on the concentration of these contaminants. Exposure to such chemicals can damage the central nervous system, respiratory system, kidney, and blood system if entered human body [17].

Exhaust gases emitting form petroleum and petrochemical industries are contaminated with hydrogen sulfide, sulfur dioxide, carbon dioxides or nitrous oxides are stored underground and can combine with natural gas. Black Sea, for example, contains 50m thick layer of hydrogen sulphide between aerobic and anaerobic water that lies after approximately 200m depth along the axis of black sea. H_2S concentration increases steadily from 300ppm at a depth of 1000m to 400ppm at 1900m. The amount of this gas is estimated at about 2.5-3.0 million tons with a concentration of 8 mg/L in 1000 m depth and 13.5 mg/L in the sea bed [18]. According to the International Energy Agency, about 43% of the world's natural gas reserves (2,580 TCF), excluding North America, are sour. The Middle East, which has the world's most sour gas reserves, contains 60% sour gas. In Russia, the world's largest natural gas producer, 34% of total reserves are sour gas

[19]. In China, recent statistics showed that millions of people are in contact with sulfur dioxide, sulfates, ozone, black carbon, flu-laced desert dust and mercury. Emission of SO_2 alone are thought to cause' harm equivalent to 12 percent of China's GNP. NOx---the main cause of urban smog---have raised 3.8 percent over 25 years of period. And it is expected to be doubled by 2020. In Russia, recent statistics showed that 14 million people are in contact with sulfur dioxide, heavy metals (nickel, copper, cobalt, lead, selenium), phenols and hydrogen sulfide where the Mining and Smeltering works are located nearby [20].

In Arab countries, the situation is similar where many countries do not control release of greenhouse gases, or fail to implement existing legislation. These problems are often compounded by the lack of treatment, unsafe transport, concentration in urban areas and inadequate management [21]. Agency for Toxic Substances & Disease Registry, USA has classified hydrogen sulfide as the top 35 of the 1,689 National Priorities List of hazardous substances identified by the U.S. Environmental Protection Agency (EPA) that need urgent treatment before entering into the environment [22]. Therefore, removing this gas or decreasing its concentrations to the permitted levels before discharging becomes a challenging issue.

Several technological processes can be performed to remediate hydrogen sulfide from downstream were adsorption can be employed efficiently at trace level with low cost. It is a mass transfer process that involves contact of a solid (adsorbent) with a fluid containing the target solute (adsorbate). The surface area of the adsorbent generally governs adsorption efficiency and selectivity as a result of accumulating of the adsorbate on the surface of the adsorbent. The adsorbent materials are classified into three categories:

(1) Oxygen-containing compounds which are hydrophilic and polar in nature. Examples of these materials are silica gel and zeolites.

(2) Polymer-based compounds. These compounds are either polar or non-polar functional groups in a porous polymer matrix.

(3) Carbon-based compounds which are hydrophobic and non-polar, including materials such as activated carbon.

Several research efforts were performed to use different adsorbent for removal of hydrogen sulfide from gas stream. Following table summarizes the adsorption of H_2S on various adsorbents.

Table 2–1: Adsorption capacities of H_2S on Different Adsorbents.

Material	Adsorption Capacity(mg/g)	Reference
Coal based Impregnated AC	9.3	[23]
Oxidized activated carbon fiber	4.57	[24]
MDEA-modified SBA-15	5.98	[25]
Fine particle rubber media (FPRM)	0.12	[26]
Peach and apricot Stone	3.65	[27]
CO_2acivated red pine wood	0.255 cm^3/g	[28]
Sewage sludge and metal sludge	20.1	[29]
MIL-53	0.714	[30]
10Zn/MSU-1 and 20Cu/MSU-1	42.3 and 19.2	[31]

2.3 Adsorption of Dyes

There are various industries including textiles, printing, food, paper and pulp, dyeing and leather industries those discharges voluminous amount of wastewater bearing dyes and pigments. Colored water not only damages the aesthetics of environment as well as poses a serious threat to aquatic ecosystem by hampering light penetration to water bodies. Among different types of treatment technologies to remove dyes from wastewater, adsorption is one of most promising option especially when the adsorbent is cheap and does not need any additional pretreatment for its activation. Calcium rich fly ash carbon adsorbs 98% of Congo red by chemisorption from solution under optimum conditions of temperature, pH and concentrations. Thermodynamics studies show the endothermic and spontaneous adsorption [32]. I D Mall et al. compare the efficiency of the removal of Congo red by commercial grade activated carbon with Bagasse fly ash (BFA) and favorable adsorption of dye onto fly ash adsorbent as compared to commercial adsorbent [33].

Table 2–2: Uptake capacities of different dyes on fly ash based adsorbents

Dye	Adsorbent	Adsorption Capacity (mol/g)	Isotherm Model	References
Congo Red	Fly ash	4.47×10^{-5}	Freundlich	[32]
Egacid orange II	Coal fly ash	3.05×10^{-4}		[34]
Acid blue 29 Acid blue 9 Acid red 91	Fly ash adsorbent	3.25×10^{-6} 5.43×10^{-6} 2.34×10^{-6}	Freundlich	[35]
Rhodamine B	Fly ash	1.15×10^{-5}	Langmuir	[34]
Crystal violet	Coal fly ash	9.76×10^{-5}	Freundlich	[36]
Orange-G	Baggase fly ash			[33]
Methylene Blue	Nitric acid treated fly ash	2.2×10^{-5}	Ridlich-Peterson	[37]
	sodium hydroxide treated fly ash	8.0×10^{-6}	Langmuir and Freundlich	[38]
	Thialand fly ash	1.6×10^{-6}		[39]
	Coal fly ash	14.4×10^{-5}	Langmuir	[40]
	Fly ash-F	1.85×10^{-5}	Langmuir	[34]

2.4 References

[1] A.L. Kohl, R.B. Nielsen, Gas purification, 5th ed., Gulf Publishing Company, Houston, 1997.

[2] J. Wu, P. Wang, W. Pan, L. Zhao, L. Gu, P. He, Experimental study on flue gas emission removed by modified activated carbons, in: 2010 International Conference on Advances in Energy Engineering, ICAEE 2010, pp. 355-358.

[3] R. Shawabkeh, A. Harahsheh, H_2S removal from sour liquefied petroleum gas using jordanian oil shale ash, Oil Shale, 24 (2007) 109-116.

[4] M.F. Irfan, J.H. Goo, S.D. Kim, Effects of NO, NO2, CO and SO2 on NO oxidation over Pt/TiO2 for hybrid fast SCR process, Environmentalist, 1-7.

[5] X.f. Bai, Y. Cao, W. Wu, Photocatalytic decomposition of H2S to produce H2 over CdS nanoparticles formed in HY-zeolite pore, Renewable Energy.

[6] S. Andini, R. Cioffi, F. Colangelo, F. Montagnaro, and L. Santoro, "Adsorption of chlorophenol, chloroaniline and methylene blue on fuel oil fly ash.," *J. Hazard. Mater.*, vol. 157, no. 2–3, pp. 599–604, Sep. 2008.

[7] S. O. Bada and S. Potgieter-vermaak, "Evaluation and Treatment of Coal Fly Ash for Adsorption Application," no. 12, pp. 37–48, 2008.

[8] M. Azhar Uddin, Y. Shinozaki, N. Furusawa, T. Yamada, Y. Yamaji, and E. Sasaoka, "Preparation of activated carbon from asphalt and heavy oil fly ash and

coal fly ash by pyrolysis," *J. Anal. Appl. Pyrolysis*, vol. 78, no. 2, pp. 337–342, Mar. 2007.

[9] A. Al-Shawabkeh, H. MATSUDA, and M. HASATMI, "ComDarative Reactivity of Treated FBC- aid PCC-Fly Ash fbr SO2 Removal," *Can. J. Chem. Eng.*, vol. 73, no. October, 1995.

[10] F. Adib, A. Bagreev, and T. J. Bandosz, "Adsorption / Oxidation of Hydrogen Sulfide on Nitrogen-Containing Activated Carbons," no. 12, pp. 1980–1986, 2000.

[11] S. Y. J. Przepiorski and A. Oya, "Structure of K 2 Co 3 -loaded activated carbon fiber and its deodorization ability against H 2 S gas," vol. 37, pp. 1881–1890, 1999.

[12] A. L. Yaumi, I. a. Hussien, and R. a. Shawabkeh, "Surface modification of oil fly ash and its application in selective capturing of carbon dioxide," *Appl. Surf. Sci.*, vol. 266, pp. 118–125, Feb. 2013.

[13] B. Rubio and M. T. Izquierdo, "Coal fly ash based carbons for SO2 removal from flue gases.," *Waste Manag.*, vol. 30, no. 7, pp. 1341–7, Jul. 2010.

[14] S. Wang, Y. Boyjoo, and A. Choueib, "A comparative study of dye removal using fly ash treated by different methods.," *Chemosphere*, vol. 60, no. 10, pp. 1401–7, Sep. 2005.

[15] M. Visa and A. Duta, "TiO2/fly ash novel substrate for simultaneous removal of heavy metals and surfactants," *Chem. Eng. J.*, vol. 223, pp. 860–868, May 2013.

[16] F. Caiazzo, A. Ashok, I. a. Waitz, S. H. L. Yim, and S. R. H. Barrett, "Air pollution and early deaths in the United States. Part I: Quantifying the impact of major sectors in 2005," Atmos. Environ., vol. 79, pp. 198–208, Nov. 2013.

[17] H. Sciences, A. M. Ghouri, and F. Member, "ENVIRONMENTAL POLLUTION :," no. April 2011, pp. 276–285.

[18] B. Sea, H. Energy, and H. Storage, "Possibilities of Production and Storage of Hydrogen in the Black Sea," no. June, pp. 1–8, 2006.

[19] D. Huo, "The Global Sour Gas Problem | Stanford Energy Club," 2012. [Online]. Available: https://energyclub.stanford.edu/journalitem/the-global-sour-gas-problem/.

[20] N. Nickel, Company Report on Air Pollution Reduction Measures in 2006 and Plans for 2007, in, 2007.

[21] BCRC-Cairo, Regional Workshop for Arab States on the Environmentally Sound Destruction of POP and Decontamination of POP Containing Waste in the Context of Basel Convention and Stockholm Convention, in, Amman, Jordan, 2005.

[22] ATSDR, CERCLA Priority List of Hazardous Substances, in, Department of Health and Human Services, USA. URL: http://www.atsdr.cdc.gov/cercla/05list.html, 2007.

[23] Y. Xiao, S. Wang, D. Wu, and Q. Yuan, "Experimental and simulation study of hydrogen sulfide adsorption on impregnated activated carbon under anaerobic conditions.," J. Hazard. Mater., vol. 153, no. 3, pp. 1193–200, May 2008.

[24] W. Feng, S. Kwon, E. Borguet, and R. Vidic, "Adsorption of hydrogen sulfide onto activated carbon fibers: effect of pore structure and surface chemistry.," Environ. Sci. Technol., vol. 39, no. 24, pp. 9744–9, Dec. 2005.

[25] Q. Xue and Y. Liu, “Removal of minor concentration of H2S on MDEA-modified SBA-15 for gas purification,” J. Ind. Eng. Chem., vol. 18, no. 1, pp. 169–173, Jan. 2012.
[26] N. Wang, J. Park, and T. G. Ellis, “The mechanism of hydrogen sulfide adsorption on fine rubber particle media (FRPM).,” J. Hazard. Mater., vol. 260, pp. 921–8, Sep. 2013.
[27] A. C. Lua and T. Yang, “Theoretical and experimental SO2 adsorption onto pistachio-nut-shell activated carbon for a fixed-bed column,” Chem. Eng. J., vol. 155, no. 1–2, pp. 175–183, Dec. 2009.
[28] K. Sakanishi, Z. Wu, A. Matsumura, I. Saito, T. Hanaoka, T. Minowa, M. Tada, and T. Iwasaki, “Simultaneous removal of H2S and COS using activated carbons and their supported catalysts,” Catal. Today, vol. 104, no. 1, pp. 94–100, Jun. 2005.
[29] W. Yuan and T. J. Bandosz, “Removal of hydrogen sulfide from biogas on sludge-derived adsorbents,” Fuel, vol. 86, no. 17–18, pp. 2736–2746, Dec. 2007.
[30N. Heymans, S. Vaesen, and G. De Weireld, “A complete procedure for acidic gas separation by adsorption on MIL-53 (Al),” Microporous Mesoporous Mater., vol. 154, pp. 93–99, May 2012.
[31] D. Montes, E. Tocuyo, E. González, D. Rodríguez, R. Solano, R. Atencio, M. a. Ramos, and A. Moronta, “Reactive H2S chemisorption on mesoporous silica molecular sieve-supported CuO or ZnO,” Microporous Mesoporous Mater., vol. 168, pp. 111–120, Mar. 2013.
[32] B. Acemioğlu, “Adsorption of Congo red from aqueous solution onto calcium-rich fly ash.,” J. Colloid Interface Sci., vol. 274, no. 2, pp. 371–9, Jun. 2004.
[33] I. D. Mall, V. C. Srivastava, and N. K. Agarwal, “Removal of Orange-G and Methyl Violet dyes by adsorption onto bagasse fly ash—kinetic study and equilibrium isotherm analyses,” Dye. Pigment., vol. 69, no. 3, pp. 210–223, Jan. 2006.
[34] P. Janos, “Sorption of dyes from aqueous solutions onto fly ash,” Water Res., vol. 37, no. 20, pp. 4938–4944, Dec. 2003.
[35] K. RAMAKRISHNA and T. VIRARAGHAVAN, “Dye removal using low cost adsorbents,” Water Sci. Technol., vol. 36, no. 2–3, pp. 189–196, 1997.
[36] D. Mohan, K. P. Singh, G. Singh, and K. Kumar, “Removal of Dyes from Wastewater Using Flyash, a Low-Cost Adsorbent †,” Ind. Eng. Chem. Res., vol. 41, no. 15, pp. 3688–3695, Jul. 2002.
[37] S. Wang, L. Li, H. Wu, and Z. H. Zhu, “Unburned carbon as a low-cost adsorbent for treatment of methylene blue-containing wastewater,” J. Colloid Interface Sci., vol. 292, no. 2, pp. 336–343, Dec. 2005.
[38] S. Wang and Z. H. Zhu, “Sonochemical treatment of fly ash for dye removal from wastewater.,” J. Hazard. Mater., vol. 126, no. 1–3, pp. 91–5, Nov. 2005.
[39] K. Yamada, K. Haraguchi, C. C. Gacho, B. P. Wongsiri, and M. L. Pena, “Removal of Dyes from Aqueous Solution by Sorption with Coal Fly Ash,” pp. 1–6, 2003.

[40] “Fly ash for colour removal from synthetic dye solutions.” Online Available: http://connection.ebscohost.com/c/articles/8462090/fly-ash-colour-removal-from-synthetic-dye-solutions.

CHAPTER 3

Thermochemical Treatment of Fly Ash for Synthesis of Mesoporous Activated Carbon

This paper is submitted to "Journal of thermal analysis and Calorimetry"

3.1 Introduction

Activated carbon (AC) is one of the most promising adsorbents that is used for many environmental, medical, analytical, and industrial applications. It is characterized as a material with a high surface area and a well-developed pore size distribution. The main precursors used for the production of AC are lignocellulosic, coal, and petroleum pitch raw materials [1-3]. Fly ash is a solid waste material that is produced during the combustion of coal and fossil fuel. It has a substantial carbon content (45-90 mass %), which is suitable a source for the production of AC. The carbon content and the experimental conditions influence the pore structure and the surface morphology of the produced carbon. Chemical activation using different metal salts and/or oxidizing agents leads to the dehydration and pyrolysis of the raw material at low temperature [4]. Thermal treatment in the presence of carbon dioxide, steam, or partially oxidizing gases develops a pore structure in the AC which significantly increases the surface area. Further chemical treatment with reagents containing various functional groups can also enhance the carbon selectivity and adsorption capacity for target solutes and gases. Many research efforts have focused on the production of activated carbonaceous materials by chemical and/or thermal treatment of fly ash. Izquierdo and Rubio evaluated coal fly ash as a starting material for the production of activated carbon by steam activation at 900^{o}C [5]. They found that increasing the activation temperature has a substantial effect on the surface area and the pore volume. Purnomo et al. studied the effect of the activation methods on the properties of AC produced from bagasse fly ash [6]. They showed that the chemical activation using KOH followed by thermal treatment in the presence of carbon dioxide can form a microporous carbon matrix. Mofarrah et al. treated oil fly ash

(OFA) with a mixture of nitric and hydrochloric acids followed by activation using phosphoric acid at 550-800 ^{o}C [7]. A maximum surface area of 148.3 m^2/g was achieved at an activation temperature of 800^{o}C. Other investigators have shown that increasing the carbon to metal oxide ratio in the ash matrix as well as the activation temperature can increase the surface area, pore volume, and hence the adsorption capacity [8-15]. These efforts, to our knowledge, were not focused on optimizing the experimental conditions to improve the surface properties of AC.

In this study, the effects of the varying composition of a mixture of the three oxidizing agents (nitric, sulfuric and phosphoric acids) combined with the thermal treatment of OFA at several temperatures on the production of mesoporous AC were evaluated. The surface properties, morphology, and the yield of the produced AC samples were also determined.

3.2 MATERIALS AND METHODS

3.2.1 Materials

OFA was received from the Rabigh power plant, Saudi Arabia. Prior to activation, it was dried at 110 °C, sieved with 45 μm mesh, and stored in capped containers. The reagents used such as nitric, sulfuric and phosphoric acids and ammonium hydroxide are of analytical reagent grade and were procured from Sigma-Aldrich and Sharlau chemical companies. Carbon dioxide and nitrogen are of 99.999% purity and were supplied by the Saudi Industrial Gases Company.

3.2.2 Chemical Activation of OFA

Twenty one OFA samples were treated with a mixture of the three oxidizing agents of varying composition as shown in Table3.1. In a typical run, a 10 g sample was refluxed with 200 mL of the acid mixture at the boiling point of ca. 110^{o}C for 4 h. Then the reaction mixture was cooled to room temperature (22±1^{o}C) and was filtered. The AC produced was washed several times with hot and double distilled water to remove the acids from the pores of the AC. The treated OFA cake was dried at 110^{o}C and stored for further use.

Table 3–1: Composition of the oxidizing agent used in the activation of OFA

Oxidizing Agent No.	H_2SO_4 /vol %	HNO_3 /vol %	H_3PO_4 /vol %
1	0	0	100
2	0	20	80
3	0	40	60
4	0	60	40
5	0	80	20
6	0	100	0
7	20	0	80
8	20	20	60
9	20	40	40
10	20	60	20
11	20	80	0
12	40	0	60
13	40	20	40
14	40	40	20
15	40	60	0
16	60	0	40
17	60	20	20
18	60	40	0
19	80	0	20
20	80	20	0
21	100	0	0

3.2.3 Physical Treatment of OFA

The chemically treated OFA samples were further activated with CO_2 at elevated temperatures (330, 660 and 990^oC) in a tubular furnace. A portion of each of the chemically treated samples (6 g) was placed in a stainless steel reaction tube (of 1 cm ID and 20 cm length) and CO_2 was passed at a flow rate of 1 L/min and a pressure of 2 bars. The temperature of the furnace was increased at a rate of 10^oC/min to the desired value and held for 30 min. Then the sample was removed from the furnace, cooled to room temperature (22±1 ^oC) and stored in capped containers, after determining the weight, for characterization and functionalization.

The degree of burn-off, α (mass %) is calculated using equation 1;

$$\alpha = \frac{w_i - w_f}{w_i} \qquad (1)$$

Where w_i is the initial mass of chemically treated fly ash and w_f is the final mass of sample after CO_2 activation.

3.2.4 Surface Modification of OFA

The thermally activated samples were first refluxed with concentrated nitric acid to functionalize the carbon surface with carboxylic groups, filtered, and washed well prior to refluxing with ammonium hydroxide (50 mL at 90°C) for 4 h. The functionalized samples were dried at 110°C and characterized for their surface properties and morphology.

3.2.5 Characterization of AC

The surface area and the pore size distribution were determined using a Micromeritics ASAP 2020 BET analyzer. A sample of ca. 0.4 g was degassed at 300^{o}C for 2 h under vacuum prior to making N_2 adsorption-desorption measurements at 77 K. The hysteresis curves were recorded and the BET surface area was determined at $0.35P_o$. The pore size distribution was estimated using the Barret-Joyner-Halenda (BJH) surface/volume mesopore analysis. Surface morphology was determined using a JSM6400A JEOL Scanning Electron Microscope in conjunction with an Energy Dispersive X-ray (EDX) spectrometry option operated at 15 kV. The samples were first coated with a thin layer of gold prior to obtaining the SEM images. Spot analyses were conducted in triplicate to determine the elemental composition of the specimens.

Fourier transform infrared (FTIR) spectroscopic analysis was performed using an FPC FTIR Perkin Elmer spectrometer. Dried AC samples were mixed with KBr powder and compressed to form transparent disks using a hydraulic press. These disks were further dried at 110°C to minimize moisture interference, prior to obtaining the FTIR spectra using the transmission mode in the 500 to 4000 cm^{-1} range. Thermogravimetric analysis (TGA) was performed on a SDT Q600 Model combined TGA-DSC analyzer, which was calibrated with calcium oxalate and aluminum supplied by SDT. Samples of 5-10 mg were heated from 300 to 1073 K at a rate of 10 K/min with a nitrogen flow rate of 10 mL/min. The mass of the samples was recorded as a function of the temperature. Thermal analysis was carried out in a differential scanning calorimeter, DSC (TA-Q1000). The program involves heating from 310 K to 573 K at a rate of 5 K/min with a hold at 378 K

for 3 minutes to remove water vapor. The different samples were scanned at the same conditions to assess the impact of the treatment on the DSC heating curve.

3.3 Results and Discussion

Elemental composition of raw and treated OFA is shown in Table3.2. Raw OFA is a black colored material that contains a high percentage of unburned carbon (77.4 mass %) and a significant amount of mineral oxides such as alumina, silica, and alkali and alkali earth metal oxides. Sulfur percentage in the ash sample is the second highest at 9.32 mass %, formed as a result of burning sulfur containing organic materials, pyrites and/or sulfates [16]. When the ash was refluxed with the acid mixture, the metal oxide content decreases due to the removal mineral oxides by leaching. Sulfur is also reduced from 9.32 to 0.51 mass %. The oxidation of the ash sample increases the percentage of oxygen containing functional groups on its surface to yield an activated carbon with 79.38% carbon and 20.06% oxygen. Additional thermal treatment results in the dissociation of the oxygenated functional groups to yield samples with 83.6 mass% carbon and 15.65 mass % oxygen. Further treatment with ammonium hydroxide significantly decreases the oxygen content to 1.35 mass % yielding a sample with a total carbon content of 97.26 mass %.

Table 3–2: Elemental composition of treated and untreated OFA

Elements	OFA /mass %	Chemically treated /mass %	Thermochemically treated and HNO_3 etched /mass %	Thermochemically treated and NH_4OH functionalized /mass %
C	77.40	79.38	83.61	97.26
O	7.10	20.06	15.65	1.35
S	9.32	0.51	0.62	1.36
Al	0.25	-	-	-
Mg	1.41	-	-	-
Ca	0.23	-	-	-
V	1.29	-	-	-
Ni	0.68	-	-	-
Zn	0.40	-	-	-
Si	0.08	0.05	0.12	0.02
Fe	0.14	-	-	-

3.3.1 Surface Area and Pore Size Distribution

The curves for the adsorption and desorption of nitrogen on chemically and thermochemically treated OFA displaying hysteresis are shown in Fig.3.1. Raw fly ash demonstrates steep sorption steps (Type H2) with a low monolayer capacity due to the relatively large pore size. Chemically treated samples showed a higher monolayer capacity of 0.3 mmol N_2/g with a stepwise sorption hysteresis appearing at a relative pressure higher than $0.35P/P^o$. This is attributed to the capillary condensation in the

mesoporous structure (Type IV), which occurs due to the spontaneous filling of the internal capillary surface accompanied by the loss of the stability of the adsorption films on capillary walls [17]. When this sample is further thermally treated in the presence of CO_2 a narrow adsorption-desorption hysteresis appeares at P/Po > 0.4 with the formation of more micro and mesopores in the carbon matrix. As a consequence, the monolayer coverage increases to 6.3mmol/g and the total surface area increases from 4.05m^2/g to 375.7 m^2/g when the chemically treated sample is subjected to thermal treatment at 990 ^oC.

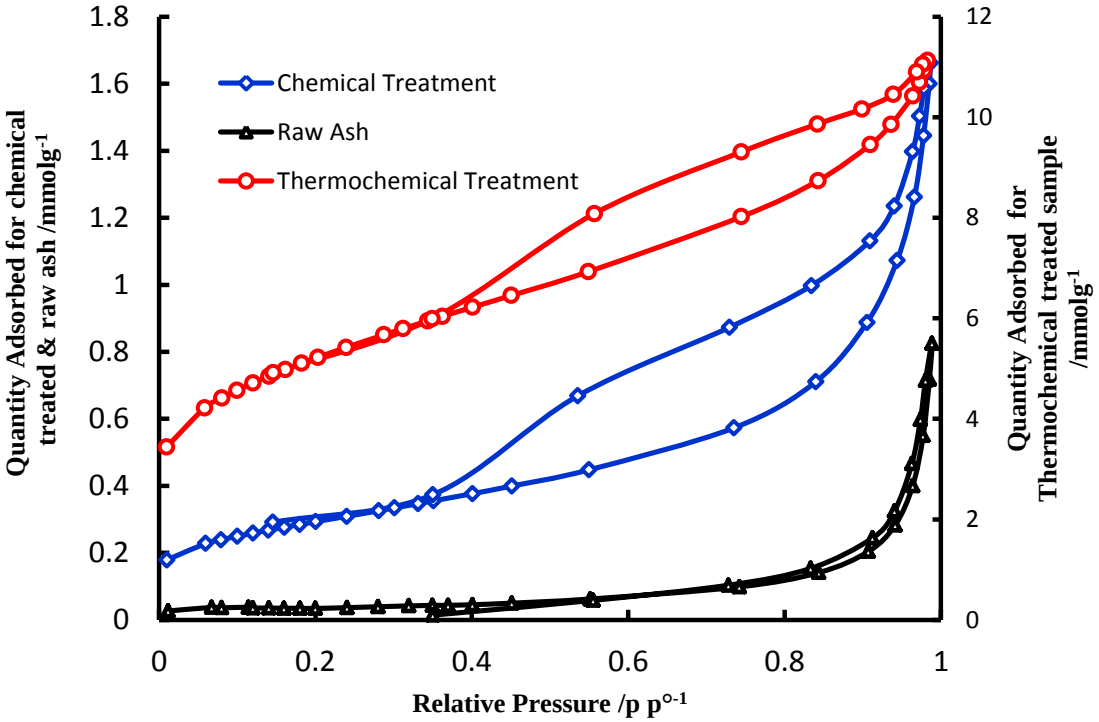

Figure 3-1: Adsorption-desorption hysteresis for N_2 on treated and untreated ash.

The impact of the composition of the acid mixture on the surface area of the AC is illustrated in Fig.3.2. Fig.3.2 (a) shows that in the absence of sulfuric acid a mixture of 20 vol. % HNO_3 and 80 vol. % H_3PO_4 gives the highest surface area after chemical treatment. Further increase in the percentage of nitric acid decreases the surface area as a result of pore damage. This trend is also present in thermally treated samples but with a less degree of pore damage (Fig.3.2 (b)). The effect of addition of sulfuric acid is pronounced, leading to the opening of more pores during thermal treatment and hence increasing the surface area. An increased surface area of 303.4, 338.5 and 375.7 m^2/g was achieved for samples thermochemically treated with 60, 40, and 20 vol. % H_2SO_4, respectively.

The effects of the acid mixture on the pore structure of the AC produced by chemical treatment are presented in Fig.3.3. Raw ash samples display a broad pore distribution in the range of 50-1000 Å and the incremental pore volume increases with increasing pore diameter. The presence of mineral oxides in the ash matrix leads to a blockage in the pores and hence contributes to the decrease of the total pore volume. Upon treatment with the acid mixture some of the minerals are leached out, which increases the carbon porosity. The magnitude of the increase is affected by the composition of the acid mixture. Fig.3.3(a) shows that an increase of the ratio of nitric to phosphoric acid increases both micropores and mesopores. Although the initial treatment with 100 vol. % H_3PO_4 does not change the pore structure, the incremental pore volume decreases with increasing pore size. Similar findings are obtained when samples are treated with 100% HNO_3, which increases the incremental pore volume at a lower pore radius producing better micropores and

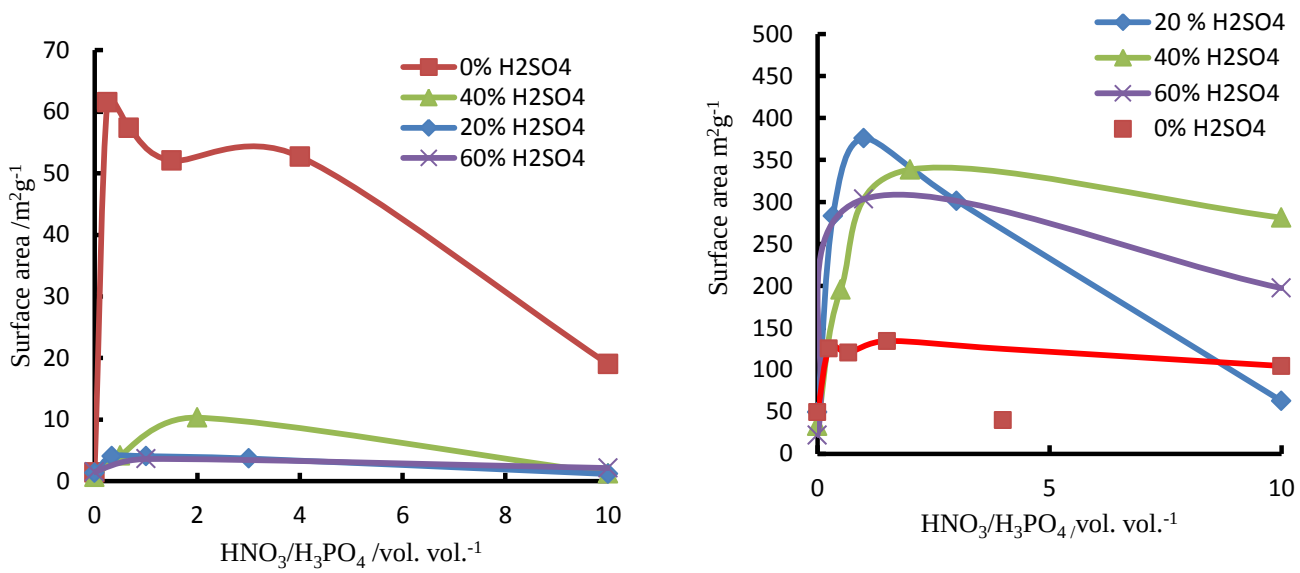

(a) (b)

Figure 3-2: Effect of the acid composition and thermal treatment on the surface area of active carbon; (a) Surface area after chemical treatment, (b) Surface area after chemical and physical treatment.

mesopores. The increase in the ratio of nitric acid to phosphoric acid leads to the opening of more micropores and mesopores, which leads to an increased contribution to the total pore volume as in the case of the treatment by 80 vol. % HNO_3. This can be attributed to the promotion of the crosslinking reaction of carbon by the acid. Phosphoric acid initiates splitting of the weak connecting bridges within the carbon structure in the ash samples. This is followed by the recombination of the fragmented structure to form stronger linkages, forming a larger structural carbon unit [18]. Similar finding were reported by Yakout and El-Deen [19] for the pyrolysis of the cellulosic structure of olive stone by phosphoric acid. They found that phosphoric acid can release tar from the cellulose cross-linked framework and hence promote porosity [19]. These results are also supported by previous investigations [20, 21]. During treatment nitric acid can also remove impurities and other oxidized char materials that block pore channels. Higher concentrations of nitric acid can destroy the pore walls and hence decrease the pore volume [22]. An optimum concentration of 20 vol. % HNO_3 and 80 vol. % H_3PO_4 produces the largest micropore and mesopore volume of 0.023 cm^3/g which accounts for 24.1% of total pore volume. Combined effects of nitric and sulfuric acids (Fig.3.3 b) or sulfuric and phosphoric acids (Fig.3.3 c), on the other hand, does not have any effect on the opening of pores of the AC structure. This may be attributed to the strong action of both acids, which could significantly damage the pore structure. Sulfuric acid shows pore opening ability similar to that for the 20 vol. % HNO_3 and 80 vol. % H_3PO_4 mixture, which can be related to the net O/H ratio of ca. 1.66-2 for the acid mixture. A study of the combined effects of the three acids (Fig.3.3 d) shows that an increase in the percentage of

phosphoric acid increases the micropore and mesopore volume to a value of 0.017 cm^3/g for the sample activated with 20 vol. % H_2SO_4, 20 vol. % HNO_3, and 60 vol. % H_3PO_4.

Thermal treatment of ash samples increases the pore volume by 2-20 times when compared to that obtained with chemical treatment alone. As shown in Error! Reference ource not found., the percentage of micropores and mesopores has increased in all samples. For example, in the sample treated with 20 vol. % HNO_3, 40 vol. % H_2SO_4, and 40 vol. % H_3PO_4 and further thermally treated at 990^oC the total pore volume is $0.3cm^3/g$ when compared to $0.056cm^3/g$ for the sample before thermal treatment. The percentage of micropores and mesopores increases from 0.9 to 4.5% and 10.7 to 32%, respectively, when thermally treated. Increasing the carbonization temperature to 990^oC results in the release of volatile organic compounds from the pores. In addition, this will burn-off a percentage of carbon in the structure, which generates more micropores in the ash matrix [23].

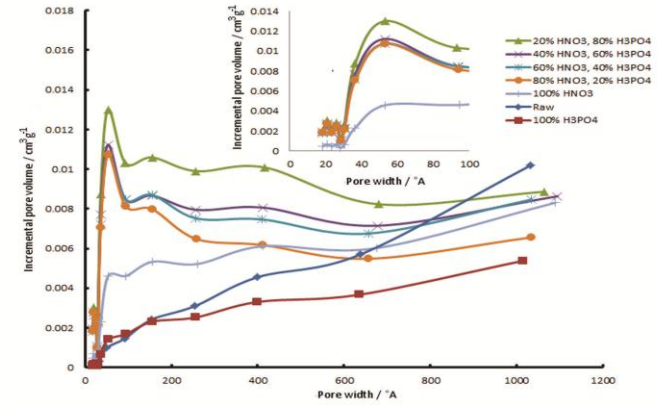

(a)

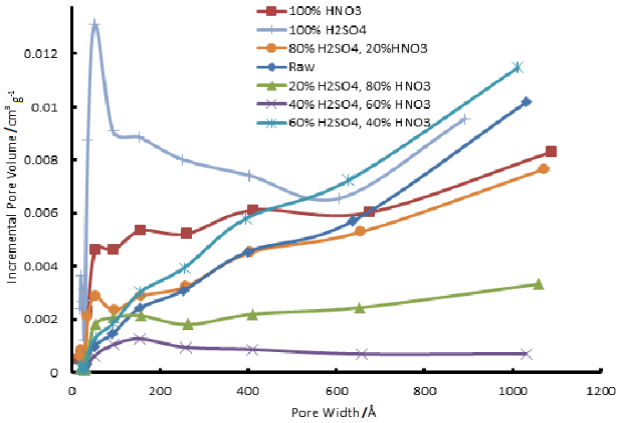

(b)

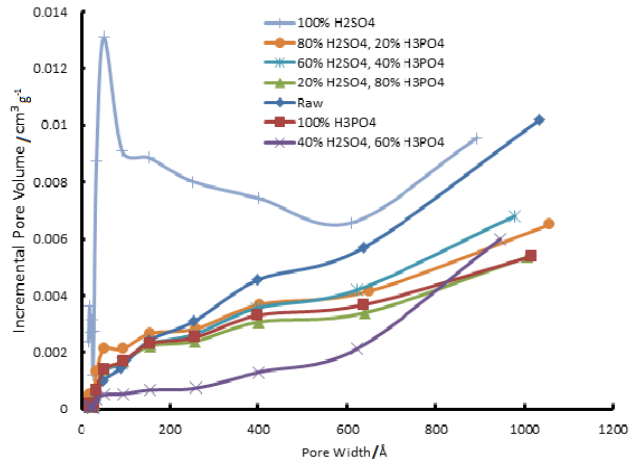

(c)

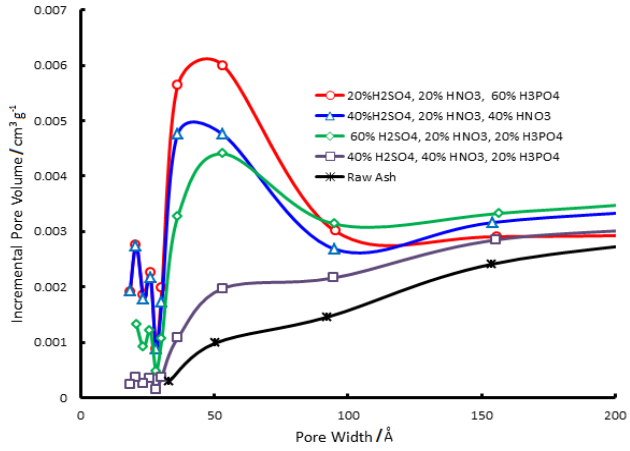

(d)

Figure 3-3: Effect of the composition of the acid mixture on the pore size of chemically treated samples; (a) Effect of the ratio of nitric acid to phosphoric acid on the pore size distribution, (b) Effect of the ratio of sulfuric acid to nitric acid on the pore size

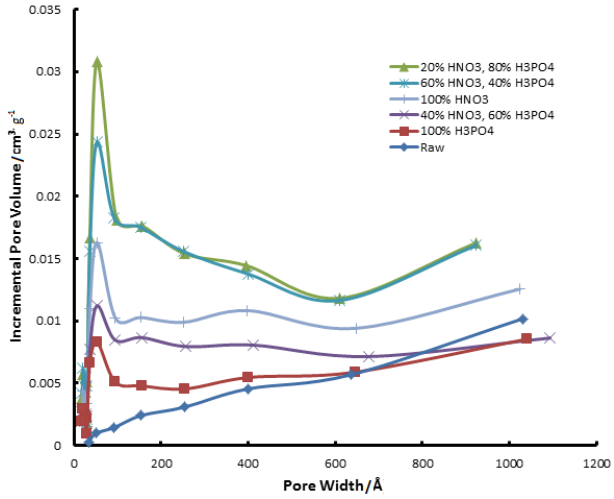

(a)

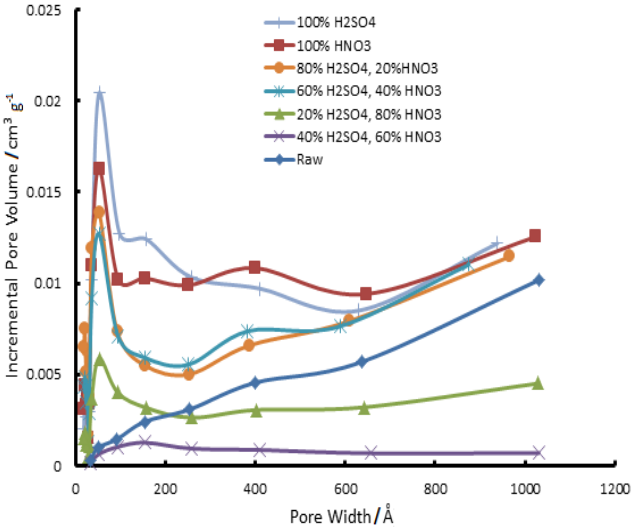

(b)

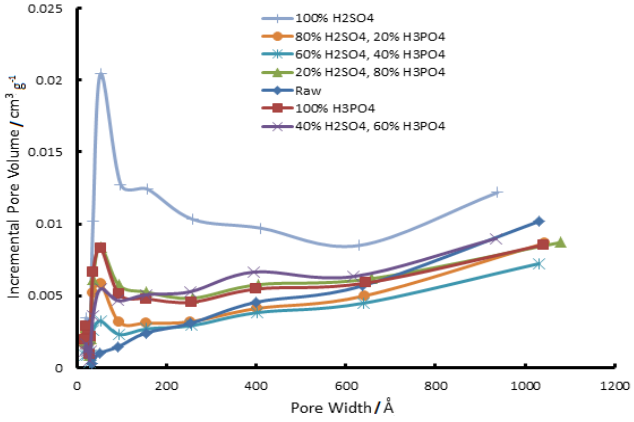

(c)

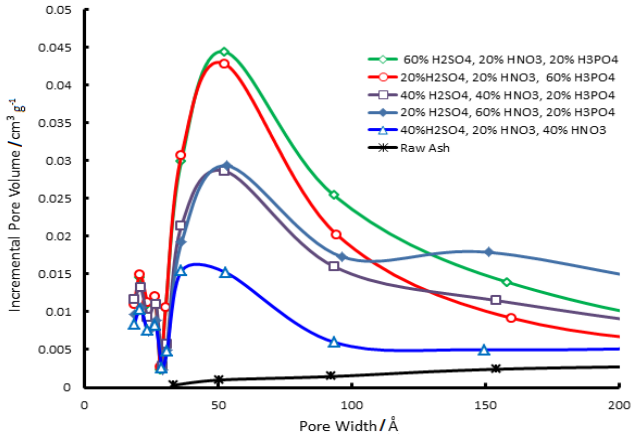

(d)

Figure 3-4: Effect of the composition of the acid mixture on the pore size of thermochemically treated samples; (a) Effect of the ratio of nitric acid to phosphoric acid and thermal treatment, (b) Effect of the ratio of sulfuric acid to nitric acid and thermal treatment

3.3.2 FTIR Spectroscopy

FTIR spectra of OFA and AC are shown in Fig.3.5. The spectrum of the untreated OFA has three major peaks; 3430 cm^{-1} attributed to either absorbed water molecules or dissolved volatile species; 1625 cm^{-1} due to the stretching mode of the carbonyl (C=O) group bonded to conjugated carbon atoms; and 1115 cm^{-1} due to C-O stretching [24]. Upon chemical treatment with the mixture of 20 vol. % H_2SO_4, 40 vol. % HNO_3 and 40 vol. % H_3PO_4 a new peak appears at 1715 cm^{-1} corresponding to carbonyl C=O stretching. The peak at 1115 cm^{-1} shifts to 1230 cm^{-1}, which is due to the C–OH stretching vibrations [25]. Further treatment with CO_2 at 990^oC results in two more peaks at 2854 and 2924 cm^{-1}, which correspond to symmetric stretching and asymmetric stretching of aliphatic C-H species, respectively. On the other hand, this sample loses all major peaks when it is soaked and refluxed with concentrated nitric acid, which is attributed to the damage of the activated ash structure [26]. The broad band at 1580 cm^{-1} is assigned to the stretching of the aromatic ring coupled to highly conjugated carbonyl groups [42]. When this AC is refluxed with ammonium hydroxide, peaks related to amine functional groups appear at 3330, 2335, 1590, and 1100 cm^{-1}. These peaks are assigned to (–NH–) stretching, –C≡N, –NH– bending vibrations and C-N stretching vibrations, respectively [27].

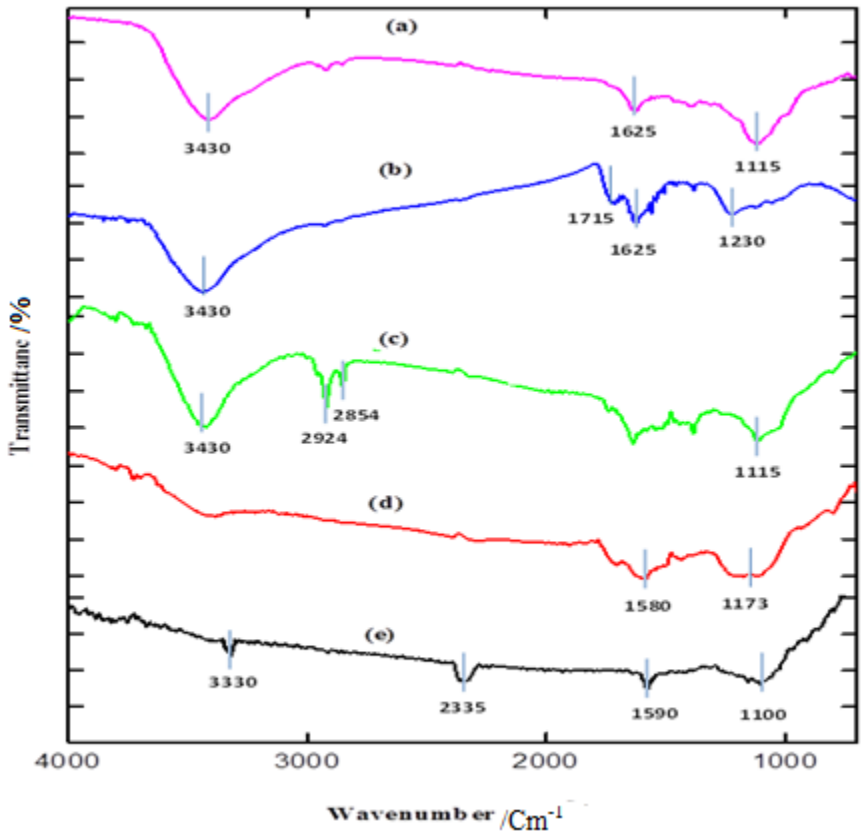

Figure 3-5: FTIR spectra for (a) Raw OFA, (b) Chemically treated OFA, (c) Thermochemically treated OFA, (d) Thermochemical treatment followed by HNO_3 itching, and (e) Thermochemical treatment followed by NH_4OH functionalization.

3.3.3 Surface Morphology

SEM image showing the morphology of raw OFA is shown in Fig.3.6 (a), which confirms the presence of carbon spherical particles in the range of 10-100 μm with small cavities and pits at the micro level. Also, there are some aggregates of irregular shape containing mineral oxides (white areas). Chemical treatment with acids reduces the size of the carbon particles to 5-50 μm and generates pores of varying sizes (Fig.3.6 b). Some of these particles are filled with mineral oxides while others have become more porous. Additional thermal treatment yields an even more porous ash with the disappearance of the mineral oxides. Further treatment with HNO_3 fractures the carbon particles leading to broken pore walls and irregular particle shapes. On the other hand, the sample treated with strong ammonium hydroxide does not show any particle damage.

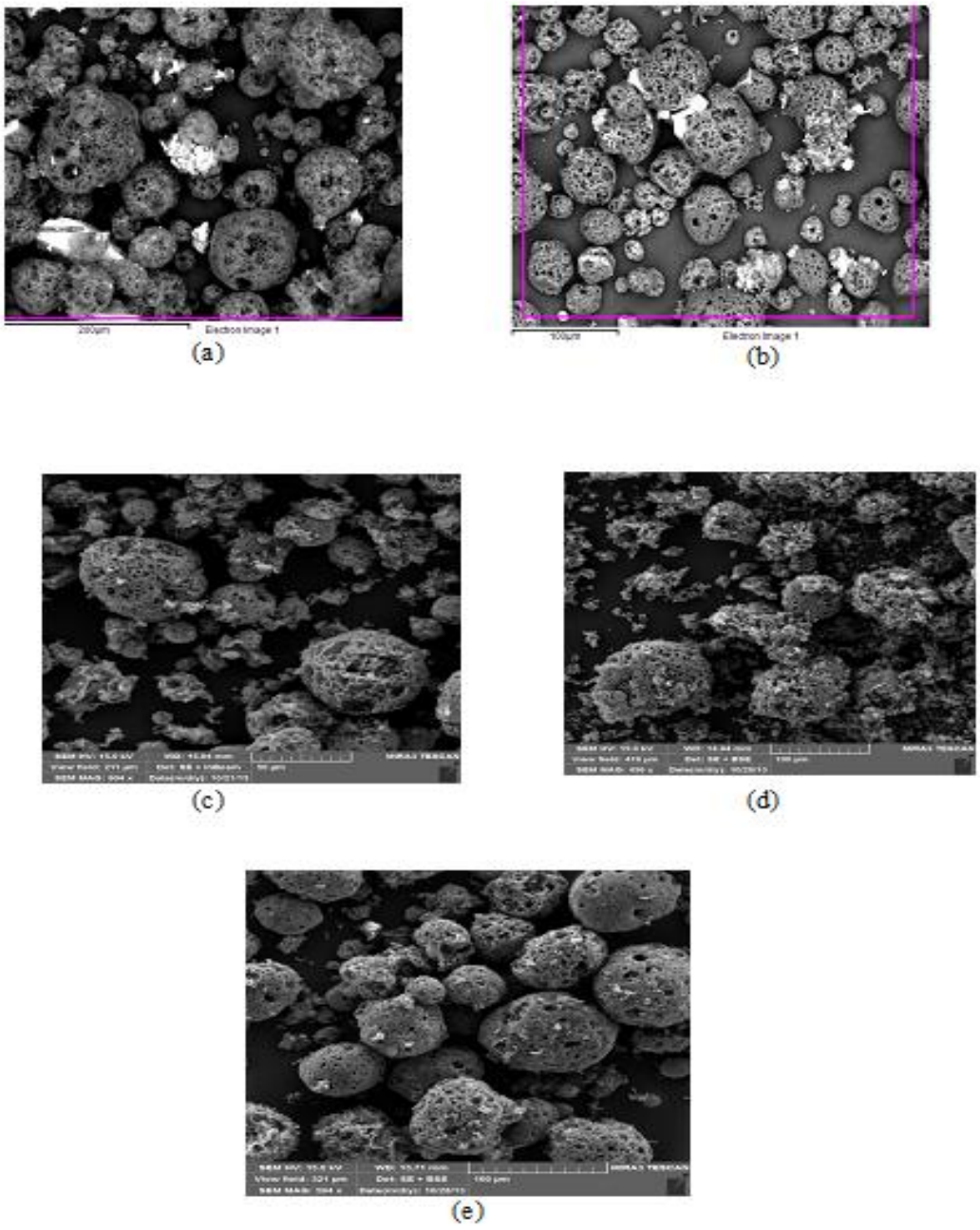

Figure 3-6: SEM images for activated ash; (a) Ash before treatment, (b) Chemically treated ash, (c) Thermochemically treated ash, (d) Thermochemical treatment followed by HNO_3 itching, and (e) Thermochemical treatment followed by NH_4OH functionalization.

3.3.4 X-ray Diffraction Characterization

X-Ray diffractograms for ash samples treated by different methods and AC samples are shown in Error! Reference source not found.**7**. Raw OFA shows two broad peaks in the ange of 22-24 and 9-10 2θ Which are related to silica and Ca-Mg-silicate (tremolite), respectively Also, major peaks appear at 29.5 2θ and 20.26 2θ representing calcite ($CACO_3$) and quartz, respectively [28]. When this sample is treated with acids the broad peak at 9-10 2θ disappears as a result of leaching of silicates from the sample matrix. Further thermal treatment followed by acid etching and NH_4OH functionalization lead to a decrease in the oxygen content.

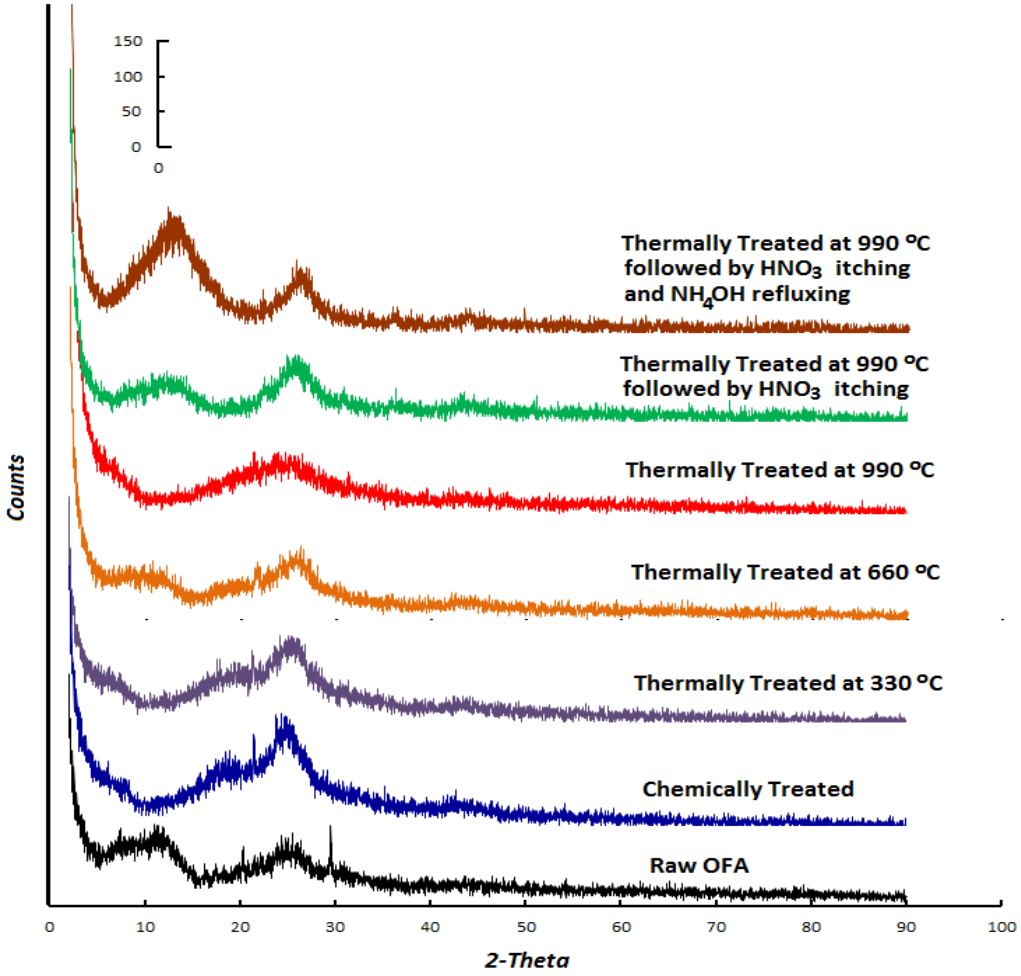

Figure 3-7: X-ray diffractograms of raw and treated ash

3.3.5 Thermo Gravimetric Analysis

Thermogravimetric analysis (TGA) was performed on raw fly ash, and chemically treated and thermally treated fly ash samples to determine their thermal stability using an SDT Q600 instrument from TA Instruments Inc. TGA scans were obtained under a nitrogen environment, with a purge flow rate of 20 mL/min from 300 to 1073K at a heating rate of 10K/min to determine the thermal parameters of each sample. The raw fly ash (Fig.3.8a) shows one-step degradation, whereas chemically treated ash (Fig.3.8b) shows a three-step degradation profile. This three-step degradation of chemically treated ash is due to the presence of volatile organic compounds. The initial degradation (5%) and char yield for raw fly ash and chemically treated ash are at 753K and 70% and 370K and 42%, respectively. Ash treated thermally (Figs.3.8c-e) at 660 ˚C and 990 ◦C displays a one-step degradation profile, whereas the sample treated at 330 ˚C displays a three-step rapid degradation. Above 660 ˚C fly ash does not contain any volatile compounds due to their decomposition at lower temperatures. In terms of char yield, fly ash treated at 660˚C shows higher values than the samples treated at 330˚C and 990˚C. The thermochemically treated samples (HNO_3 etched and NH_4OH functionalized) show similar degradation profiles (Fig.3.8g). These samples degrade rapidly when compared to other samples due to the presence of readily removed volatile organic compounds. These samples demonstrate a maximum degradation at approximately 323K and other degradations in the samples after HNO_3 etching and NH_4OH functionalization are around 553K, 723K, and 953K and 473K, 753K, and 953K, respectively. The NH_4OH treated fly ash sample has a higher char yield percentage than the HNO_3 treated sample.

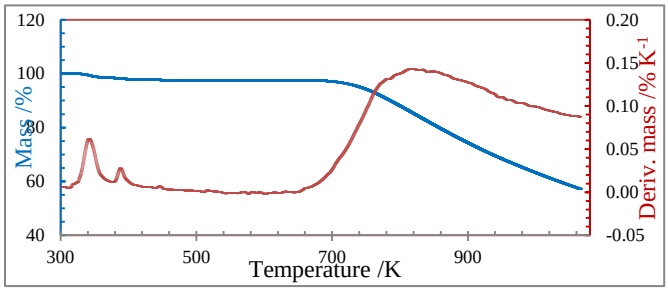

(a)

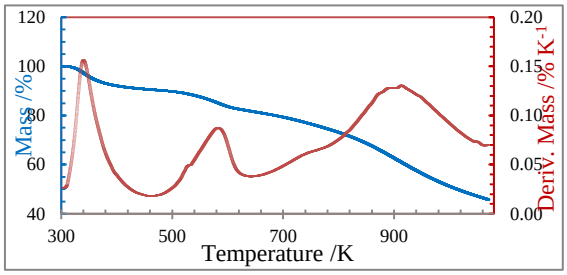

(b)

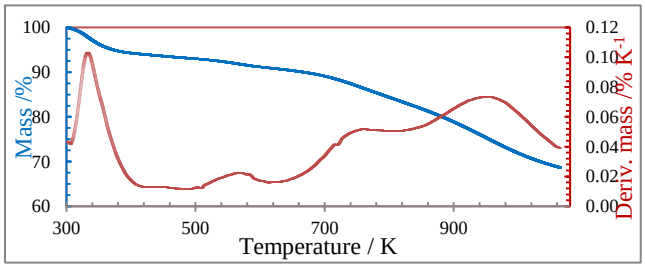

(c)

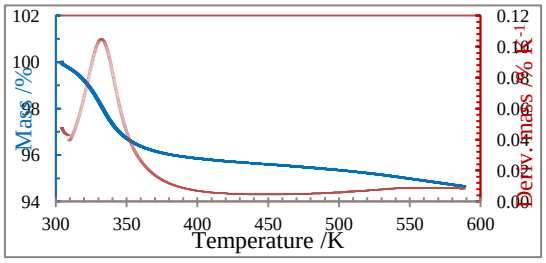

(d)

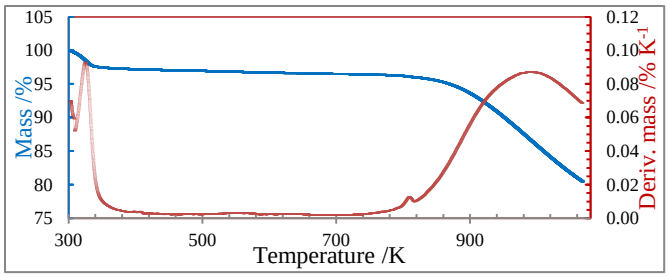

(e)

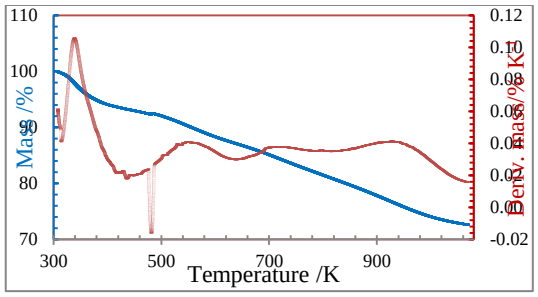

(f)

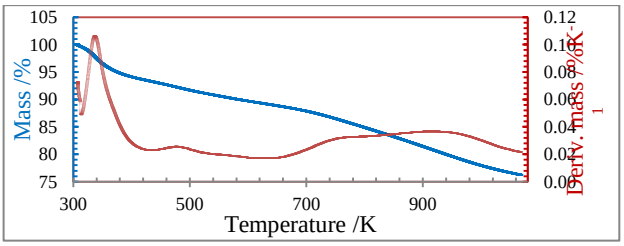

(g)

Figure 3-8: Thermogravimetric analysis of ash samples; (a) Raw ash, (b) Chemically treated ash, (c) Thermal treatment at 330°C, (d) Thermal treatment at 660°C, (e) Thermal treatment at 990°C, (f) Thermochemical treatment followed by HNO_3 itching, and (g) Thermochemical treatment followed by NH_4OH

3.3.6 Thermal Analysis

The results of the DSC analysis for treated and untreated ash samples are shown in Fig. 3.11. All curves show a strong endotherm below 373K. This is likely due to adsorption of water vapor from air just before sample loading and during storage. The endotherm is strong in the case of raw ash which was stored for a longer period of time. The heating above the boiling point of water and holding the temperature at 378K for 3 minutes is assumed to remove the adsorbed water. For raw and thermally treated ash samples, the heating curve was almost flat and did not show any significant variation above 400K. This is true for raw ash and samples treated at 603K (330^{o}C), 933K (660^{o}C) and 1263K (990^{o}C). However, the chemically treated samples showed increase in heat flow (exothermic behavior) above 490K. The sample that was thermochemically treated and then functionalized by NH_4OH showed the highest increase in heat release. This suggests that this treatment was successful in incorporating amine functional groups on the surface of ash.

3.3.7 Effect of the Carbonization Temperature on the Carbon Yield

Activation temperature has a noticeable impact on the characteristics and the yield both OFA and the produced AC. While the increasing carbonization temperature increases the surface area and the pore volume of AC, it has an adverse effect on the yield. Fig.3.9 shows the effect of the ratio of nitric acid to phosphoric acid on the carbon yield. Fig.3.9 (a) shows that in the presence of sulfuric acid the increase in the ratio of HNO_3/H_3PO_4 leads to a decrease in the yield. At lower acid ratios (i.e., $HNO_3/H_3PO_4 < 1$) the carbon yield undergoes a steep decrease. For a sample treated with only nitric and phosphoric

acids increasing the HNO_3/H_3PO_4 ratio from 0 to 1 results in a decrease in the carbon yield from 100 to 60%. The addition of 20 vol. % sulfuric acid into this activation mixture further decreases the yield to 43%. This can be attributed to the burning of some of the carbon atoms in the ash matrix to produce carbon dioxide. A similar trend is observed in the case of thermal treatment, but to a lesser extent especially at higher nitric to phosphoric acid ratios (Fig.3.9 b). The overall yield after both chemical and thermal treatments shows a decrease from 100% to values of 40 to 20% (Fig.3.9 c). There is an inverse correlation between the surface area and the yield, which indicates that increasing the surface area is at the expense of the carbon yield (Fig.3.10). For example, the sample that is thermochemically treated with 20 vol. % H_2SO_4, 40 vol. % HNO_3, and 40 vol. % H_3PO_4 at 990^oC has the highest surface area of 375.69m^2/g and the lowest yield of 20%. In addition, the plot shows a sample with a surface area of ca. 200 m^2/g corresponding to a 60% yield and another with a surface area of ca. 300 m^2/g corresponding to a 35% yield.

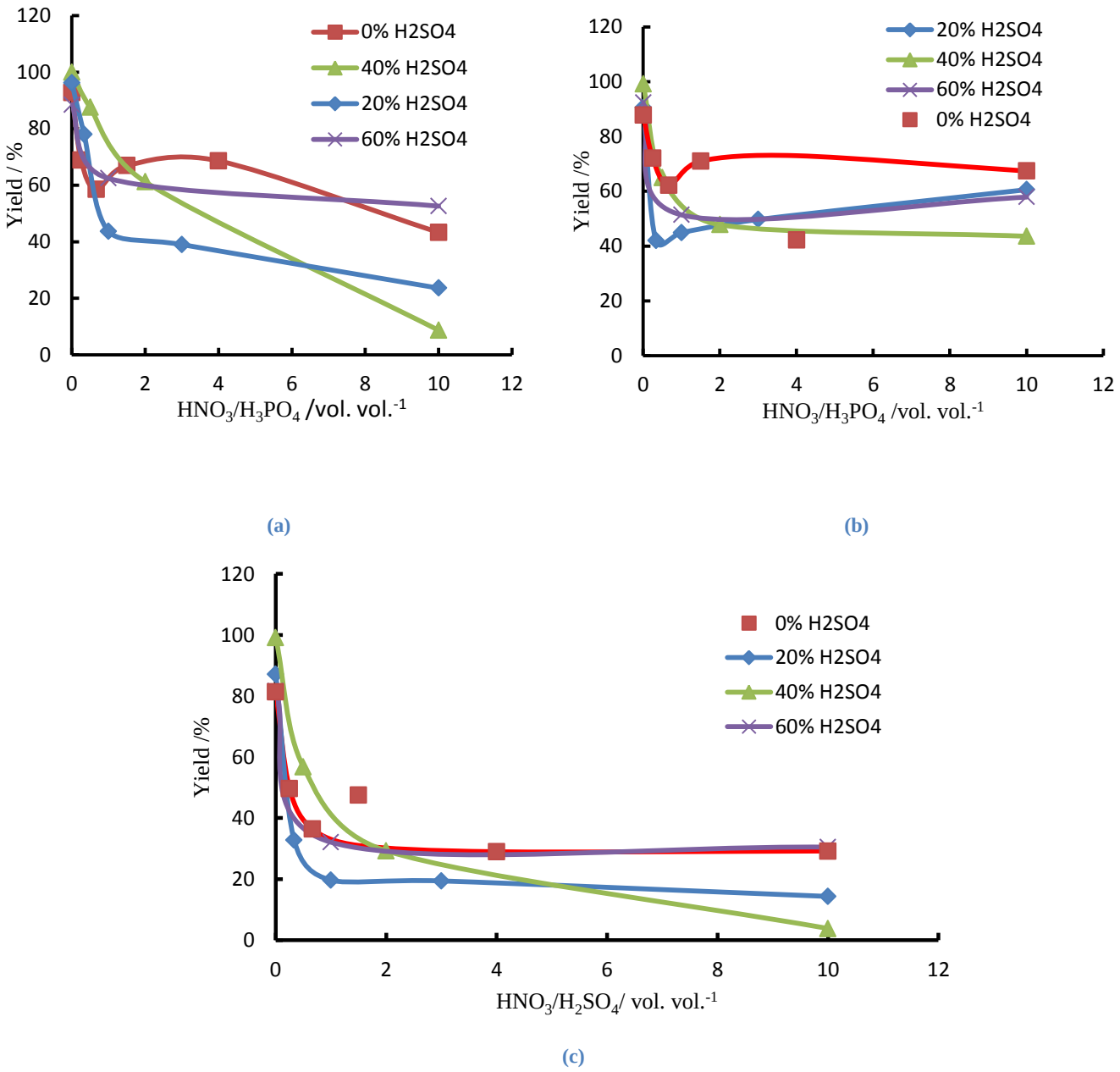

Figure 3-9: Activated carbon yield obtained after successive treatments for OFA; (a) Yield after chemical treatment, (b) Yield after thermal treatment, and (c) Overall yield after both chemical and thermal treatment

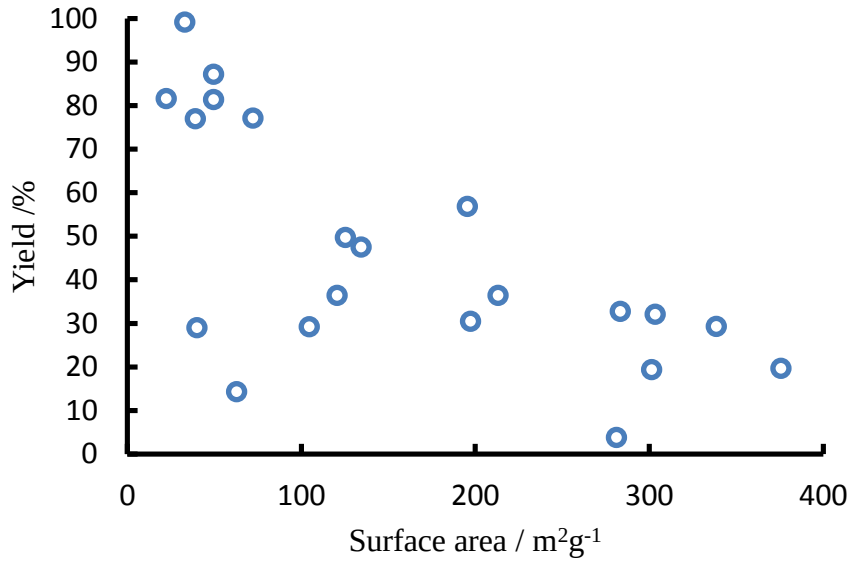

Figure 3-10: Correlation between yield and surface area of activated carbon obtained after different thermochemical treatments at 990°C.

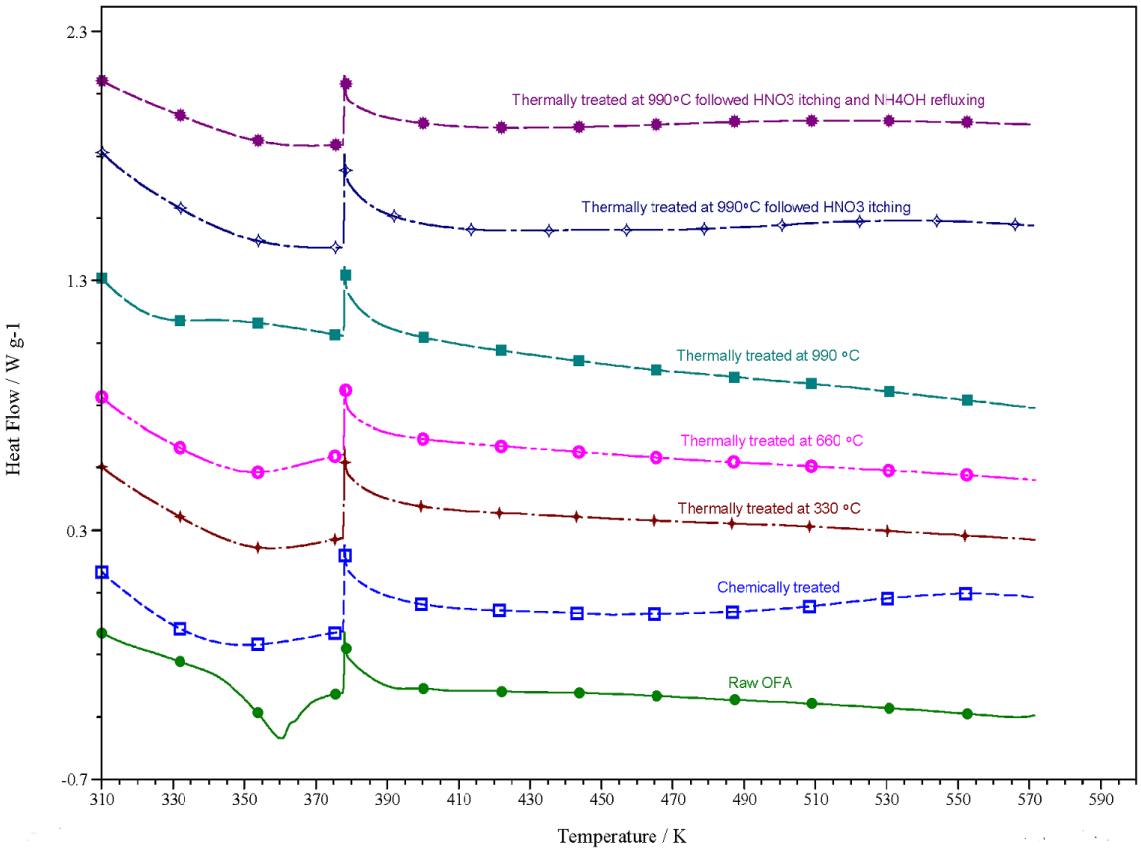

Figure 3-11: DSC (Differential Scanning Calorimetry) of raw and treated ash

3.4 CONCLUSION

Activated carbon was produced from oil fly ash using thermochemical treatment at elevated temperatures. The effect of the composition of the acid mixture was studied and it was observed that more macropores and mesopores are formed. Thermal treatment enhances the generation of micropores. The thermochemical treatment leads to the generation of more micropore and mesopore volumes and hence increases the surface area of the produced AC. An optimum composition of 20 vol. % H_2SO_4, 40 vol. % HNO_3, and 40 vol. % H_3PO_4 for chemical treatment of OFA followed by thermal treatment using CO_2 at 990^oC provides the highest surface area of 375.69m^2/g but the yield is low at 20%. An increase of the concentration of nitric acid results in the decrease of the surface area as a result of pore damage. This trend is also present in thermally treated samples, but with a lesser degree of pore damage. SEM images show that the treatment with acids reduces the size of carbon particles to 5-50 µm and generates pores of varying sizes. Thermochemical treatment results in a total pore volume of 0.3cm^3/g when compared to 0.056cm^3/g achieved before thermal treatment. The percentage of micropores and mesopores increases from 0.9 to 4.5% and 10.7 to 32%, respectively. The waste OFA material is shown to be a potential raw material for the production of activated carbon.

3.5 References

[1] Kandah MI, Shawabkeh R, Al-Zboon MA. Synthesis and characterization of activated carbon from asphalt. Applied Surface Science. 2006;253(2):821-6.

[2] Shawabkeh RA, Al-Harthi M, Al-Ghamdi SM. The synthesis and characterization of microporous, high surface area activated carbon from palm seeds. Energy Sources, Part A: Recovery, Utilization and Environmental Effects. 2014;36(1):93-103.

[3] Shawabkeh R, Rockstraw DA, Bhada RK, inventors; Activated carbon feedstock. USA2001.
[4] Wang X, Li D, Li W, Peng J, Xia H, Zhang L et al. Optimization of Mesoporous Activated Carbon from Coconut Shells by Chemical Activation with Phosphoric Acid. 2013, vol 4. 2013.
[5] Izquierdo MT, Rubio B. Carbon-enriched coal fly ash as a precursor of activated carbons for SO2 removal. Journal of Hazardous Materials. 2008;155(1–2):199-205. doi:http://dx.doi.org/10.1016/j.jhazmat.2007.11.047.
[6] Purnomo CW, Salim C, Hinode H. Effect of the activation method on the properties and adsorption behavior of bagasse fly ash-based activated carbon. Fuel Processing Technology. 2012;102(0):132-9. doi:http://dx.doi.org/10.1016/j.fuproc.2012.04.037.
[7] Mofarrah A, Husain T, Bottaro C. Characterization of activated carbon obtained from Saudi Arabian fly ash. Int J Environ Sci Technol. 2014;11(1):159-68. doi:10.1007/s13762-013-0370-5.
[8]. Rubio B, Izquierdo MT, Mayoral MC, Bona MT, Andres JM. Unburnt carbon from coal fly ashes as a precursor of activated carbon for nitric oxide removal. Journal of Hazardous Materials. 2007;143(1–2):561-6. doi:http://dx.doi.org/10.1016/j.jhazmat.2006.09.074.
[9] Gao Y, Zhang H, Chen J. Vapor-phase sorption of hexachlorobenzene on typical municipal solid waste (MSW) incineration fly ashes, clay minerals and activated carbon. Chemosphere. 2010;81(8):1012-7. doi:http://dx.doi.org/10.1016/j.chemosphere.2010.09.008.
[10] Azhar Uddin M, Shinozaki Y, Furusawa N, Yamada T, Yamaji Y, Sasaoka E. Preparation of activated carbon from asphalt and heavy oil fly ash and coal fly ash by pyrolysis. Journal of Analytical and Applied Pyrolysis. 2007;78(2):337-42. doi:http://dx.doi.org/10.1016/j.jaap.2006.09.004.
[11] Liu Y, Guo Y, Zhu Y, An D, Gao W, Wang Z et al. A sustainable route for the preparation of activated carbon and silica from rice husk ash. Journal of Hazardous Materials. 2011;186(2–3):1314-9. doi:http://dx.doi.org/10.1016/j.jhazmat.2010.12.007.
[12] Wu F-C, Wu P-H, Tseng R-L, Juang R-S. Preparation of activated carbons from unburnt coal in bottom ash with KOH activation for liquid-phase adsorption. Journal of Environmental Management. 2010;91(5):1097-102. doi:http://dx.doi.org/10.1016/j.jenvman.2009.12.011.
[13] Davini P. Behaviour of activated carbons obtained from mixtures of oil-fired fly ash and oil refining pitch. Carbon. 2003;41(8):1559-65. doi:http://dx.doi.org/10.1016/S0008-6223(03)00104-0.
[14] Mishra SB, Langwenya SP, Mamba BB, Balakrishnan M. Study on surface morphology and physicochemical properties of raw and activated South African coal and coal fly ash. Physics and Chemistry of the Earth, Parts A/B/C. 2010;35(13–14):811-4. doi:http://dx.doi.org/10.1016/j.pce.2010.07.001.
[15]D e Lima LS, Quináia SP, Melquiades FL, de Biasi GEV, Garcia JR. Characterization of activated carbons from different sources and the simultaneous adsorption of Cu, Cr, and Zn from metallurgic effluent. Separation and Purification Technology. 2014;122(0):421-30. doi:http://dx.doi.org/10.1016/j.seppur.2013.11.034.

[16] Mandal PK, Mandal TK. Electrostatic precipitator performance in Indian pulverized coal based thermal power stations - problems and solutions. Water Energy Res Dig. 1996;19(4):31-40.
[17] Seaton NA. Characterization of porous solids III Edited by J. Rouquerol, F. Rodriguez-Reinoso, K. S . W. Sing & K. K.Unger, Elsevier Science, Amsterdam, 1994, xiv + 802 pp., US$265.50. ISBN 0 444 81491 4. Journal of Chemical Technology & Biotechnology. 1996;65(1):106-. doi:10.1002/(sici)1097-4660(199601)65:1<106::aid-jctb7361>3.0.co;2-n.
[18] Jagtoyen M, Groppo J, Derbyshire F. Activated carbons from bituminous coals by reaction with H3PO4: The influence of coal cleaning. Fuel Processing Technology. 1993;34(2):85-96. doi:http://dx.doi.org/10.1016/0378-3820(93)90093-J.
[19] Yakout SM, Sharaf El-Deen G. Characterization of activated carbon prepared by phosphoric acid activation of olive stones. Arabian Journal of Chemistry. (0). doi:http://dx.doi.org/10.1016/j.arabjc.2011.12.002.
[20] Hsu L-Y, Teng H. Influence of different chemical reagents on the preparation of activated carbons from bituminous coal. Fuel Processing Technology. 2000;64(1–3):155-66. doi:http://dx.doi.org/10.1016/S0378-3820(00)00071-0.
[21]. Baquero MC, Giraldo L, Moreno JC, Suárez G, amp, x et al. Activated carbons by pyrolysis of coffee bean husks in presence of phosphoric acid. Journal of Analytical and Applied Pyrolysis. 2003;70(2):779-84. doi:http://dx.doi.org/10.1016/S0165-2370(02)00180-8.
[22] Bazuła PA, Lu A-H, Nitz J-J, Schüth F. Surface and pore structure modification of ordered mesoporous carbons via a chemical oxidation approach. Microporous and Mesoporous Materials. 2008;108(1–3):266-75. doi:http://dx.doi.org/10.1016/j.micromeso.2007.04.008.
[23] Herawan SG, Hadi MS, Ayob MR, Putra A. Characterization of Activated Carbons from Oil-Palm Shell by CO2 Activation with No Holding Carbonization Temperature. The Scientific World Journal. 2013;2013:6. doi:10.1155/2013/624865.
[24] Malarvizhi TS, Santhi T. Lignite fired fly ash modified by chemical treatment for adsorption of zinc from aqueous solution. Res Chem Intermed. 2013;39(6):2473-94. doi:10.1007/s11164-012-0774-8.
[25] Shafeeyan MS, Daud WMAW, Houshmand A, Shamiri A. A review on surface modification of activated carbon for carbon dioxide adsorption. Journal of Analytical and Applied Pyrolysis. 2010;89(2):143-51. doi:http://dx.doi.org/10.1016/j.jaap.2010.07.006.
[26] Shin Y-R, Jung S-M, Jeon I-Y, Baek J-B. The oxidation mechanism of highly ordered pyrolytic graphite in a nitric acid/sulfuric acid mixture. Carbon. 2013;52(0):493-8. doi:http://dx.doi.org/10.1016/j.carbon.2012.10.001.
[27] B. Shrestha, J. Kour, P.L. Homagai, M.R. Pokhrel, K.N. Ghimire. Surface Modification of the Biowaste for Purification of Wastewater Contaminated with Toxic Heavy Metals- Lead and Cadmium. , Adv Chem Eng Sci. 2013; 3: 178–84.
[28] Morkel J, Kruger S, Vermaak M. Characterization of clay mineral fractions in tuffisitic kimberlite breccias by X-ray diffraction. The Journal of The South African Institute of Mining and Metallurgy. 2006;106.

CHAPTER 4

Synthesis of Activated Carbon from Oil Fly Ash for Removal of H_2S from Gas Stream

This paper was published in Applied Surface Science on February 1, 2015

4.1 Introduction

Hydrogen sulfide is one of the major pollutants. The presence of H_2S in natural gas results in major corrosion and environmental problems. Hydrogen sulfide is toxic and most harmful toxin gas for human and animals. It becomes fatal when its concentration exceeds 500 ppm [1–4]. On the other hand, the presence of H_2S at concentrations higher than 5.5 mg/m^3in natural gas leads to sulfur stress cracking that reduces life of processing and handling equipment. To overcome these adverse effects, several commercial technologies have been used forH_2S removal from natural gas. Amine sweetening process is widely used in industries to lower the concentration of $H_2S$to the target level imposed by customers and downstream processors[5,6]. This method is costly in term of heat required for regeneration and also produces unwanted by-products. Other treatment processes, such as membrane separation and biological treatment, either suffer from low selectivity or they are not feasible at the larger scales [7]. Adsorption, on the other hand, can be used to capture H_2S at trace levels with relatively low cost of adsorbent. This process becomes especially attractive option when an adsorbent material, such as oil fly ash (OFA), is available in large quantities and for low cost. This OFA is by-product of many industrial and power generation plant operations[8]. OFA usually causes environmental pollution problems and requires safe disposal. Therefore, utilization of waste OFA in removing H_2S is expected to solve more than one environmental problem. The adsorption capacity of a material largely depends on its surface area. Generally, the higher specific surface area of an adsorbent results in the higher uptake capacity.

Since OFA is pozzolanic in nature, it contains mainly unburned carbon (~80%) with some inorganic oxides like SiO_2, Fe_2O_3, Al_2O_3, and CaO and traces of heavy metals[9].

According to a survey conducted by American Coal Ash Association (ACAA) over 100 million tons of coal combustion products were produced in 2012, where only 38% of total coal combustion products were used beneficially [10]. However, utilization rate of fly ash has increased greatly in China reaching up to 67% in 2010 compared to 20% rate in 1999[11]. Majority of fly ash is used in blended cements, filler for metal matrix composites, as raw material for metal recovery and as filler for polymers [12–18].Recently, OFA has gained particular attention as potential adsorbent for several adsorbate due to its high carbonaceous contents and low cost [19–21]. Izquierdo et al studied SO_2 removal using activated carbon (AC) produced from oil agglomerated coal fly ash. They compare the adsorption efficiency of anthracite coal based fly ash activated carbon with bituminous-lignite blended coal fly ash activated carbon and concluded that the latter is superior with 28mg/g uptake capacity [21]. With some chemical treatment, the porosimetric characteristics of ash may be enhanced to obtain a high surface area AC. Thus obtained, AC can be used to remove pollutants from flue gas. Our group used treated OFA for the adsorption of CO_2 under different flow conditions. A removal capacity of 240mg CO_2/g-treated OFA was achieved. The interactions between CO2and ash surface were reported to be endothermic in nature [19, 20].

Various treatment strategies could be implemented to increase the porosity and create some ordering of structure like in the synthesis of Zeolites [22–25]. For example, external heating of fly ash with acid mixture involves various sulfonation and nitrification reactions including the formation of phosphate functional groups. As a result oxides of sulfur and nitrogen and carbon dioxide are released during the chemical activation

process [26, 27]. Treatment of fly ash with acids also introduces hydrophilic groups like carboxylic and hydroxyl groups on the surface of ash [28].

Several kinds of carbon based adsorbents have been employed to capture H_2S from gas stream. These adsorbents include agro based activated carbon[29,30], coal based and impregnated activated carbon[31,32].The use of fly ash as a precursor of activated carbon is advantageous due to abundant availability and one step activation procedure as compared to conventional production of activated carbon by two step activation. The literature on the utilization of OFA in the removal of $H_2S$from natural gas is scarce. Therefore, the objective of this study is to investigate the synthesis of AC from OFA and its application in the removal of H_2S from natural gas. This objective will be achieved by successive chemical and physical treatments of OFA at different conditions using activation agents. The efficiency of such physico-chemical activation will strongly influence the potential of using OFA as a cheap source for AC for application in H_2S gas removal from natural gas.

4.2 Materials and Methods

4.2.1 Materials

Synthetic natural gas containing 50 ppm H_2S in methane was supplied by Saudi Gas Company. The Pyrex glass ware was washed with demineralized water and dried in the oven at 105°C. Other Chemicals used are explained in Section 3.2.1.

4.2.2 Activation of Oil Fly Ash

The activation procedure was same as explained in the Section 3.2.2 & 3.2.3.

4.2.3 Treatment with NH4OH and HNO3

Explain in the section 2.2.4.

4.2.4 Characterization of Activated OFA

4.2.4.1 Surface area and pore size determination

Micrometrics ASAP 2020 instrument was used to determine the BET surface area pore volume and other surface properties of sample like pore size distribution. A sample of 0.43gtreated OFA was degassed at 573K for 2h under vacuum, and then N2 gas was adsorbed-desorbed at 77K.Micro-pore volume was determined by the t-plot method[33].

4.2.4.2 Surface morphology

AJEOL Scanning Electron Microscopy (Model JSM6400) in conjunction with Energy Dispersive Spectrophotometer (EDX) operated with 15kV accelerating voltage was used to analyze the morphology of ash samples. Each sample was coated with a thin layer of gold before the analysis. Elemental composition of the sample was determined by analyzing the X-ray spectrum generated through spot analysis**.**

4.2.4.3 FTIR measurements

Presence of functional groups at the surface of activated OFA was analyzed using FPC FTIR Perkin Elmer spectrophotometer. A sample of 1.0g of AC ash was mixed with 1.0g of KBr powder and hydraulically pressed at10 Ton/m2 to prepare a thin uniform pellet. The pellet was oven dried at 110°C to prevent any interference with moisture. All FTIR spectrums were obtained in the transmission mode.

4.2.5 H2S breakthrough experiments

An adsorption column (length = 12cm, I.D = 1cm) connected with N_2 and CH_4/H_2S gas cylinders, was used for break through adsorption/desorption experiments (Fig.4.1). The column was packed with 2.0g treated OFA sample. Initially, the column was purged with N_2 at a flow rate of 0.4 L/min for 15 min. Then a gas mixture containing 50ppm H_2S and CH_4 as balance was introduced to the column at 0.4 L/min, 20% RH at 22^oC and 1 atm pressure. Exit H_2S concentration was continuously monitored by MultiRAE IR sensor every 2s until reaching the saturation. Some gas samples were analyzed using GC-MS spectrophotometer to check the reliability of the gas meter. After the completion of the adsorption cycle the valve was switched to N_2 at 1 atm to start desorption cycle. The concentration of H_2S in the exit gas was measured continuously and stopped when the exit concentration of H_2S reaches zero ppm. The adsorption capacity was calculated from adsorption run using equation 4.1.

$$q = \frac{C_o \times F}{M} \int_0^{t_e} \left(1 - \frac{C}{C_o}\right) dt \qquad (4.1)$$

Where q = equilibrium adsorption capacity, mg/g

t_e = exhaust/saturation time of adsorbent.

C_o& C = Initial and concentration at time t, respectively, mg/cm^3

F = gas mixture flow rate, L/min

M = mass of adsorbent, g

t = time, min

The adsorption capacity after the desorption process was calculated using the area between adsorption and desorption curves. This capacity is the working capacity of the

column. In this way we can define the regeneration efficiency (RE) of the column for the given dimension as follows:

$$RE\ (\%) = \frac{\text{Capacity after desorption}}{\text{Capacity before desorption}} \times 100 = \frac{q_{de}}{q_{ad}} \times 100 \qquad (4.2)$$

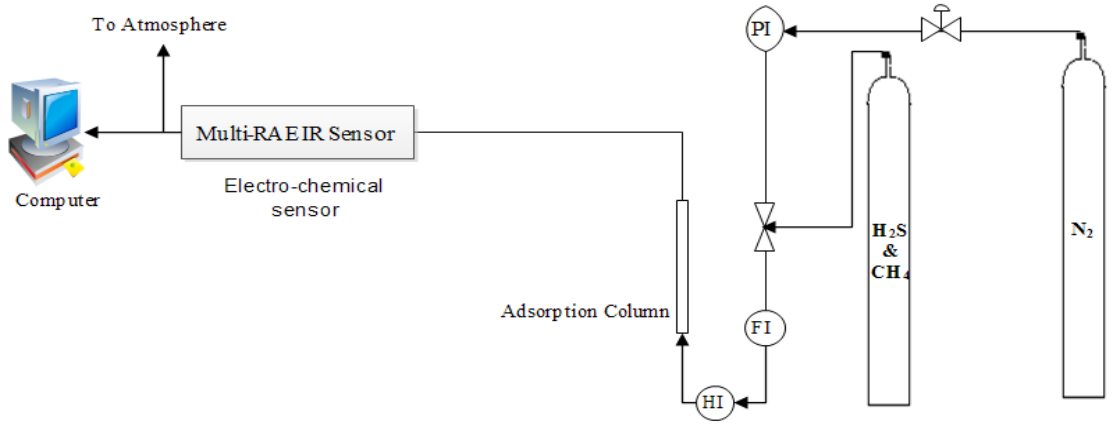

Figure 4-1: Experimental setup for H_2S breakthrough adsorption/desorption measurements (PI: Pressure Indicator, FI: Flow meter, HI: Humidity Indicator)

4.3 Results and Discussion

4.3.1 Synthesis and Characterization of AC

The activation of OFA with acid affects the porosity of ash compared to the raw material. The BET surface areas were determined from N_2 adsorption isotherms at 77K.Table 4.1summarizes the results of BET analyses after acid and physical treatment with CO_2. The acid treatment of OFA has leached out almost all major inorganic matter and increases the porosity. The surface area of acid treated OFA depends on the oxidation ability of the acid mixture. Based on O/H ratio in the chemical formula of the acid, the oxidation tendency of the acid increases according to the order HNO_3> H_2SO_4> H_3PO_4. Chemical treatment with mixtures of HNO_3/H_3PO_4 (without H_2SO_4) generates the highest

surface area corresponding to 57.34m^2/g compared to single individual acid treatment. The incorporation of H_2SO_4 increases the degree of oxidation of the surface and makes the pore walls thinner thus easily damaged by HNO_3. As a result micropores get enlarged to mesopores and consequent diminishing of surface area values. For a combination of H_3PO_4/H_2SO_4, the acid treatment of ash experienced a very small weight loss of 0.1% as compared to other combinations and produces 0.66 m^2/g BET surface area except for only H_2SO_4 for which surface area is 8.41 m^2/g. This may be attributed to damage of pore structure or the formation of phosphate layer which covers the pore structure [34]. When ash was treated with a strong oxidizing mixture, consisting of only HNO_3/H_2SO_4 the weight loss was 91.3%. This shows strong oxidation conditions can destroy the carbon structure and pose a negative impact, results in decreasing the surface area to a value less than that of raw OFA (i.e.2.63 m^2/g).

Surface activation with the three acids at different volume ratios produced higher values of surface area compared to untreated OFA. Different acid compositions have different impact on weight loss of OFA. However, OFA treated with higher ratio of HNO_3/H_2SO_4mixture showed a higher degree of weight loss in comparison with

H_3PO_4/H_2SO_4. Raw OFA samples treated with a combination of the three acids generated the higher surface areas after CO_2 activation. Samples having surface area greater than 250m^2/g experienced a burn-off greater than 50%. This shows that the surface of OFA treated with more oxidizing mixture is more prone to the reaction of CO_2 with carbon that is essential in generating micro porosity, which leads to an increase of the surface area. Out of all different acid formulations covered in this study, OFA sample activated with 20% H_2SO_4, 40% HNO_3 and 40% H_3PO_4(i.e. sample # 4) generated the highest surface

area (~375.69m^2/g)after CO_2 activation as shown in the table 2. Consequently, OFA samples treated with this acid composition are further characterized for pore size distribution.

Table 4–1: Impact of Physicochemical Treatment on BET surface areas

No.	Percentage of acids			Chemical Treatment		CO_2 Activation	
	H_2SO_4	HNO_3	H_3PO_4	Weight Loss (%)	BET surface area (m^2/g)	Burn off (%) after CO_2 activation	BET surface area (m^2/g)
1	0	0	100	7.3	1.40	12.2	49.60
2	0	40	60	41.5	57.34	37.8	120.59
3	0	100	0	56.7	19.02	32.6	104.61
4	20	40	40	56.3	4.05	55.1	375.69
5	40	0	60	0.1	0.66	0.8	33.07
6	40	20	40	12.5	4.14	35.1	195.52
7	40	60	0	91.3	1.23	56.4	281.22
8	100	0	0	20.5	8.41	3	72.15
9	0	0	0	-	2.63	5.61	7.49

Figure 4.2 shows the pore size distribution for ash samples before and after treatment with acid mixture of 20%H2SO_4, 40%HNO_3 and 40%H_3PO_4. The original ash sample has low pore size distribution and the pore volume increases with the increase in pore width. The total pore volume is related to the macropores for raw ash. Activation with acid mixture has increased the mesopore volume and decreases the macropores with an increase of total pore volume of 0.0257cm^3/g over the original ash sample. Further treatment with CO_2 at 990^oC has opened up more micro and mesopores while macropores

has decreased with an average mesopore size of 50 A°. When the sample was treated with CO_2 at elevated temperatures micropores were generated with an average pore size of 50 Å compared to 109 Å obtained after acid treatment. Functionalization of selected samples with HNO_3 has increased the pore size to 54 Å but the surface area decreased to 39 m^2/g from its original value of 375m^2/g. This could be attributed to the damage of the pore network by generating aggregation and alignment in the ash structure. Subsequent surface modification of selected sample with HNO_3 and NH_4OH enlarged some of the micropores to produce more mesopores as shown in Table 4.2

Surface area has been reduced from 375 m^2/g of $AC_{acid\text{-}CO2}$ to 80 m^2/g and 39 m^2/g during functionalization with NH_4OH and HNO_3, respectively. This is likely due to the decrease in pore volume. High surface area of $AC_{acid\text{-}CO2}$ allows both (NH_4OH & HNO_3) functionalizing agents to penetrate inside and react readily with carbon particles. The total pore volume (Table 4.2) of $AC_{acid\text{-}CO2\text{-}NH4OH}$ and $AC_{acid\text{-}CO2\text{-}HNO3}$ is higher than that of $AC_{acid\text{-}CO2}$ which is due to higher meso and macro porosity. Consequently, the average pore size decreased from 280˚A to 53˚A and 54˚A for $AC_{acid\text{-}CO2\text{-}NH4OH}$ and $AC_{acid\text{-}CO2\text{-}HNO3}$, respectively.

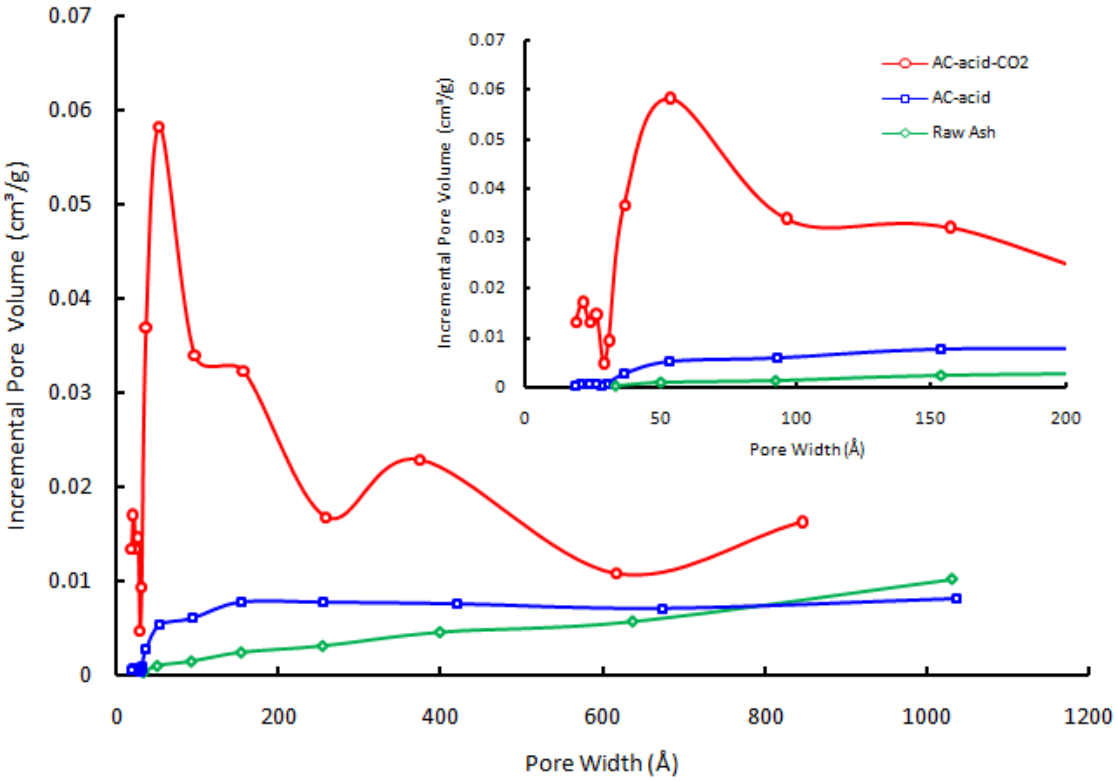

Figure 4-2: Pore size distribution of ash sample before and after treatment.

Table 4–2: Textural properties of sample # 04 at different stages of activation and functionalization

Sample ID	S_{BET} (m^2/g)	t-plot micro-pore Volume, V_{micro}, (cm^3/g)	Total Pore Volume, $V_{0.99}$, (cm^3/g)	*V_{meso} (cm^3/g)	Average Pore Size (4v/A) (Å)
Raw OFA	2.63	0	0.03	0.03	280
AC_{acid}	4.05	0.0010	0.0557	0.0547	109
$AC_{acid\text{-}CO2}$	375.69	0.0791	0.3002	0.2211	50
$AC_{acid\text{-}CO2\text{-}NH4OH}$	80.27	0.0672	0.3895	0.3223	53
$AC_{acid\text{-}CO2\text{-}HNO3}$	39.03	0.0600	0.3530	0.2930	54

* $V_{meso} = V_{0.99} - V_{micro}$, AC = Activated Carbon

The EDX results of selected OFA treated samples are summarized in Table 4.3. The results show increase in oxygen to carbon ratio due to the leaching of some elements from raw OFA. Sulfur is reduced from 7.1% to 0.51 wt% after acid treatment. The possible reasons are either oxidation of sulfur to SO_2 or the removal of free elemental sulfur during the washing step or a combination of these two processes. Sulfur dioxide is produced due to the strong interaction of HNO_3withsulfate and pyrite sulfur in untreated OFA [9]. Subsequent CO_2 activation of acid treated ash breaks up some carbon bonding from the structure of ash and produces gaseous CO and carbon surface with oxygen chemisorbed on to it known as "surface-oxygen complex". Under the reaction conditions, surface-oxygen complex may either become stable and inhibit further reaction of CO_2 with carbon surface by blocking the reaction sites or it decomposes to CO leaving a free surface carbon atoms available for further reaction [35].

Table 4–3: Average Atomic composition of sample # 4 after the activation of OFA

Element	AC_{acid}	$AC_{acid-CO2}$	$AC_{acid-CO2-NH4OH}$	$AC_{acid-CO2-HNO3}$
Carbon (%)	79.43	95.71	96.79	83.61
Oxygen (%)	20.06	3.35	1.67	15.77
Sulfur (%)	0.51	0.93	1.54	0.62
O/C	0.252	0.035	0.017	0.188
Weight Loss (%)	56.2	55.1	11	35

*AC = 'AC' stands for Activated Carbon and subscript shows the activation procedure

4.3.2 Morphology

SEM images (Fig.3.6) show that ash particles are composed of spheres, spheroids, and some agglomerates, and mostly are porous in nature. The size of ash particles varies from few to several microns. Similar values were also reported in the previous studies [36,37]. SEM analysis of raw sample (Fig. 3.6(a)) depicts the large cenospheres which are mixed with aggregates of particles. The pores are clearer and randomly located at the surface. Some pores of macro range can also be seen. After chemical treatment with the acid mixtures most of the metallic constituents are removed from the external surface and are at lower concentration inside the cenospheres. These observations are consistent with the tabulated data obtained from EDX spot analysis (Table4.3). An increase in oxygen content is due to oxidation of OFA while the percentage of sulfur is very low and all other minerals are removed. Presence of sulfur in the acid treated sample shows bonding with carbon inside the cenospheres. Some broken fly ash particles can also be seen due to the strong attack of concentrated mixture of acids. Physical activation has a significant influence on the porosity development and all the particles contain micro- and mesopores (Fig.3.6(c)). Similar results were obtained for AC prepared from coal fly ash[37,38].Functionalizing the selected sample with NH_4OH blocks some of the micropores and produces more mesopores as shown in the fig. 3.6(d) while the action of HNO_3 broke the activated carbon particles (Fig.3.6(d)) and severely affect the porosity as can also be seen from Table 4.2.

Spot analysis of selected sample was done to determine the percentage of carbon, oxygen and sulfur. Oxygen to carbon ratio shows the degree of oxidation after each activation process (Table 4.3). It is evident that the percentage of sulfur depends on the degree of

oxidation as oxygen replaces sulfur on the surface of OFA [39]. On the other hand, physical activation with CO_2at high temperature decreases oxygen to carbon ratio since all functional groups will leave the surface at high activation temperature. Subsequent surface modification of selected sample #4 with either NH_4OH or HNO_3 shows different behavior against each functionalizing agent as shown in the Table 4.3.

The heating of $AC_{acid\text{-}CO2}$ with ammonium hydroxide increases the basicity of activated carbon by introducing nitrogen containing groups to carbon surface. In addition, post treatment of $AC_{acid\text{-}CO2}$ with HNO_3 leads to oxidation of carbon at the surface. The decrease in O/C ratio in $AC_{acid\text{-}CO2\text{-}NH4OH}$in comparison with $AC_{acid\text{-}CO2}$ supports this fact. Post treatment of $AC_{acid\text{-}CO2}$ with HNO_3leads to oxidation of carbon at the surface. This is confirmed by the increase of O/C ratio from 0.035 to 0.188as shown in Table 4.3. FTIR studies were performed to confirm the nitrogen and acidic containing functional groups on the surface of $AC_{acid\text{-}CO2\text{-}NH4OH}$and $AC_{acid\text{-}CO2\text{-}HNO3}$, respectively. Due to the intense oxidation conditions during HNO_3functionalization, the material has experienced a higher weight loss as compared to treatment of $ACacid_{\text{-}CO2}$ with ammonium hydroxide.

4.3.3 FTIR Analysis

FTIR analysis was performed to determine the type of functional groups and their intensities on the surface of OFA. Each sample was scanned from $500cm^{-1}$ to $4000cm^{-1}$and the percentage of transmission was examined (Fig.3.5). A broad band appears between $3100\text{-}3550cm^{-1}$ for raw OFA with a minimum at $3430cm^{-1}$. This is due to stretching vibration of free and associated hydroxyl groups (-OH) on the virgin ash. In raw OFA, the peaks at $1625cm^{-1}$ and $1115cm^{-1}$ between $1100\text{-}1650cm^{-1}$ may be due to conjugated hydrocarbon bonded carbonyl (C=O) group stretching and C-O stretching,

respectively[40]. It is shown that broad peak centered at 3430cm^{-1}remains even after acid treatment of fly ash (i.e. Fig. 2.5(b)) and subsequent CO_2 activation of acid treated fly ash (i.e. Fig. 4(c)). Two peaks can be observed for AC_{acid} at 1715cm^{-1}, 1625cm^{-1}which correspond to carbonyl (C=O) and C=C group stretching respectively. The peak at 1115cm^{-1} in Fig.3.5(a) shifts to 1230cm^{-1} after acid treatment (Fig.3.5 (b)) due to aryl association and can be assigned to C–OH stretching vibrations[41]. Two Consecutive small peaks in Fig.3.5(c) at 2924cm^{-1} and 2854 cm^{-1} correspond to asymmetric and symmetric C-H stretching in aliphatic compounds, respectively. The peak at 1230cm^{-1} for AC_{-acid} shifts back to low wavenumber at 1115cm^{-1}in $AC_{acid-CO2}$. But this new peak in $AC_{acid-CO2}$ has less intensity than the same peak in raw ash. This may be attributed to alkyl substituted C-O stretch. The existence of these groups is likely due to the reaction of CO_2 with carbon structure. Further activation of $AC_{acid-CO2}$ with either HNO_3 or ammonium hydroxide produces different FTIR spectrum as shown in the Fig.3.5(d) and 4(e), respectively. Oxidation of $AC_{acid-CO2}$with nitric acid leads to the disappearance of the peaks at wavenumbers higher than 2000cm^{-1}.A broad band at 1580cm^{-1} in the $AC_{acid-CO2-HNO3}$ is assigned to stretching of aromatic ring coupled to highly conjugated carbonyl groups [42]. A wide band between 1000cm^{-1} to 1250cm^{-1} in $AC_{acid-CO2-HNO3}$cannot be assigned to a single group due to superimposed overlapping of bands. Some researchers' assigns this wide band as C-O stretching vibrations in ether and phenolic structures present in different structural environments [42–44].On the other hand, ammonium hydroxide treatment of $AC_{acid-CO2}$ produces four major peaks at 3330cm^{-1}, 2335cm^{-1}, 1590cm^{-1}, and 1100 cm^{-1} as shown in Fig.3.5(e). These peaks can be assigned to amine (–NH–) stretching, –C≡N, –NH– bending vibrations and C-N stretching vibrations,

respectively [45–48]. Yofa et al reported similar results for AC prepared from rice straw [49]. Therefore, the FTIR results support and explain the previous findings on O/C ratio due to HNO_3 and NH_4OH treatments.

4.3.4 H_2S Breakthrough measurements of adsorption bed packed with activated OFA

Small pore size, large surface area and basic surface functional groups play an important role in the adsorption of acidic gas molecules[50]. Figures 4.4-4.6 show the breakthrough curves of columns packed with different AC adsorbents. The adsorbents were produced through different physicochemical activations and surface modifications of OFA. Breakthrough times and equilibrium capacities of raw and activated OFA samples were calculated and the results are given in Table 3.4. OFA activated with the mixture of three acids and raw OFA show approximately the same (very short) breakthrough times (Table 4.4), but the adsorption and desorption curves are quite different from each other as shown in Fig.4.4. It is expected that H_2S is strongly attached to raw OFA surface due to the strong host/guest attractions in the presence of mineral matter. However, after acid treatment of raw OFA sample, the surface is oxidized through formation of acidic carbonyl functional groups. The oxidized surface would likely give **a** rise to repulsive surface forces relative to H_2S. Hence, the tendency of the adsorption–desorption process would be almost physical for AC_{acid} compared to raw OFA sample (Fig.4.4).

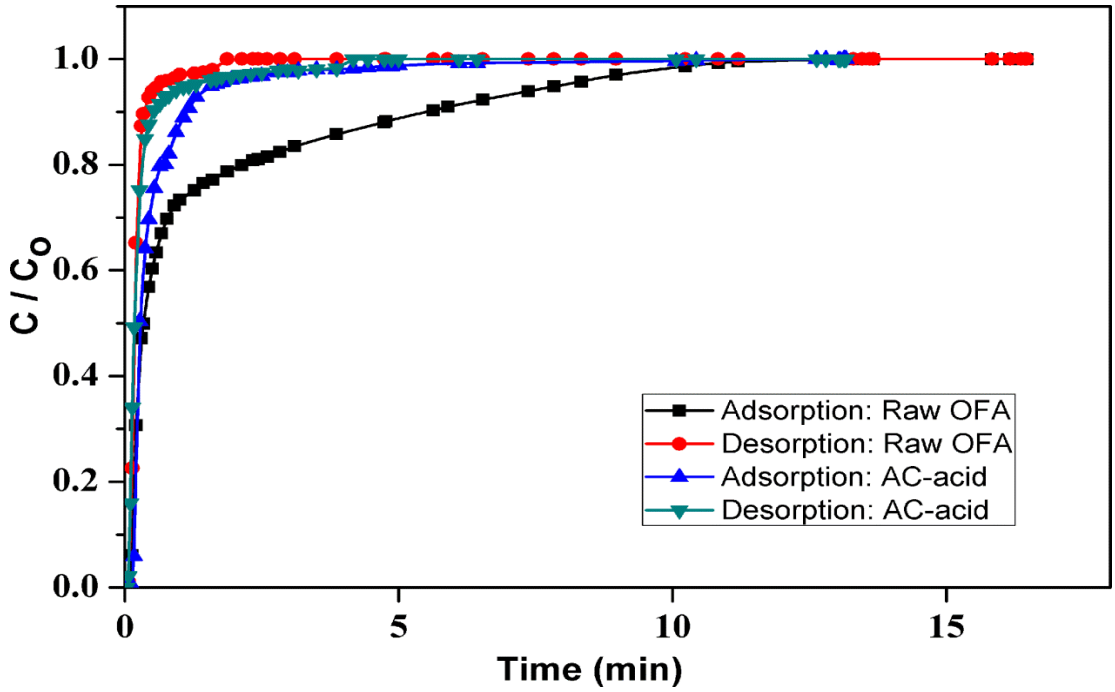

Figure 4-3: Adsorption-Desorption breakthrough curves for Raw OFA and after Acid treatment (Pressure = 1atm, Temperature = 22°C, Relative Humidity = 20%, Flow rate = 0.4L/min).

The H_2S breakthrough test with $AC_{acid\text{-}CO2}$ shows that the adsorbed amount of H_2S has increased (Fig.4.5).The same figure also shows desorption curve**.** The desorbed amount can be viewed as physically attached to the surface of OFA during the adsorption step, while retained amount can be considered as chemically adsorbed. According to BET analysis shown in the previous section, the surface area, micro pore volume and total basicity increases and all acid groups vanished at higher temperature during CO_2activation. The decrease in the desorbed amount can be explained on the basis of Micro Pore filling theory. The theory which states that pores of smaller diameter will adsorb more solute at lower concentration because of higher adsorption potential exerted by the walls[51].

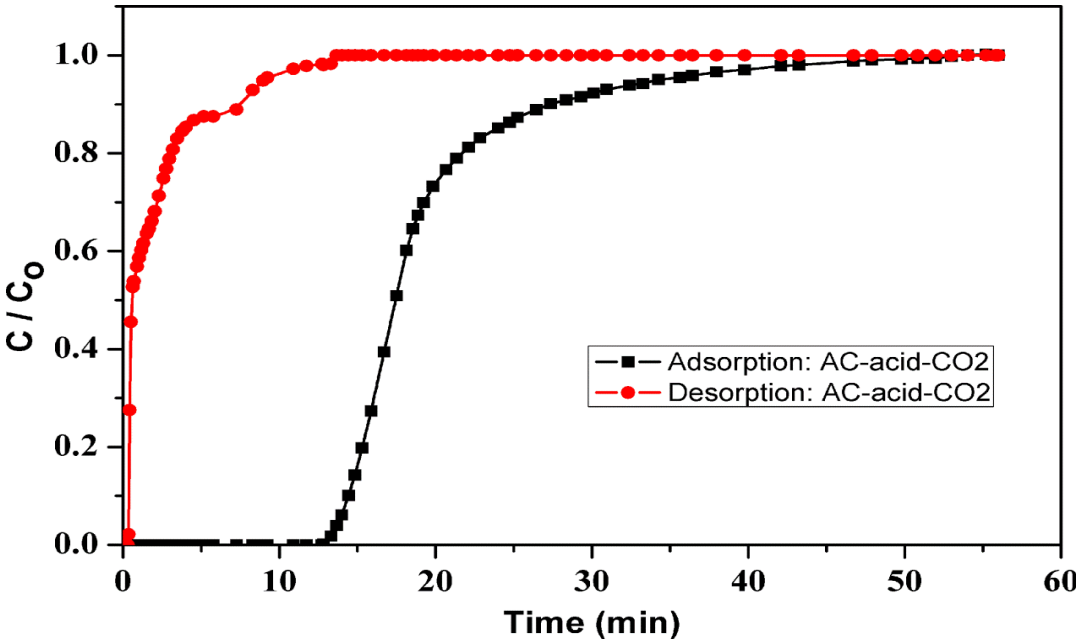

Figure 4-4: Adsorption-Desorption breakthrough curves after physic-chemical treatment of OFA (Pressure = 1atm, Temperature = 22°C, Relative Humidity = 20%, Flow rate = 0.4L/min)

Table 4–4: Equilibrium capacity and break-through time of H_2S after conducting adsorption tests

Sample type	Equilibrium capacity (mg/g)	Adsorption capacity left after desorption (mg/g)	Regeneration efficiency (%)	Break Through Time (sec)
Raw OFA	0.0231	0.0192	83.41	6
AC_{acid}	0.0088	0.0036	40.96	8
$AC_{acid\text{-}CO2}$	0.2966	0.2639	89.00	770
$AC_{acid\text{-}CO2\text{-}NH4OH}$	0.3001	0.2594	86.43	450
$AC_{acid\text{-}CO2\text{-}HNO3}$	0.1035	0.0573	55.34	36

Figure 4.6 shows the H_2S breakthrough results for NH_4OH and HNO_3 treated $AC_{acid\text{-}CO2}$ samples. Ammonium hydroxide treatment of previously developed activated carbon i.e. $AC_{acid\text{-}CO2}$ gives almost the same result as$AC_{acid\text{-}CO2,}$ although the surface area is reduced for $AC_{acid\text{-}CO2\text{-}NH4OH}$sample. This can be attributed to the nitrogen functionalities attached to the surface of carbon. As compared to NH_4OH treatment, HNO_3 treatment again increases the oxidation of the surface, which in turn reduces the equilibrium capacity of H_2S. More acidic surface of adsorbent inhibits the dissociation of H_2S, hence decreases the concentration of hydrogen sulfide ions. Low concentration of these ions promotes the formation of high-valent sulfur compounds like SO_2 and sulfuric acid which leads to low H_2S removal capacity. On the other hand, adsorbent surface with pH in the basic range favors the dissociation of H_2S to hydrogen sulfide ions, i.e., HS^-. These ions are oxidized to form sulfur polymers having ring or chain like shape yielding higher H_2S removal capacities[51–54].

Regeneration efficiency was calculated for different AC samples using equation 4.2 and the results are given in Table 4.4. It is essential to effectively regenerate loaded adsorbent in industrial applications (such as pressure swing adsorption) for economic feasibility of the process. Regeneration efficiency is an indicator of reusability of any sorbent. Table 4.4 shows that regeneration efficiency of raw OFA sample is ~83%. Both the equilibrium capacity and regeneration efficiency of AC_{acid} are the lowest compared to all other samples. The reason behind this observation is already mentioned that this sample possess repulsive functional groups on its surface. However, activation of this sample by CO_2 at high temperature increases both the capacity and regeneration efficiency, which can lead to a potential commercial application.

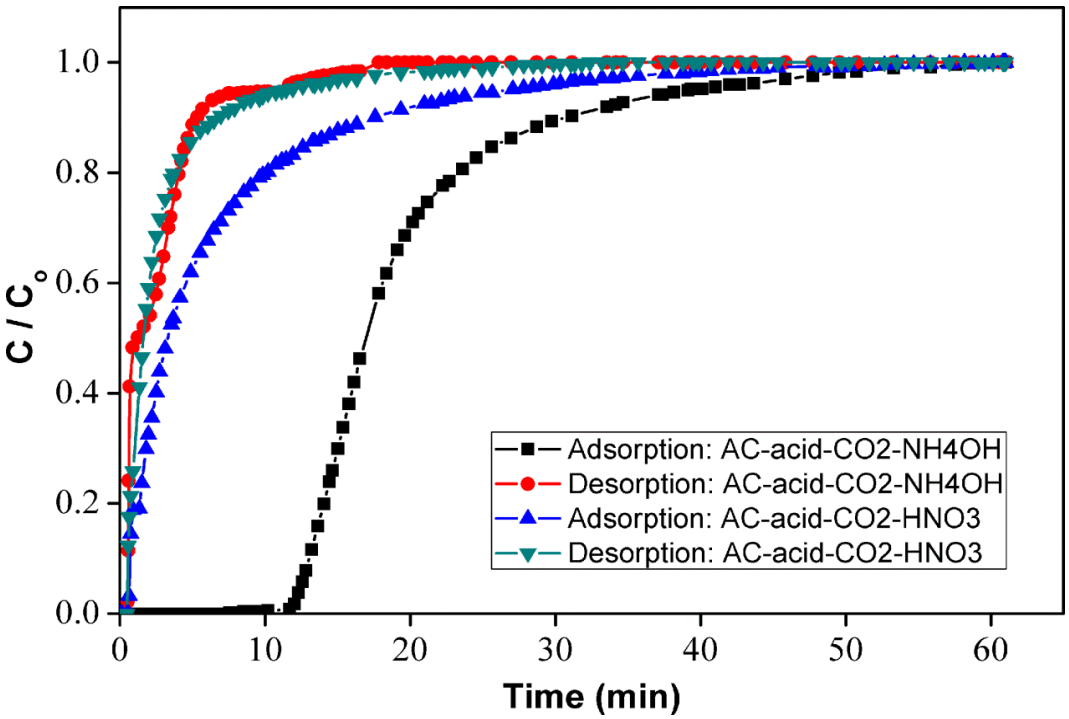

Figure 4-5: Breakthrough curves of physic-chemically treated OFA after functionalizing with HNO_3 and NH_4OH (Pressure = 1atm, Temperature = 22°C, Relative Humidity = 20%, Flow rate = 0.4L/min)

4.4 Conclusions

Due to low cost and large amount of unburned carbon, OFA may become an attractive choice for the removal of H_2S from natural gas. Physicochemical treatments not only remove the mineral matter from ash but also result in a product with very high surface area. BET analysis shows an increase in the surface area from few square meters per gram to 375m^2/g. SEM images showed more micro-pores, well developed particle size and porous structure due to activation with CO_2at high temperature. It is demonstrated that proper combination of surface porosity and functional groups can lead to a suitable adsorbent for H_2Sremoval. Amine treatment after CO_2 activation leads to the formation of nitrogen functionalities on the carbon surface at the expense of reducing the surface area. The results are confirmed by FTIR and BET analyses. On the other hand, HNO_3 functionalization of high surface area activated carbon has an adverse effect. The equilibrium capacity is reduced from 0.2966 mg/g to 0.1035 mg/g. The results indicate

that the presence of more acidic functionalities on the surface reduces the H_2S adsorption efficiency from the gas mixture. Regeneration efficiency of the samples show that acid treatment followed by CO_2 activation at high temperature give the best option for removal of H_2S for OFA. Finally, physicochemical activation of waste OFA sample can convert a waste product to valuable adsorbent and also can solve waste disposal problem.

4.5 References

[1] Y. Elsayed, M. Seredych, A. Dallas, T.J. Bandosz, Desulfurization of air at high and low H2S concentrations, Chem. Eng. J. 155 (2009) 594–602.

[2] P. Forzatti, L. Lietti, Catalyst deactivation, 52 (1999) 165–181.

[3] W.J. Powers-Schilling, Olfaction: Chemical and psychological consideration, in: Nuisance Concern Animal. Management: Odor and Flies, Gainesville, Florida, 1995.

[4] Y. Xiao, S. Wang, D. Wu, Q. Yuan, Catalytic oxidation of hydrogen sulfide over unmodified and impregnated activated carbon, Sep. Purif. Technol. 59 (2008) 326–332.

[5] R. Álvarez-Cruz,B.E. Sánchez-Flores, J. Torres-González, R. Antaño-López, F. Castañeda, Insights in the development of a new method to treat H2S and CO2 from sour gas by alkali, Fuel. 100 (2012) 173–176.

[6] M. Tagliabue, C. Rizzo, N.B. Onorati, E.F. Gambarotta, A. Carati, F. Bazzano, Regenerability of zeolites as adsorbents for natural gas sweetening: A case-study, Fuel. 93 (2012) 238–244.

[7] J.I. Huertas, N. Giraldo, S. Izquierdo, Removal of H2S and CO2 from Biogas by Amine Absorption, in: D.J. Markoa (Ed.), Mass Transfer in Chemical Engineering Process, In Tech Europ, 2011, pp. 132–150.

[8] M. Sharma, C. Guria, A. Sarkar, A.K. Pathak, Recycle of waste fly ash: A rheological Investigation, Int. J. Sci. Environ. Technol. 1 (2012) 285–301.

[9] R. Shawabkeh, M.J. Khan, A. a. Al-Juhani, H.I. Al-Abdul Wahhab, I. a. Hussein, Enhancement of surface properties of oil fly ash by chemical treatment, Appl. Surf. Sci. 258 (2011) 1643–1650.

[10] American Coal Ash Association, Coal Combustion Product (CCP) Production & Use Survey Report, 2012.

[11] Z. Tang, S. Ma, J. Ding, Y. Wang, S. Zheng, Current status and prospect of fly ash Utilization in China, in: 2013 World Coal Ash Conference, 2013, pp. 22–27.

[12] R.A. Shawabkeh, Adsorption of chromium ions from aqueous solution by using activated carbo-aluminosilicate material from oil shale., J. Colloid Interface Sci. 299 (2006) 530–6.

[13] T.P.D. Rajan, R.M. Pillai, B.C. Pai, K.G. Satyanarayana, P.K. Rohatgi, Fabrication and characterisation of Al–7Si–0.35Mg/fly ash metal matrix

composites processed by different stir casting routes, Compos. Sci. Technol. 67 (2007) 3369–3377.
[14] R. Navarro, J. Guzman, I. Saucedo, J. Revilla, E. Guibal, Vanadium recovery from oil fly ash by leaching, precipitation and solvent extraction processes., Waste Manag. 27 (2007) 425–38.
[15] Q. Zeng, K. Li, T. Fen-Chong, P. Dangla, Surface fractal analysis of pore structure of high-volume fly-ash cement pastes, Appl. Surf. Sci. 257 (2010) 762–768.
[16] M. a. Al-Ghouti, Y.S. Al-Degs, A. Ghrair, H. Khoury, M. Ziedan, Extraction and separation of vanadium and nickel from fly ash produced in heavy fuel power plants, Chem. Eng. J. 173 (2011) 191–197.
[17] K.T. Hideaki Tokuyama, Susumu Nii, Fumio Kawaizumi, Characterization of Al-Cu alloy reinforced fly ash metal matrix composites by squeeze casting method, Int. J. Engg. Sci. Technol.5 (2013) 71–79.
[18] A.K. Senapati, A. Bhatta, S. Mohanty, P.C. Mishra, B.C. Routra, An extensive literature review on the usage of fly ash as a reinforcing agent for different matrices, Int. J. Innov. Sci. Mod. Eng., vol. 2, no. 3(2014) 4–9.
[19] A.L. Yaumi, R.Aww.K. ShaWabkeh, ilbnesllvaleed A. Hussem,United States Patent, US 8,545,781 B1, 2013.
[20] A.L. Yaumi, I. a. Hussien, R. a. Shawabkeh, Surface modification of oil fly ash and its application in selective capturing of carbon dioxide, Appl. Surf. Sci. 266 (2013) 118–125.
[21] B. Rubio, M.T. Izquierdo, Coal fly ash based carbons for SO2 removal from flue gases., Waste Manag. 30 (2010) 1341–7.
[22] A. Alastuey, E. Herna, X. Querol, N. Moreno, J.C. Uman, F. Plana, Synthesis of zeolites from coal fly ash : an overview, Int. J. Coal Geol.50 (2002) 413–423.
[23] M. Wdowin, M. Franus, R. Panek, L. Badura, W. Franus, The conversion technology of fly ash into zeolites, Clean Technol. Environ. Policy. (2014).
[24] M. Visa, A. Duta, TiO2/fly ash novel substrate for simultaneous removal of heavy metals and surfactants, Chem. Eng. J. 223 (2013) 860–868.
[25] M.M. Maroto-valer, Z. Lu, Y. Zhang, Z. Tang, Sorbents for CO2 capture from high carbon fly ashes, Waste Manag. 28 (2008) 2320–2328.
[26] B. Bournonville, A. Nzihou, P. Sharrock, G. Depelsenaire, Stabilisation of heavy metal containing dusts by reaction with phosphoric acid: study of the reactivity of fly ash., J. Hazard. Mater. 116 (2004) 65–74.
[27] R.A. Shawabkeh, Synthesis and characterization of activated carbo-aluminosilicate material from oil shale, Microporous Mesoporous Mater. 75 (2004) 107–114.
[28] E.D. Dimotakis, M.P. Cal, J. Economy, M.J. Rood, S.M. Larson, Chemically treated activated carbon cloths for removal of volatile organic carbons from gas streams: evidence for enhanced physical adsorption., Environ. Sci. Technol. 29 (1995) 1876–80.
[29] J. Kazmierczak, P. Nowicki, R. Pietrzak, Sorption properties of activated carbons obtained from corn cobs by chemical and physical activation, Adsorption. 19(2013) 273–281.

[30] H.S. Choo, L.C. Lau, A.R. Mohamed, K.T. Lee,Hydrogen sulfide adsorption by alkaline impregnated coconut shell activated carbon, J. Eng. Sci. Technol. 8 (2013) 741–753.
[31] D. Choi, J. Lee, S. Jang, B. Ahn, D. Choi, Adsorption dynamics of hydrogen sulfide in impregnated activated carbon bed, Adsorption. 14 (2008) 533–538.
[32] A. Bagreev, J. Angel Menendez, I. Dukhno, Y. Tarasenko, T.J. Bandosz, Bituminous coal-based activated carbons modified with nitrogen as adsorbents of hydrogen sulfide, Carbon. 42 (2004) 469–476.
[31] Hsi, Hsing-Cheng. 2013. "Effects of Sulfur, Nitric Acid, and Thermal Treatments on the Properties and Mercury Adsorption of Activated Carbons from Bituminous Coals." Aerosol and Air Quality Research: 730–738. doi:10.4209/aaqr.2012.07.0177. http://www.aaqr.org/Doi.php?id=29_AAQR-12-07-OA-0177&v=13&i=2&m=4&y=2013.
[32] Mun, M J. 1997. "Activated Carbons from Spanish Coals . 3 . Preoxidation Effect on Anthracite Activation" 0624 (12): 785–791.
[33] B.C. Lippens, J.H. De Boer, Studies on Pore Systems in Catalysts, J. Catal. 4(1965) 319–323.
[34] B.S. Girgis, A.-N. a. El-Hendawy, Porosity development in activated carbons obtained from date pits under chemical activation with phosphoric acid, Microporous Mesoporous Mater. 52 (2002) 105–117.
[35] H. Marsh, F.R. Reinoso, Activated Carbon, 1st ed., Elsevier Ltd, New York, 2006.
[36] A. Mofarrah, T. Husain, C. Bottaro, Characterization of activated carbon obtained from Saudi Arabian fly ash, Int. J. Environ. Sci. Technol. (2013).
[37] C.M. López-Badillo, J. López-Cuevas, C. a. Gutiérrez-Chavarría, J.L. Rodríguez-Galicia, M.I. Pech-Canul, Synthesis and characterization of BaAl2Si2O8 using mechanically activated precursor mixtures containing coal fly ash, J. Eur. Ceram. Soc. 33 (2013) 3287–3300.
[38] Z. Lu, M.M. Maroto-Valer, H.H. Schobert, Catalytic effects of inorganic compounds on the development of surface areas of fly ash carbon during steam activation, Fuel. 89 (2010) 3436–3441.
[39] M.J. Khan, A. a. Al-Juhani, R. Shawabkeh, A. Ul-Hamid, I. a. Hussein, Chemical modification of waste oil fly ash for improved mechanical and thermal properties of low density polyethylene composites, J. Polym. Res. 18 (2011) 2275–2284.
[40] T.S. Malarvizhi, T. Santhi, S. Manonmani, Acid treated lignite fired fly ash for the removal of Zn(II) ions from aqueous solution,Int. J. Chem. Sci. Appl.4 (2013) 84–96.
[41] M.S. Shafeeyan, W.M.A.W. Daud, A. Houshmand, A. Shamiri, A review on surface modification of activated carbon for carbon dioxide adsorption, J. Anal. Appl. Pyrolysis. 89 (2010) 143–151.
[42] C. Moreno-Castilla, M.. López-Ramón, F. Carrasco-Marín, Changes in surface chemistry of activated carbons by wet oxidation, Carbon. 38 (2000) 1995–2001.
[43] A.M. Youssef, M.B. Dawy, M.A. Akland, A.M. Abou-Elanwar, EDTA versus nitric acid modified activated carbon for adsorption studies of lead, J. Appl. Sci. Res. 9 (2013) 897–912.

[44] J.R. Ferraro, L.J. Basile, eds., Fourier Transform Infrared Spectroscopy: Applications to Chemical System, 4th ed., ACADEMIC PRESS, INC., New york, 1985.
[45] B. Bagheri, M. Abdouss, M.M. Aslzadeh, Efficient Removal of Cr3+ , Pb2+ and Hg2+ Ions from Industrial Effluents by Hydrolyzed/Thioamidated Polyacrylonitrile Fibres,Iran. Polym. J. 19 (2010) 911–925.
[46] P. Drużkowski, M. Ćwiżewicz, K. Świder, M. Radlik, B. Samojeden, Comparison of SCR catalyst effectiveness based on modified activated carbon promoted Cu in NH3-SCR,URL:http://gdri.pl/abstrakty/Samojeden%20B.pdf.
[47] B. Shrestha, J. Kour, P.L. Homagai, M.R. Pokhrel, K.N. Ghimire, Surface Modification of the Biowaste for Purification of Wastewater Contaminated with Toxic Heavy Metals — Lead and Cadmium, Adv. Chem. Eng. Sci. 3 (2013) 178–184.
[48] J.K. Koech, Q. Shao, F.N. Mutua, Y. Wang, Application of Hydrazine Hydrate in the Synthesis of Octa (aminophenyl) silsesquioxane (OAPS) Poss, Adv. Chem. Eng. Sci. 3 (2013) 93–97.
[49] E.R. Elswick, M. Mastalerz, Progression in sulfur isotopic compositions from coal to fly ash: Examples from single-source combustion in Indiana, Int. J. Coal Geol. 73 (2008) 273–284.
[50] R.T. Yang, Adsorbents: Fundamentals and applications, John Wiley & Sons, Inc., New Jersey, 2003.
[51] W. Feng, S. Kwon, E. Borguet, R. Vidic, Adsorption of hydrogen sulfide onto activated carbon fibers: Effect of pore structure and surface chemistry., Environ. Sci. Technol. 39 (2005) 9744–9.
[52] M. Abe, K. Kawashima, K. Kozawa, H. Sakai, K. Kaneko, Amination of activated carbon and adsorption characteristics of Its aminated surface, Langmuir. 16 (2000) 5059–5063.
[53] F. Adib, A. Bagreev, T.J. Bandosz, Adsorption/Oxidation of hydrogen sulfide on nitrogen-containing activated carbons, Langmuir. 16 (2000) 1980–1986.
[54] T.J. Bandosz, On the adsorption/oxidation of hydrogen sulfide on activated carbons at ambient temperatures., J. Colloid Interface Sci. 246 (2002) 1–20.

CHAPTER 5

Adsorption of H_2S onto activated oil fly ash: Kinetics and Modeling

This paper is ready for submission

5.1 Introduction

Hydrogen sulfide (H_2S) is an airborne pollutant causing both acute and chronic health problems depending on exposure time and toxicant concentration [1,2]. At low concentration around 10-20ppm (parts per million) starts eye-irritation and goes to respiratory paralysis above 300ppm level. Five minute exposure to 500-1000ppmv concentration might lead to a death [3,4]. Apart from its toxicity to human, it can also be harmful for catalyst even at 1ppm concentration[5,6]. Getting rid of H_2S from air and industrial stream is beneficial for both life and industry.

Various H_2S abatement technologies have been practiced industrially to meet the strict environment regulations of toxic gas emission. These methods include absorption using alkanolamines solutions [7,8], oxidation of H_2S to sulfur by Claus Process [9,10], biological oxidation to sulfuric acid [11] and adsorption using carbonaceous or metal adsorbent [12]. All these methods have their own benefits and limitations which make them suitable for specific applications. Among these techniques, adsorption is preferred for treating gas streams that have lower concentration of H_2S [13,14]. Activated carbon is widely used as an adsorbent due to its low cost, high surface area and porous structure. In order to make the adsorption process economically feasible, the precursor of activated carbon should be of such materials that are either abundant in nature or produced as waste or by-product in industries[15,16]. Fly ash derived activated carbon represents a promising option for H_2S capture to existing specialized activated materials and molecular sieves that tend to be costly and hamper the viability of H_2S sorption on a big scale. Huge amount of fly ash has been released from utility industries every year but only 30% is being utilized of total amount (700million per year) generated worldwide

[17]. In US, out of 150million ton fly ash per year only 27% is reused in different application while remaining is disposed of as landfill or surface impounded[18]. Depending upon the fuel (i.e. solid or liquid) being burned, the constituents of fly ash vary considerably, but all the fly ash comprises of unburned carbon with some inorganic oxides like Aluminum oxide (Al_2O_3), Silicon dioxide (SiO_2) and traces of heavy metals. Exploiting the use of fly ash as a precursor of activated carbon is advantageous due to its cheap source, availability, and one step activation procedure as compared to conventional production of activated carbon by two step activation.

Several studies have been reported on the utilization of fly ash for the adsorption of individual toxicant in an aqueous solution or from flue gas. Salvatro Andidi et al were used oil fly ash to adsorbed 2-chlorophenol (CP), 2-chloroaniline (CA) and methylene blue (MB) from aqueous solutions. Adsorption was highest for 2-chlorophenol (CP) and quite low for other two organics [19]. Bada et al. investigated the adsorption capabilities of chemically treated and heat treated fly ash samples. They used Hydrochloric acid for chemical treatment and found relatively higher specific surface area as compared to heat treated fly ash. This increased surface area was achieved due to the corrosion of the outer layer of the fly ash to ash to disintegrate its stable glassy layer[20]. Md. Azhar Uddin et al. prepared an activated carbon for adsorption applications by the pyrolysis of mixture of fly ash with road paving asphalt dissolved in kerosene at 650^oC in N_2 atmosphere. They showed macropore diameter of the sample increased by an asphalt ratio[21]. A Al-shawabkeh et al. prepared Calcium hydroxide treated fly ash adsorbent and tested it for SO_2 adsorption. SO_2 was chemically adsorbed and showed first order kinetics[22]. Bagreeve et al studied the NaOH modified activated carbon for the adsorption of H_2S and

concluded that adsorption capacity was increased with loading of NaOH and insensitive to pore structure and surface area [23]. Prezeprioski et al also reported a significant improvement in adsorption capacity of H_2S after treating activated carbon with K_2CO_3 [24]. It is concluded that the presence of alkali metals on the activated carbon surface helps to dissociate the H_2S molecule and hence increases the uptake capacity. From the literature, it is revealed that not only the porosity but also the surface chemistry is important to enhance the adsorption capacity of AC. Higher surface area and very fine micropores exerts strong interactions between adsorbate gas molecules and carbon structure and results physical adsorption but on the other hand the presence of OH functional group or the cations dissociates the H_2S and promote chemisorption[1].

The present study aimed at equilibrium and column breakthrough study of H_2S adsorption on a packed with alkaline treated activated carbon derived from oil fly ash. The effects of operating variables like temperature, influent concentration of H_2S, and the flow rate of gas stream and inlet pressure have been investigated. Different isotherm models like Langmuir, Freundlich, Sips and dual site Langmuir (DSL) models were tested to fit the experimental adsorption data. Yoon-Nelson model, Thomas model and Clark model were fitted with experimental data.

5.2 Materials and Methods

5.2.1 Materials

A sample of raw oil fly ash (OFA) was received from the Rabigh (RB) power plant located in Saudi Arabia. The raw ash was dried overnight at 110°C in the oven to remove moisture content, sieved to 45µm mesh, and stored in closed containers for later use.

Elemental composition of raw material is given in Table 5.1 showing higher percentage of carbon exists in the sample. Nitric and orthophosphoric acids were of analytical grades supplied by Panreac Company, Spain. 2M Potassium hydroxide (Provided by Merck Chemical Company, Germany) solution was prepared by dissolving an appropriate amount in deionized water in one liter volumetric flask. Synthetic natural gas containing 50 and 100 ppm H_2S in methane was supplied by Saudi Gas Company. All glass wares were of Pyrex, washed with distilled water and dried in an oven at 105°C.

5.2.2 Preparation of activated OFA and Surface modification with aqueous KOH

In a typical run, a sample of 10g OFA powder was treated with 200ml of an acid mixture in a round-bottom flask at 115°C for four hours under total reflux condition. An acid mixture comprises of 20% HNO_3 and 80% H_3PO_4. Then activated sample was filtered to obtain the solid residue. The residue was rinsed repeatedly with distilled water to wash out the acid contents until the pH of spent acid reached 5. Finally, the solid residue was dried in an oven at 110°C for 5 hours. The elemental composition of activated carbon determined by Energy Dispersive Spectrometer (EDX) is given in table 4.1. Initially the raw sample contains mainly unburned carbon and other mineral oxides with traces of heavy metals. Interaction of acid mixture with ash results in several nitrification and phosphate reactions and practically leaches out almost all inorganic oxides from the ash while some organically bounded sulfur left in the carbon structure. This is due to the fact that nitric acid can only mildly attack organic sulfur than pyrite and sulfate form of sulfur in the fly ash [25–28]. For alkali functionalization of activated carbon, 5g of dried oil fly ash activated carbon was mixed with 50ml of 2M KOH solution in a round-bottom flask

and heated at 100°C for 4 hours at total reflux. Then, the mixture was cooled, filtered and washed with 500 ml water. Filter cake was dried in an oven at 110°C and saved in a closed cap bottle for further characterization and adsorption tests.

Table 5–1: Elemental Composition of raw and acid treated oil fly ash

Element	C	S	O	Al	Mg	Ca	V	Ni	Cu	Zn	Si	Fe
Raw OFA (%)	77.40	7.10	9.32	0.25	1.41	0.23	1.29	0.68	1.70	0.40	0.08	0.14
F-AC	88.05	1.39	10.56	All in negligible percentage								

* OFA = oil Fly ash, FA-AC = Fly ash Activated Carbon after acid treatment

5.2.3 Analysis and Characterization of OFA

5.2.3.1 BET (Brunauer–Emmett–Teller) Surface area analysis

Explained in Section 4..2.4.1

5.2.3.2 FTIR measurement

Explained in section 4.2.4.3

5.2.3.3 X-ray diffraction spectrometry (XRD)

The phase identification of the fly ash sample which is in a powdery form, were determined by the X-ray diffractometry using a Phillips PW 1830 diffractometer with a copper anode. It was operated at 40 kV and 40 mA for 1 h from 0° to 80° over the range of 2q and High Score Plus software was used for the identification of the phases present.

5.2.3.4 Energy dispersive X-ray (EDX) analysis

Explained in Section 3.2.4.2

5.2.4 H_2S Adsorption capacity tests

Procedure is explained in section 4.2.5

5.3 Results and Discussion

5.3.1 Porosimetric Characteristics

The porosimetric features of raw oil fly ash and its derived substances are presented in the table 5.2. The precursor material has small BET surface area and negligible micro-pore volume. Acid treatment induces porosity to ash by removing inorganic matter cotton from the surface and produces a porous carbon. The BET surface area increases to 61.54m^2/g from its initial value of 2.75m^2/g. By functionalizing the activated carbon with aqueous KOH reduces the micro pore volume and hence surface area. This is due to possible action of KOH in the inner pores of carbon.

The BJH pore size distribution (Fig. 5.1) of FA-AC_{KOH} shows that mesopore accounts for 91%of the pore area and 4.7% is the only micro pore area and remaining is the macro pore. While in the acid activated fly ash mesopores accounts for almost same percentage (i.e. 90.4%) of the pore area and remaining 8% and 1.5% are contributed by micropores and macropores respectively. This pore area distribution depicts the heterogeneity of the surface and we characterize it as meso porous adsorbent as can also be seen from Fig.5.1. The hysteresis (Fig. 5.2) in both FA-AC and FA-AC_{KOH} is same which also confirms that the mesoporous area in FA-AC_{KOH} is almost same as its precursor. Although the FA-AC

has more surface area than FA-AC_{KOH} but the surface modification with alkali treatment increases its adsorption capacity several times as can be seen in the subsequent sections.

Table 5–2: Porosity Characteristics of raw and activated ash sample

Porosity Characteristics	**Raw OFA**	**FA-AC**	**FA-AC_{KOH}**
BET Area (m^2/g)	2.75	61.54	35.24
Langmuir surface area (m^2/g)	4.4	105.79	58.35
t-plot micropore volume (cm^3/g)	8.60E-05	0.0031	0.0022
Average BJH Adsorption Pore size (4V/A), A°	280	70	115
Average BJH Desorption Pore size (4V/A), A°	190	53	72

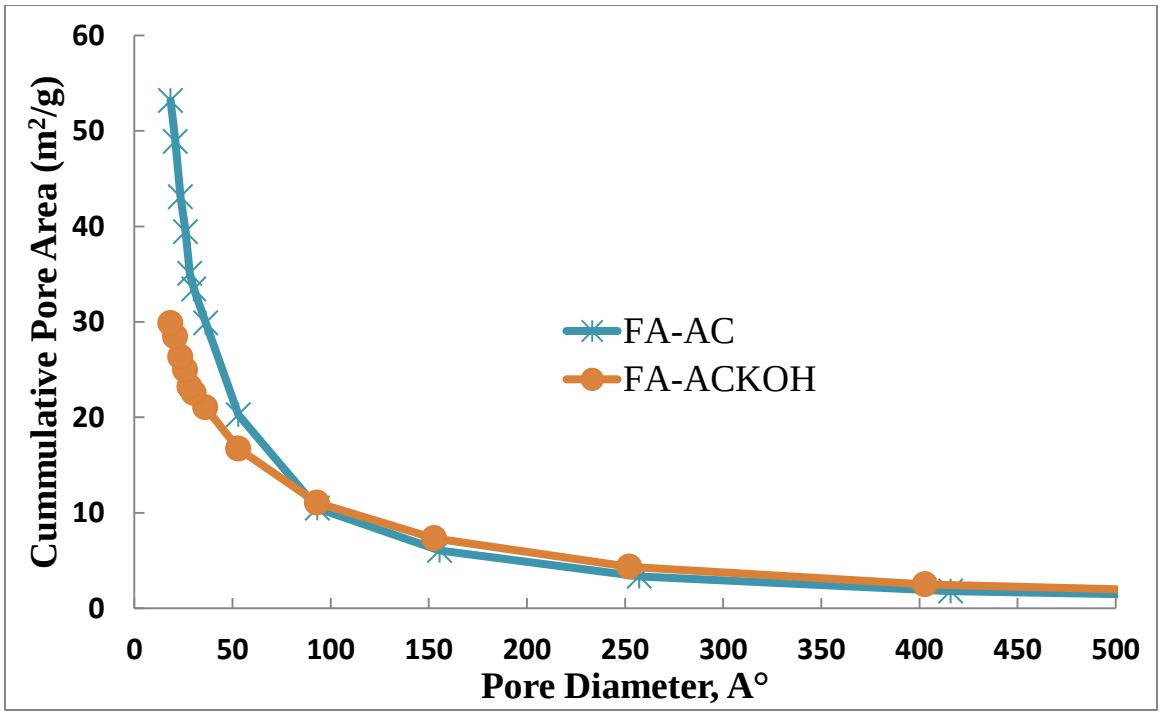

Figure 5-1: BJH pore size distribution.

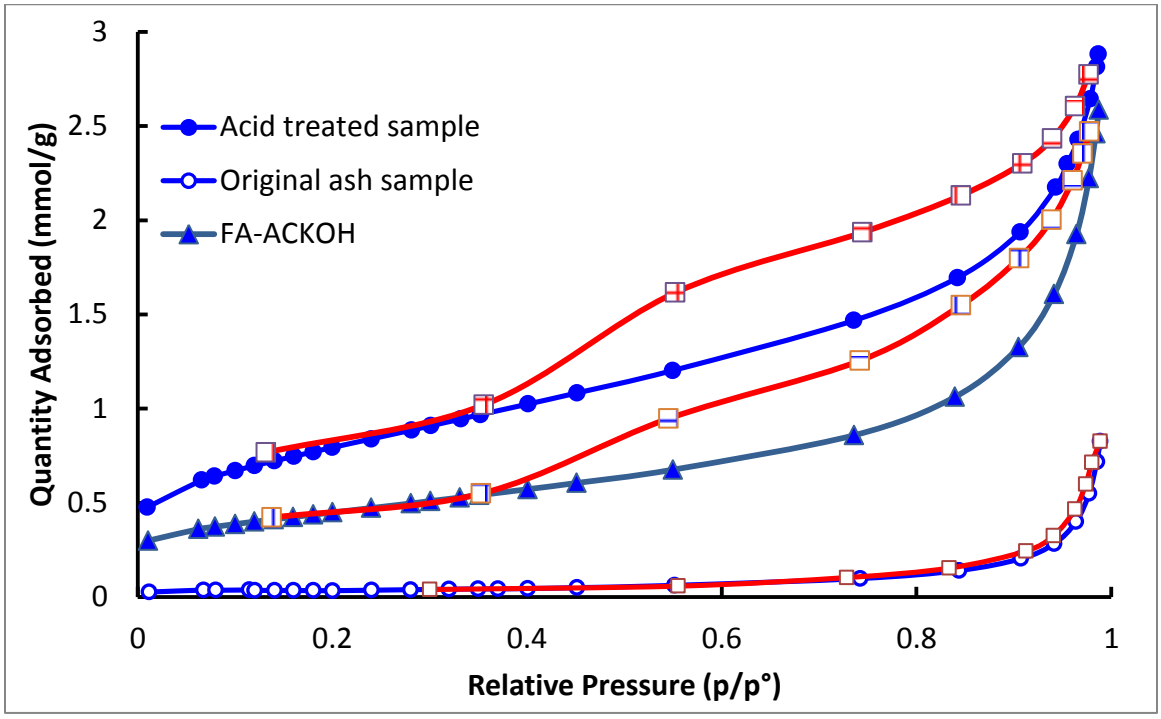

Figure 5-2: BET isotherm plot of activated fly ash carbon at different stages.

5.3.2 Fourier transforms infrared spectroscopy (FTIR)

FTIR spectrums of different ash samples are shown in the Figure 5.3. A broad band appears between 3100-3550cm^{-1} for raw fly ash with minimum at 3400cm-^{1} . This is due to stretching vibration of free and associated hydroxyl groups (-OH) on the virgin ash[29]. This stretching is because of both adsorbed water (3400cm-^{1}) and silanol group (Si-OH) on the surface. Two peaks can be observed in the raw ash at 2924cm^{-1} and 2854 cm^{-1} correspond to C-H sp^{3} stretching in aliphatic acid and O-H vibration in the molecule [30,31]. Three peaks (1625cm^{-1},1394cm^{-1} and 1115cm^{-1}) between 1100-1650cm^{-1} are indicative of C=C stretching CO_2^{-1} symmetrical stretching and C-O stretching respectively. Comparing to raw material, acid treatment of fly ash introduces oxygenated acidic surface groups mainly include phenolic hydroxyl, carboxylic and Lactones [32]. After KOH treatment, the activated carbon surface has been functionalized and hydroxyl

group is attached to the surface as indicated by corresponding peak at 3435cm^{-1}. Peak at 1630cm-^{1} is due to C=O double bond stretching vibrations of aromatic carbon[33,34]. After H_2S is being adsorbed on the KOH treated activated carbon a strong band emerges at 3435cm^{-1} which is accounted for dissociative adsorption of H_2S. This increase in intensity is due to contribution of -OH stretching of -SO-OH group. -SH group can be assigned to peak appears at 1620cm^{-1}[35–37]. Comparison of FTIR spectrum shows that the H_2S adsorption is more effective due to presence of hydroxyl groups.

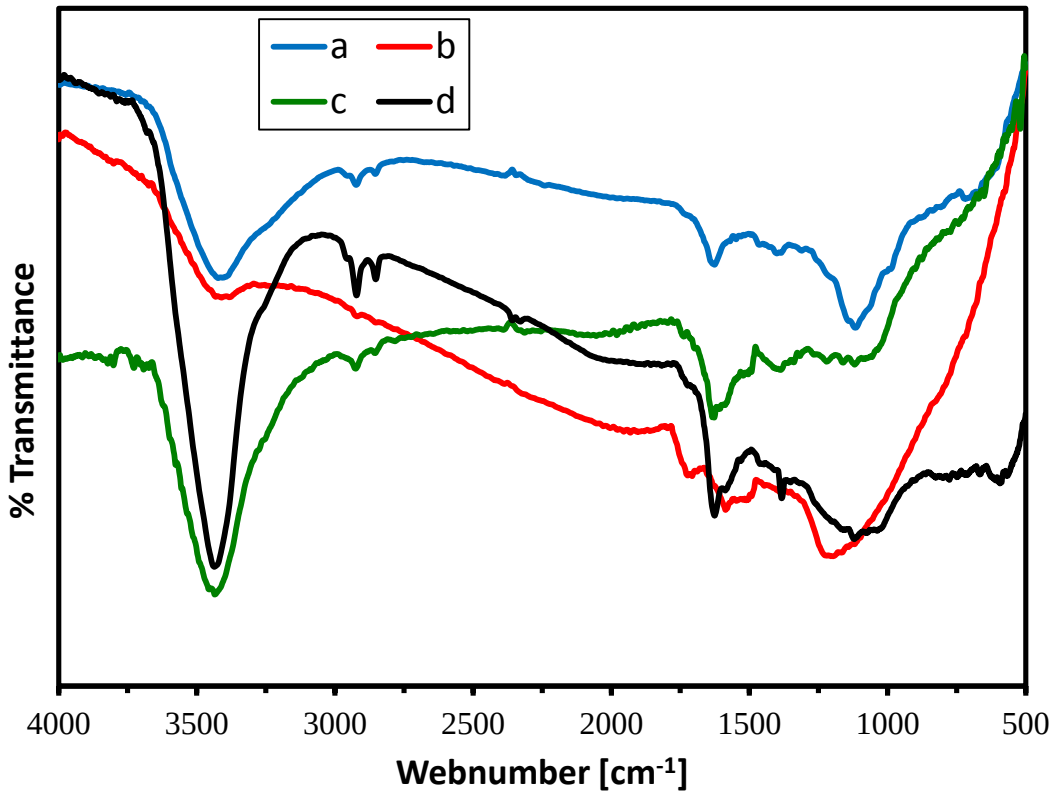

Figure 5-3: FTIR spectrum of raw (a), acid activated ash (b), KOH activated before adsorption (c) and KOH activated after adsorption (d)

5.3.3 X-ray diffraction spectrometry (XRD)

X-Ray diffraction spectroscopy (XRD) was used to analyze the ash at various stages of its use as shown in figure 4. Figure 5.4(a) shows that the dominant element of raw oily fly ash as compared to other materials is the carbon as indicated by broad peak at 25° 2θ [38,39]. Other materials in the raw OFA includes Mullite (Alumiosilicate), Zeolite, Quartz, Faujasite and Cancrinite. Small peaks at 11°,16°, 18° 2θ can be assigned to zeolite X, P and NA .A distinct peak oat 22° 2θ is because of quartz presence in the fly ash. Also the three peaks between 27° to 38° 2θ shows the presence of Faujasite, Cancrinite and Mullite phases. Furthermore a wide peak at 43°2θ shows a Sodalite followed by small peak of quartz at 76° 2θ[25,40,41]. Treatment of as received ash with mixture of acids wash out almost all the minerals as most of small peaks have not been exists further as shown in Fig 5.4(b). The intensity of the carbon peak at 25° 2θ is increased to 185% as compared to raw oil fly ash. The broadening of the carbon peak after acid activation of raw ash reflects the predominance of amorphous and porous nature of activated carbon[42]. With the KOH functionalization of activated carbon, an XRD pattern remains same except around 50% decrease in peak intensity before and after KOH treatment. This shows some surface coverage of porous carbon with alkali and hence decreases the surface area [43]. Comparing the peak before and after H_2S adsorption reveals that both differactograms trace out the same path except a clear sharp peak at $2\theta = 21.5°$. This indicates the possibility of formation of new substance i.e. K_2SO_4 as a result of chemical reaction of acidic gas with carbon surface [34,37]

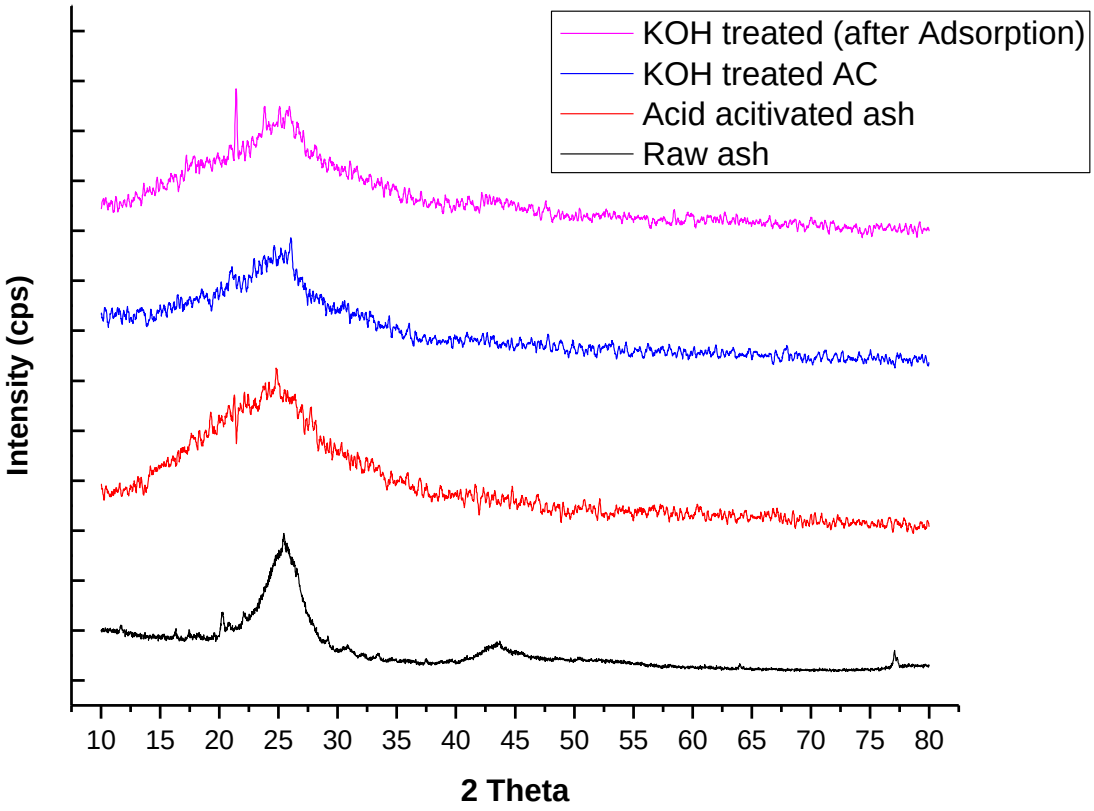

Figure 5-4: XRD Diffractograms of Raw and treated ash

5.3.4 Adsorption Thermodynamics

The adsorption equilibrium data were used to extract the thermodynamic parameters for the adsorption process such as Gibbs free energy change (ΔG*), enthalpy change (ΔH*), and entropy change (ΔS*) by the following equations (Ghosh & Bhattacharyya, 2002):

$$lnK = ln\left(\frac{q_t}{C_t}\right) = \frac{\Delta S^*_{ads}}{R} - \frac{\Delta H^*_{ads}}{RT} \qquad (5.1)$$

$$\Delta G^* = \Delta H^* - T\Delta S^* \qquad (5.2)$$

Where ΔH*, ΔS*, and ΔG* are the enthalpy, entropy and Gibbs free change for the adsorption process respectively. Gibbs free energy change is the fundamental criterion of

the process spontaneity. The values of these parameters were calculated using equation 5.1 and 5.2 and recorded in Table 5.3.

Table 5–3: Adsorption thermodynamic parameters for H_2S adsorption onto activated OFA

Temperature (K)	ΔG* (kJ/mol)	ΔH*(kJ/mol)	ΔS*(J/mol.K)
274	-8.04	-3.51	16.54
283	-8.19		
293	-8.36		
303	-8.52		

The negative value of ΔH* (-3.51kJ/mol) indicates the sorption of H_2S adsorption onto activated OFA is exothermic in nature whereas the negative values of ΔG* confirmed adsorption of H_2S is a spontaneous process and the spontaneity increases with temperature. The positive entropy change (ΔS*) indicates the affinity of the activated OFA for H_2S adsorption and the increasing randomness during the adsorption process.

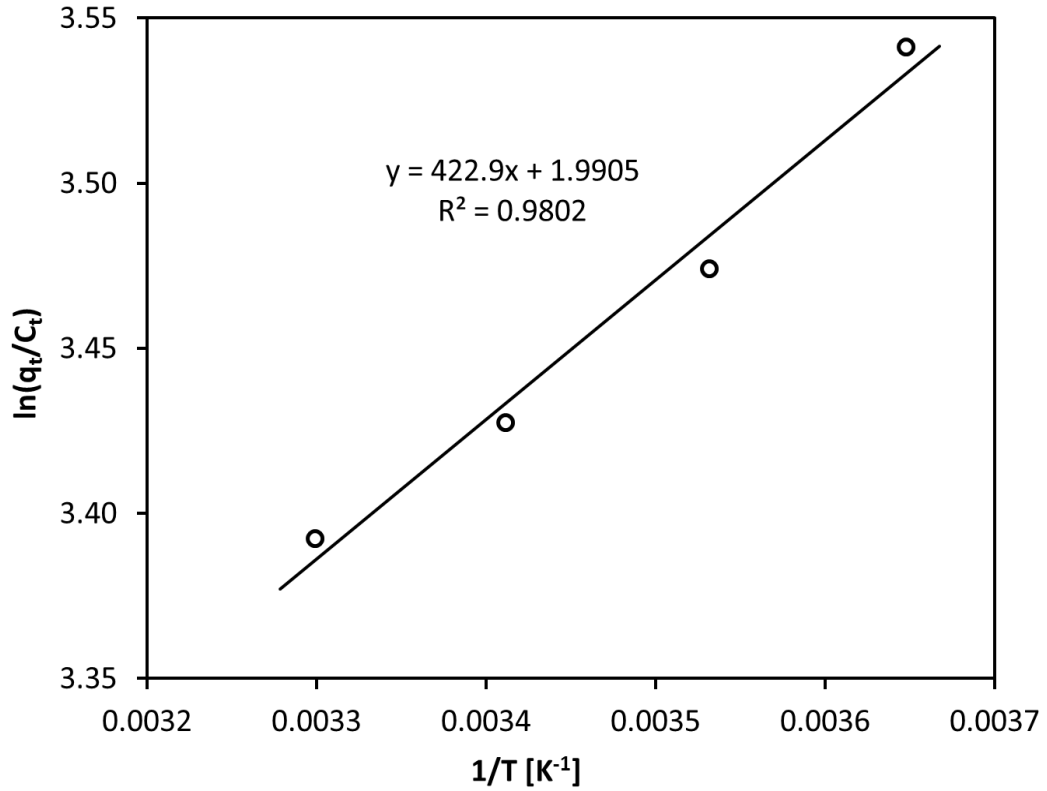

Figure 5-5: Determination of thermodynamic parameters adsorption of H_2S on activated OFA

5.3.5 Adsorption isotherms

Adsorption equilibrium data were analyzed using well-known isotherm model such as; Freundlich, Langmuir, Sips and dual site Langmuir (DSL) model. Non-linear regression method was chosen to find the isotherm parameter as the linearization often causes erroneous data treatment (Chowdhury & Saha, 2011). Parameters for different models were adjusted using the non-linear least square method. In order evaluate the goodness of fit of each model; statistical parameters were used, such as coefficient of determination (R^2), and residual sum of squares (RSS). Microsoft Excel® Solver function was used to optimized the statistical parameters RSS using the following equation:

$$\mathrm{RSS} = \sum_{1}^{n} \left(q_{\mathrm{i,\,exp}} - q_{\mathrm{i,\,model}} \right)^2 \qquad (4)$$

Where n is the number of data points, $q_{i,exp}$ and $q_{i,model}$ are the experimental and theoretical values of adsorbed amount of H_2S on OFA respectively. The correlation coefficient, R^2 gives a measure of proportion of the variability attributed to the model. The standard error, RSS gives an indication of the precision of the experimental estimation. The model with the highest of R^2 and the lowest of RSS value was chosen to be the best fitted equation. Four different models used in this study are listed with their non-linear equation in Table 5.4. Figure 5.6 and Figure 5.7 represent the typical isotherm plot using different model used. The calculated capacity and model parameters are listed in Table 5.5. It indicates that the adsorption isotherms are best fitted by dual site Langmuir (DSL) model as seen from the plot and regression coefficient values. Freundlich model underestimates at lower concentrations and overestimates at higher concentrations whereas Langmuir and Sips models are opposite (overestimates at lower concentration and underestimates at higher concentration).

Table 5–4: Isotherm model used in non-linear form

Model name	Equation	Constants and parameters
Freundlich	$q_e = K_F C_e^{1/n}$	K_F,n
Langmuir	$q_e = \frac{q_m K C_e}{(1+KC_e)}$	q_m, K
Sips	$q_e = \frac{K_S C_e^{\beta_S}}{(1+a_S C_e^{\beta_S})}$	K_S, β_S, a_S
Dual Site Langmuir (DSL)	$q_e = \frac{q_{m1} K_1 C_e}{(1+K_1 C_e)} + \frac{q_{m2} K_2 C_e}{(1+K_2 C_e)}$	q_{m1}, K_1, q_{m2}, K_2

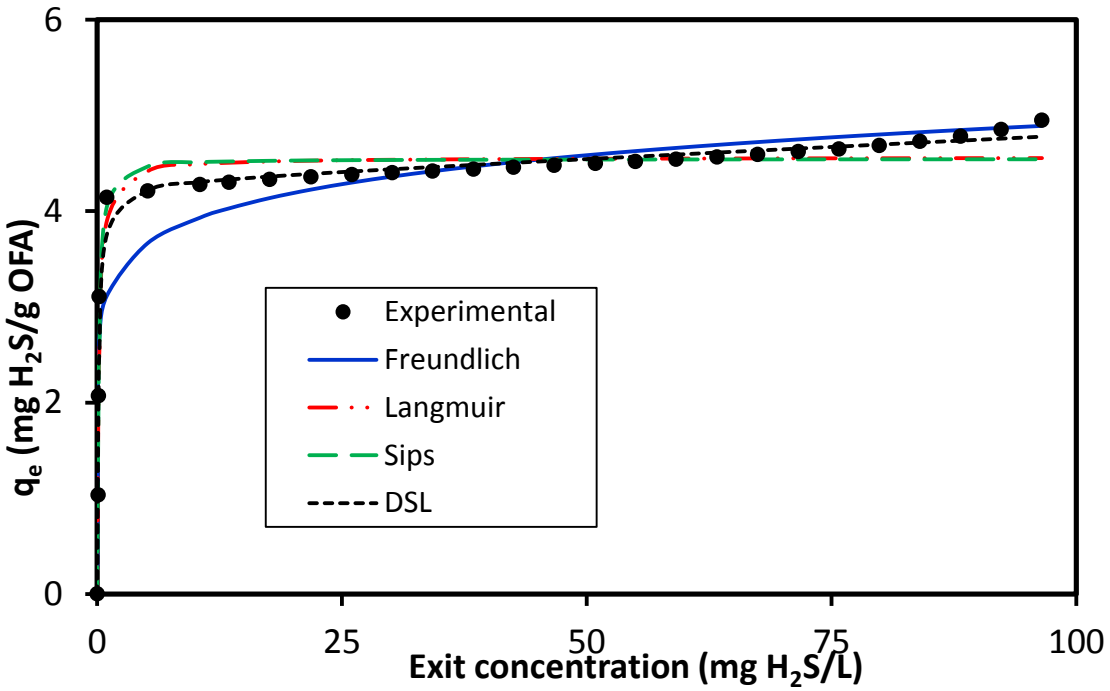

Figure 5-6: Fitting adsorption isotherm data for H_2S by different models for adsorption at 1°C and 100 ppm inlet concentration with 0.4L/min flow rate

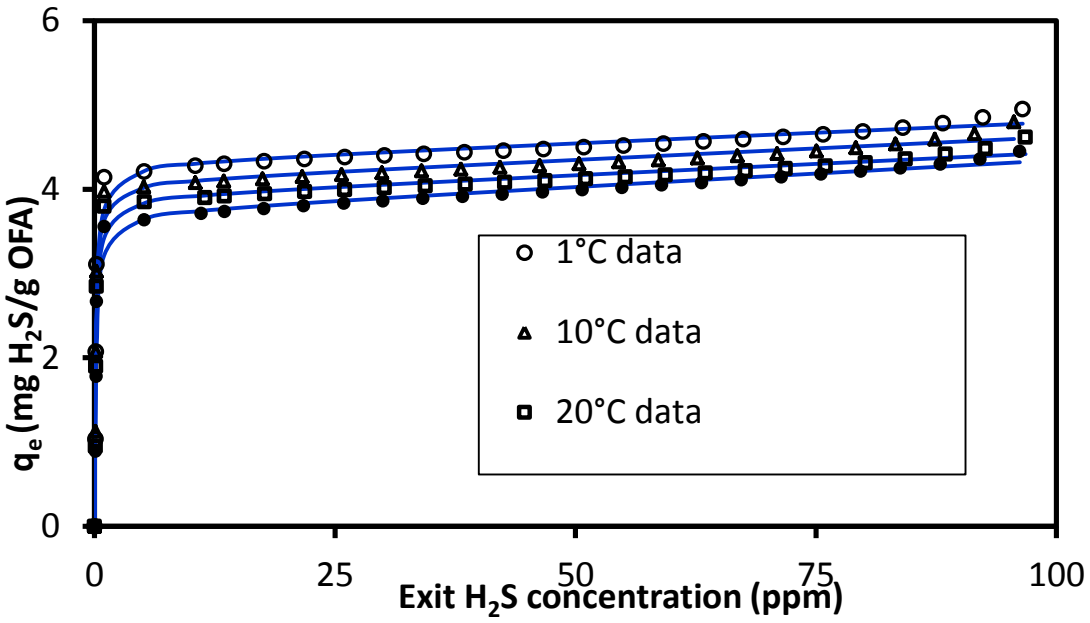

Figure 5-7: Fitting adsorption isotherm data for H_2S at different temperature with dual site Langmuir (DSL) model for 100 ppm inlet concentration and 0.4L/min flow rate

Figure 5.7 showed the experimental and DSL model fit for the adsorption runs at temperature range 1°C-30°C. It showed that the amount adsorbed on solid phase increases sharply up to a value close to 3.5-4.25 mg/g when the bed temperature in the range 1°C-30°C. The fitting of isotherms with DSL model proves that the interaction between H_2S and activated OFA involved in dual site characteristics of OFA. It means that OFA has two sites with higher and lower affinity. The exit concentration from the column outlet remains zero until the first site is covered by adsorbed H_2S. After the sharp increase in q_e due to filling of higher affinity site, adsorption goes to increase slowly by filling the lower affinity sites until the column becomes saturated. Both the saturation capacities (q_{m1}, q_{m2}) and affinities (K_1, K_2) decrease with the increase in bed temperature as it was depicted from thermodynamic study in the previous section.

Table 5–5: Isotherm parameter for different temperature runs at flow rate 0.4 L/min

Isotherm Parameters		1°C	10°C	20°C	30°C
Freundlich	K_F	5.909	5.612	5.447	5.375
	1/n	0.099	0.095	0.100	0.108
	R^2	0.881	0.891	0.884	0.899
	RSS	4.312	3.491	3.542	2.962
Langmuir	q_m	4.563	4.360	4.184	4.047
	K	3893	4399	3876	3364
	R^2	0.957	0.956	0.952	0.952
	RSS	1.541	1.421	1.469	1.405
Sips	K_s	79180	79026	78848	78697
	β_S	1.180	1.169	1.190	1.213
	a_s	17422	18188.	18928	19556
	R^2	0.961	0.959	0.956	0.955
	RSS	1.398	1.323	1.351	1.337
DSL	q_{m1}	4.310	4.089	3.913	3.716
	K_1	4454	5137	4540	4103
	q_{m2}	3.00	2.50	2.45	2.25
	K_2	1.214	1.647	1.654	2.312
	R^2	0.969	0.970	0.967	0.974
	RSS	1.115	0.920	0.979	0.728

5.3.6 Column Dynamics and Effect of Operating Conditions

Adsorption models are used to predict breakthrough curves behavior and capacity of adsorption. Experimental data were fitted with Yoon-Nelson model, Thomas model and Clark model.

Yoon-Nelson model

Yoon-nelson model is a relatively simple model to predict breakthrough behavior of adsorbate vapor or gas on solid adsorbent. This model is based on the assumption that the rate of decrease in the probability of adsorption of adsorbate molecule is proportional to the probability of the adsorbate adsorption and the adsorbate breakthrough on the adsorbent. The Yoon-Nelson model for single component system is given by the following equation:

$$\ln\left(\frac{C}{C_o - C}\right) = K_{YN}\left(t - \tau\right)$$

Where k_{YN} is Yoon-Nelson rate constant (min^{-1}), τ is the time required for 50% adsorbate breakthrough time (min).

Thomas Model

Thomas model for adsorption column breakthrough prediction is given by following equation:

$$\ln(\frac{C_0}{C} - 1) = \frac{K_{Th} q_0 X}{Q} - K_{Th} C_0 t$$

Where K_{TH} is the Thomas constant (ml min^{-1} mg^{-1}), q_o is the maximum solid-phase concentration of adsorbate (mg g^{-1}) and Q, the flow rate (mL min^{-1}). Thomas model is one of the most general and widely used methods in column performance theory. It assumes Langmuir kinetics of adsorption–desorption without axial dispersion and the reaction kinetics obeys second-order reversible reaction.

Clark Model

In 1987 Clark defined a new model for breakthrough simulation which uses the Freundlich isotherm with linear driving force mass transfer concept. The model equation can be expressed as:

$$\frac{C}{C_o} = \left(\frac{1}{1 + Ae^{-rt}} \right)^{1/n-1}$$

Where the constants A and r can be adjusted using the values of n determined from Freundlich model. For this study the value n was ~ 11 (calculated from isotherm modeling). Non-linear regression method was used to find the parameters of the different model.

Figure 5.8 shows the breakthrough curve modeling with Yoon-Nelson, Thomas and Clark model for the adsorption run at 1°C and 100 ppm inlet H_2S concentration and 0.4L/min flow rate. The fit quality (R^2) values showed that Yoon-Nelson model fits the adsorption of H_2S on activated OFA better than other model. Thomas model is more accurate at higher exit concentrations but not good at lower concentration whereas Clark model better at lower concentrations. Yoon-Nelson model was further used to explain the effect of operating conditions on the breakthrough curves.

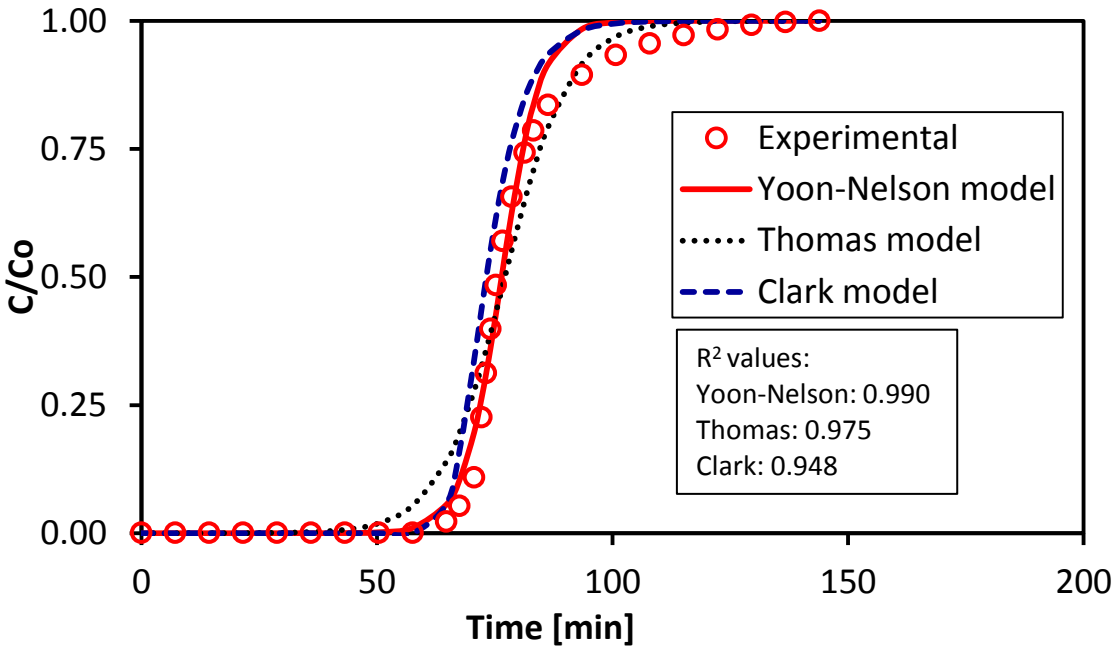

Figure 5-8: Breakthrough curve modeling with Yoon-Nelson, Thomas and Clark model for the adsorption run at 1°C and 100 ppm inlet H_2S concentration and 0.4L/min flow rate.

Effect of flow rate and concentration and inlet pressure

Figure 5.9 and Figure 5.10 represent experimental breakthrough curve and Yoon-Nelson model fit for different flow rates and inlet concentrations. The experimental and calculated values are listed in Table 5.6. The values of the regression coefficients and percentages error on calculating τ indicate that the predicted τ are very similar to the experimental one. The experimental and predicted breakthrough curves very close to each almost entire breakthrough region. Increase in flow rates and inlet concentrations shift the breakthrough curve to the left. Decreasing flow rate from 0.4 L/min to 0.2 L/min results in causes the column breakthrough time to increase three times. The inlet concentration is minimal on the breakthrough time for 100 ppm and 50 ppm inlet H_2S concentration.

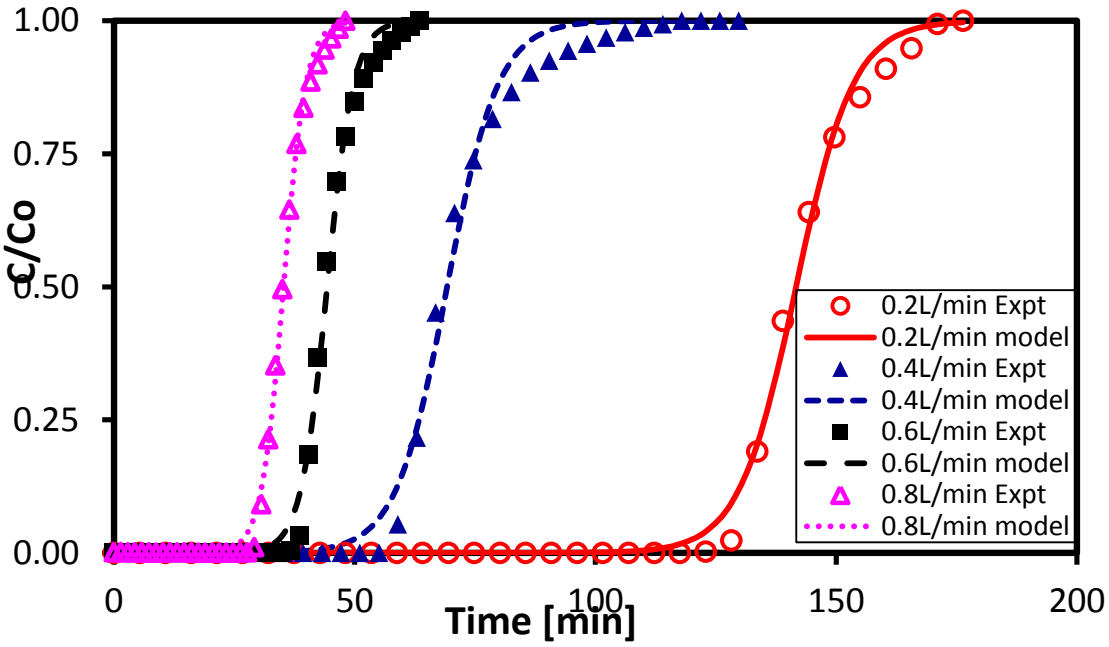

Figure 5-9: Comparison of the experimental and predicted breakthrough curves obtained at different flow rates according to the Yoon–Nelson model (temperature, 30°C; inlet conc., 100 ppm)

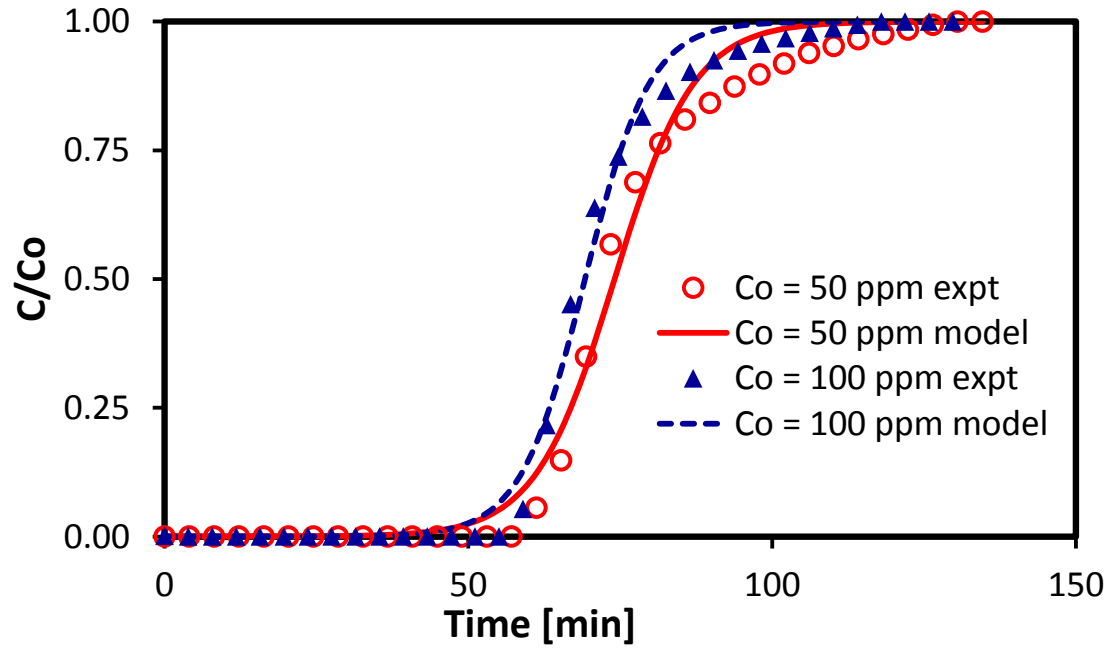

Figure 5-10: Comparison of the experimental and predicted breakthrough curves obtained at two inlet concentrations to the Yoon–Nelson model (temperature, 30°C; inlet conc., flow rate 0.4L/min)

Table 5–6: Yoon–Nelson model parameters (Effect of concentration and flow rate)

Co (ppm)	Q (L/min)	k_{YN} (min^{-1})	τ_{theo} (min)	τ_{exp} (min)	R^2	Error (%)
100	0.2	0.1689	141.68	140.30	0.996	0.99
100	0.4	0.1882	69.21	67.93	0.995	1.88
100	0.6	0.3638	44.29	49.70	0.996	-10.89
100	0.8	0.4313	35.23	35.01	0.998	0.63
50	0.4	0.1527	74.06	72.73	0.991	1.83

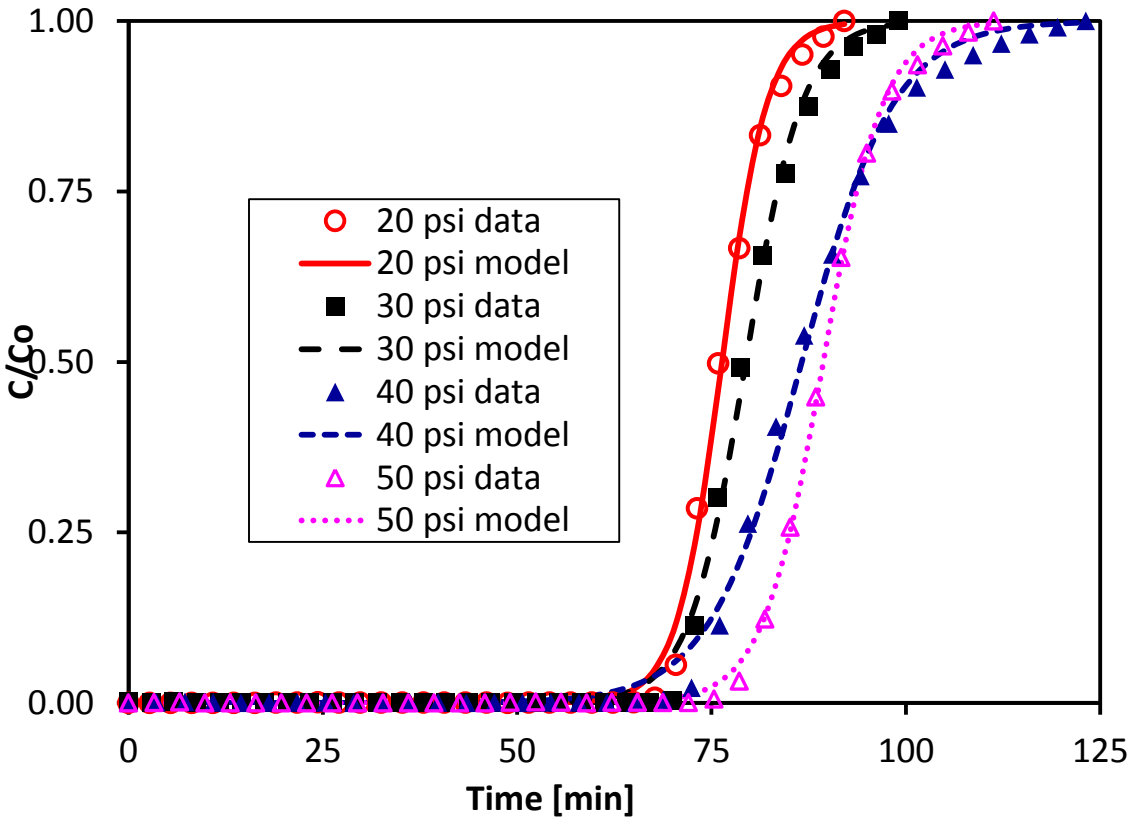

Figure 5-11: Effect operating pressure on breakthrough curve using Yoon-Nelson modeling

Table 5–7: Yoon–Nelson model parameters (Effect of Inlet pressure)

Inlet Pressure (psi)	Pressure drop (%)	Q (L/min)	k_{YN} (min^{-1})	τ_{theo} (min)	τ_{exp} (min)	R^2
20	4.17	0.4	0.342	76.34	76.15	0.997
30	4.26	0.4	0.274	79.40	79.65	0.997
40	5.15	0.4	0.186	86.61	85.75	0.996
50	5.45	0.4	00.257	89.37	89.85	0.991

Adsorption experiments were also conducted at different pressures (20 to 50 psi) to assess the effect of inlet pressure on the column breakthrough curve. The column breakthrough data were modeled using Yoon-Nelson model and it showed good agreement of data to fit the model as shown Figure 5.11. Yoon-Nelson model parameters are listed in Table 5.7. Pressure drop in column remains below 6% and the 50% breakthrough time increase from 76 to 89 min for 30 psi increase in pressure level.

5.4 Conclusion

This study suggests that a waste product (OFA) can be used a low cost adsorbent for removal of H_2S from natural gas. Physico-chemical treatment removes the undesired mineral matter from OFA and increase surface area which has boosted the adsorption capacity. H_2S uptake capacity increases up to 8.5 mg/g. Finally, physico-chemical activation of waste OFA sample can convert a waste product to valuable adsorbent and also can solve waste disposal problem. Kinetic of H_2S adsorption process follow pseudo first order model. Adsorption process is mainly physical (Ea<40kJ/mol) and spontaneous process (ΔG^* negative). DSL isotherm better explain the experimental data with dual site

adsorption characteristics of activated OFA. The utilization of activated OFA as low cost adsorbent can be effective to natural gas sweetening process as well as to solve waste disposal problems arises from power generation plant.

5.5 References

[1] W. Feng, S. Kwon, E. Borguet, R. Vidic, Adsorption of hydrogen sulfide onto activated carbon fibers: effect of pore structure and surface chemistry., Environ. Sci. Technol. 39 (2005) 9744–9.

[2] N. Wang, An investigation of H2S adsorption mechanisms on Tire Derived Rubber Particles (TDRP TM), Iowa State University, 2010.

[3] Y. Elsayed, M. Seredych, A. Dallas, T.J. Bandosz, Desulfurization of air at high and low H2S concentrations, Chem. Eng. J. 155 (2009) 594–602.

[4] Y. Xiao, S. Wang, D. Wu, Q. Yuan, Experimental and simulation study of hydrogen sulfide adsorption on impregnated activated carbon under anaerobic conditions., J. Hazard. Mater. 153 (2008) 1193–200.

[5] P. Forzatti, L. Lietti, Catalyst deactivation, 52 (1999) 165–181.

[6] E. Ashori, F. Nazari, F. Illas, Adsorption of H2S on carbonaceous materials of different dimensionality, Int. J. Hydrogen Energy. 39 (2014) 6610–6619.

[7] H.R. Godini, D. Mowla, Selectivity study of H_2S and CO_2 absorption from gaseous mixtures by MEA in packed beds, Chem. Eng. Res. Des. 86 (2008) 401–409.

[8] H. Su, S. Wang, H. Niu, L. Pan, A. Wang, Y. Hu, Mass transfer characteristics of H_2S absorption from gaseous mixture into methyldiethanolamine solution in a T-junction microchannel, Sep. Purif. Technol. 72 (2010) 326–334.

[9] M.J. Ledoux, C. Pham-huu, N. Keller, J. Nougayrède, S. Savin-poncet, J. Bousquet, Selective oxidation of H 2 S in Claus tail-gas over SiC supported NiS 2 catalyst, 61 (2000) 157–163.

[10] R.L. Mora, Sulphur condensation influence in Claus catalyst performance., J. Hazard. Mater. 79 (2000) 103–15.

[11] G.G. and Z.Z. Fred Soroushian, Yun Shang, Eliza Jane Whitman, DEVELOPMENT AND APPLICATION OF BIOLOGICAL H2S SCRUBBERS FOR TREATMENT OF DIGESTER GAS, Water Environ. Found. (2006) 3541–3547.

[12] A.D. Wiheeb, I.K. Shamsudin, M.A. Ahmad, M.N. Murat, J. Kim, M.R. Othman, Present technologies for hydrogen sulfide removal from gaseous mixtures, Rev. Chem. Eng. 29 (2013) 449–470.

[13] V. Mee, D.L. Trimm, N.W. Cant, Adsorption-Reaction Processes for the Removal of H y drogen Sulphide from Gas Streams *, 50 (1997).

[14] H.U.I.S.U.N. Choo, L.E.E.C. Lau, A.R. Mohamed, HYDROGEN SULFIDE ADSORPTION BY ALKALINE IMPREGNATED COCONUT SHELL ACTIVATED CARBON, 8 (2013) 741–753.

[15] N. Mohamad Nor, L.C. Lau, K.T. Lee, A.R. Mohamed, Synthesis of activated carbon from lignocellulosic biomass and its applications in air pollution control—a review, J. Environ. Chem. Eng. 1 (2013) 658–666.
[16] O. Hernandez-Ramirez, S.M. Holmes, Novel and modified materials for wastewater treatment applications, J. Mater. Chem. 18 (2008) 2751.
[17] J.-H. Wee, A review on carbon dioxide capture and storage technology using coal fly ash, Appl. Energy. 106 (2013) 143–151.
[18] H. Rostami, W. Brendley, Alkali ash material: a novel fly ash-based cement., Environ. Sci. Technol. 37 (2003) 3454–7.
[19] S. Andini, R. Cioffi, F. Colangelo, F. Montagnaro, L. Santoro, Adsorption of chlorophenol, chloroaniline and methylene blue on fuel oil fly ash., J. Hazard. Mater. 157 (2008) 599–604.
[20] S.O. Bada, S. Potgieter-vermaak, Evaluation and Treatment of Coal Fly Ash for Adsorption Application, (2008) 37–48.
[21] M. Azhar Uddin, Y. Shinozaki, N. Furusawa, T. Yamada, Y. Yamaji, E. Sasaoka, Preparation of activated carbon from asphalt and heavy oil fly ash and coal fly ash by pyrolysis, J. Anal. Appl. Pyrolysis. 78 (2007) 337–342.
[22] A. Al-Shawabkeh, H. MATSUDA, M. HASATMI, ComDarative Reactivity of Treated FBC- aid PCC-Fly Ash fbr SO2 Removal, Can. J. Chem. Eng. 73 (1995).
[23] A. Bagreev, T.J. Bandosz, A Role of Sodium Hydroxide in the Process of Hydrogen Sulfide Adsorption/Oxidation on Caustic-Impregnated Activated Carbons, Ind. Eng. Chem. Res. 41 (2002) 672–679.
[24] S.Y. J. Przepiorski, A. Oya, Structure of K 2 Co 3 -loaded activated carbon fiber and its deodorization ability against H 2 S gas, 37 (1999) 1881–1890.
[25] R. Shawabkeh, M.J. Khan, A. a. Al-Juhani, H.I. Al-Abdul Wahhab, I. a. Hussein, Enhancement of surface properties of oil fly ash by chemical treatment, Appl. Surf. Sci. 258 (2011) 1643–1650.
[26] M.B. Mustafa Arslan, The interaction of orthophosphoric acid and fly ash, Resour. Conserv. Recycl. 9 (1993) 295–310.
[27] M.I. Kandah, R. Shawabkeh, M.A. Al-Zboon, Synthesis and characterization of activated carbon from asphalt, Appl. Surf. Sci. 253 (2006) 821–826.
[28] M. Izquierdo, X. Querol, Leaching behaviour of elements from coal combustion fly ash: An overview, Int. J. Coal Geol. 94 (2012) 54–66.
[29] C. Hontoria-Lucas, a. J. López-Peinado, J. d. D. López-González, M.L. Rojas-Cervantes, R.M. Martín-Aranda, Study of oxygen-containing groups in a series of graphite oxides: Physical and chemical characterization, Carbon N. Y. 33 (1995) 1585–1592.
[30] A. Kumar, B. Prasad, I.M. Mishra, Isotherm and kinetics study for acrylic acid removal using powdered activated carbon., J. Hazard. Mater. 176 (2010) 774–83.
[31] M.H.M. Bakr, A.M.E. Gabre, Reduction of COD in Resin Production Wastewater Using Three Types of Activated Carbon, 1 (2013) 126–136.
[32] M.S. Shafeeyan, W.M.A.W. Daud, A. Houshmand, A. Shamiri, A review on surface modification of activated carbon for carbon dioxide adsorption, J. Anal. Appl. Pyrolysis. 89 (2010) 143–151.

[33] A. Buasri, N. Chaiyut, V. Loryuenyong, E. Phakdeepataraphan, S. Watpathomsub, V. Kunakemakorn, et al., Synthesis of Activated Carbon Using Agricultural Wastes from Biodiesel Production, (2013) 98–102.
[34] R.A. Shawabkeh, Synthesis and characterization of activated carbo-aluminosilicate material from oil shale, Microporous Mesoporous Mater. 75 (2004) 107–114.
[35] A. Travert, O. V Manoilova, A.A. Tsyganenko, F. Mauge, Effect of Hydrogen Sulfide and Methanethiol Adsorption on Acidic Properties of Metal Oxides : An Infrared Study, (2002) 1350–1362.
[36] Y. Wang, A.B.M. Saad, O. Saur, J.C. Lavalley, B.A. Morrow, FTIR study of adsorption and reaction of SO 2 and H 2 S on Na / SiO 2, 16 (1998) 279–290.
[37] Y.-W. Lee, J.-W. Park, J.-H. Choung, D.-K. Choi, Adsorption characteristics of SO2 on activated carbon prepared from coconut shell with potassium hydroxide activation., Environ. Sci. Technol. 36 (2002) 1086–92.
[38] A.M.M.S. Seehra, X-RAY DIFFRACTION ANALYSIS OF THE PARTICULATE MATTER IN RESIDUAL OIL FLYASH, (n.d.).
[39] A.L. Yaumi, I. a. Hussien, R. a. Shawabkeh, Surface modification of oil fly ash and its application in selective capturing of carbon dioxide, Appl. Surf. Sci. 266 (2013) 118–125.
[40] S. Katara, S. Kabra, A. Sharma, R. Hada, A. Rani, Surface Modification of Fly Ash by Thermal Activation : A DR / FTIR Study, 3 (2013) 299–307.
[41] N.M. Musyoka, L.F. Petrik, G. Balfour, W.M. Gitari, E. Hums, Synthesis of hydroxy sodalite from coal fly ash using waste industrial brine solution., J. Environ. Sci. Health. A. Tox. Hazard. Subst. Environ. Eng. 46 (2011) 1699–707.
[42] S. Tangjuank, N. Insuk, V. Udeye, J. Tontrakoon, Chromium (III) sorption from aqueous solutions using activated carbon prepared from cashew nut shells, 4 (2009) 412–417.
[43] S. Ilango, Equilibrium Sorption studies of Fe , Cu and Co ions in aqueous medium using activated Carbon prepared from Recinius Communis Linn ., (2008).

CHAPTER 6

Adsorption of H_2S from Natural Gas using treated Oil Fly Ash

This paper will be published in a book chapter in Conference proceedings

6.1 Introduction

Burning coal or oil at power production facilities produces a solid waste called fly ash. It comprises of silica, alumina, iron oxide and residual carbon. Some toxic elements like arsenic, cadmium, selenium, strontium, boron, chromium, cobalt and lead along with PAH (poly aromatic hydrocarbons) compounds and dioxins could also be present. These constituents vary in amount depending on the type of fuel and degree of combustion [1,2]. It is reported that 3 kg of ash are produced per 1000 L of fuel oil [3,4]. Tones of fly ash are being collected from power production facilities and are one of the major hazardous waste materials.

Currently, the most common industrial waste management practice of OFA is the dry disposal method, i.e. land disposal. Indeed, an uncontrolled and inadequate management at dumping site may cause a dispersion of particulate matter which may have major negative impact on environment [5,6]. Because of its low bulk density ($0.318/cm^3$) and fine particle size, it can travel long distances and may cast a danger to plants and animals in a variety of ways [7,8]. Although fly ash has received major attention as an environment pollutant but a close look reveals its multiple uses in various fields, and it may become a valuable resource. Nowadays, it mainly finds application as replacement of Portland cement, fillers in polymeric synthesis, asphalt and cementitious materials and in adsorption of various solutes from mixtures [9,10]. Because of carbonaceous contents and morphology of oil fly ash (OFA) has gained much attention as a low-cost adsorbent [11]. It is expected that with some chemical treatment, activated OFA can be utilized to remove toxic gases from gas mixture. Yaumi et al. modified OFA using ammonium hydroxide and studied the adsorption of CO_2 under various flow conditions. They noticed

the increase in adsorption capacity with higher concentration of CO_2 and flow rate [9]. Rubio and Izquierdo obtained promising results for SO_2 removal using activated carbon produced from oil agglomerated fly ash [12]. Wang et al. used fly ash to synthesize zeolite adsorbent for the treatment of waste water containing cationic dyes [13]. Visa and Duta synthesized a substrate by hydrothermal processing of fly ash and TiO_2 nano-powder. They reported an efficient and simultaneous removal of surfactant and heavy metals in a single step process [14].

The present study aims at increasing the surface area of raw OFA through physicochemical treatment. The produced treated OFA is used for the adsorption of H_2S. The success of such physicochemical activation in H_2S removal is expected to lead to the utilization of OFA as low cost activated carbon for removal of toxic gases such as H_2S. Materials and Methods

6.2 Raw-Material and Chemicals

Raw OFA was received from the Shuaibah power plant located in Saudi Arabia. It was dried overnight at 110°C in the oven to remove moisture and then sieved to 45µm mesh. Elemental composition and porosity characterization of raw material are given in Table6.1. The high percentage of carbon in treated ash makes it a good precursor for preparation of activated carbon. Sieved sample was saved in a closed cap bottle for future use.

The acid chemicals like nitric, phosphoric and sulfuric acid used in this study were of analytical grades and supplied by Panreac Company. CO_2 gas of 99.999% purity and natural gas containing 100 ppm H_2S were provided by Saudi Gas Company. All glass wares were of Pyrex, washed with demineralized water and dried in an oven at 105°C.

6.2.1 Activation of Oil Fly Ash (OFA)

The activation process includes two steps: acid treatment followed by CO_2 activation at higher temperature. A sample of 10 g OFA powder was treated with 200 ml of an acid mixture [comprises of 40 wt.% (16M) HNO_3, 40 wt.% (18 M) H_3PO_4 and 20 wt.% (18 M) H_2SO_4 in a round-bottom flask at 125°C for four hours under total reflux condition. The treated samples were filtered to get the solid residue. The residue was rinsed five times with distilled water to wash out the acid contents. Finally, the solid residue was dried in an oven for 5 hrs at 110°C.

After acid treatment, the dried ash was further activated with CO_2 at 990°C in a programmable Lindberg Blue M tube furnace. The furnace was programmed to increase the temperature at 50°C/min. Once the required temperature was achieved; a long horizontal column with ID of 1cm containing 6g sample was exposed to 990°C temperature for 1hr. The CO_2 was injected with inlet pressure of 2 bars at a flow rate of 1 L/min. After 1 hr of operation the furnace and CO_2 supply was switched off and sample was left to cool down to room temperature. Then the products were kept in a desiccator for further characterization. Samples with various degrees of burn off were obtained depending on their temperature of activation. The degree of burn off α (wt. %), is calculated as follows;

$$\alpha = \frac{M_i - M_f}{M_i}$$

Where M_i is the initial mass of chemically treated fly ash and M_f is the final mass of the sample after CO_2 activation.

Table 6–1: Elemental Composition and Porosimetric Characteristics of OFA

Element	Wt.%
C	84.20
O	4.67
S	6.20
Mg	0.08
Al	0.15
Ca	0.10
V	1.07
Cu	1.46
Ni	0.63
Zn	1.14
Fe	0.23
Si	0.06
BET Surface area (m^2/g)	2.03
Pore Volume (cm^3/g)	0.028
t-plot Micro pore Volume (cm^3/g)	0
Average Particle Size (4V/A) (°A)	260

6.2.2 Characterization of treated OFA

6.2.2.1 Surface area and Pore volume Determination

As explained in section 4.2.4.1

6.2.2.2 Surface Morphology

Explained in section 4.2.4.2

6.2.2.3 FTIR (Fourier Transform Infra-red Spectroscopic) Analysis

According to section 4.2.4.3.

6.2.2.4 H2S Adsorption Experiment

Described in detail in section 4.2.5

6.3 Results and Discussion

It is undoubtly accepted that adsorption capacity of a material largely depends on its porosimetric features. In general, the greater the specific surface area of an adsorbent the larger will be its uptake capacity [15, 16]. There are various reaction strategies that can be used to influence the porosity and to create some ordering of structure. In the following sections a detailed discussion on the pore development during physiochemical activation of OFA is given.

6.3.1 Development of porosity after Physicochemical treatment

Table 6.2 summarizes the variation in porosity at various stages of treatment of oil fly ash. Acid treatment of oil fly ash removes the most of the inorganic matter from the surface and inside of fly ash particles and produces micro and mesopores. Heating of ash with acid leached out most of the metals in the form of phosphates, sulfates and nitrates. Activation of ash with acid produces more mesopores than raw ash (see Fig. 6.1).Physical activation of fly ash with CO_2 at three different temperatures affects the surface area. Increases in temperature have proportional relation with porosity. With increase in temperature the weight loss also increases from 16.6% to 55%. This is because of higher reactivity of CO_2 with carbon at elevated temperature. At 330°C, reaction of CO_2 produces some micro pores as a result of which BET surface area increases. At 660°C,

both the meso porosity and micro porosity increase and surface area increases to above 100 m^2/g. Activation of acid treated ash at 990°C increases the micro and meso porosity as compared to lower temperatures. At higher temperature, removal of carbon atom first generates the micropores and pore enlarging with time produces more mesopores with the overall increase in surface area. Due to high porosity of treated OFA activated at 990°C, it was suggested to use it for break through experiments.

Table 6–2: Porosity Characteristics of Physicochemically treated fly ash

Sample	BET Surface area (m^2/g)	Weight Loss (%)	Pore Volume (Cm^3/g)	Pore Size(4V/A) (˚A)
OFA-acid	5.05	53.6	0.055	108
OFA-acid-CO_2 (*330°C)	15.65	16.6	0.063	101
OFA-acid-CO_2 (660°C)	119.76	29.3	0.095	70
OFA-acid-CO_2 (990°C)	375.06	55	0.3	49

*Bracketed number shows the temperature of activation of 'OFA-acid' during CO_2 activation

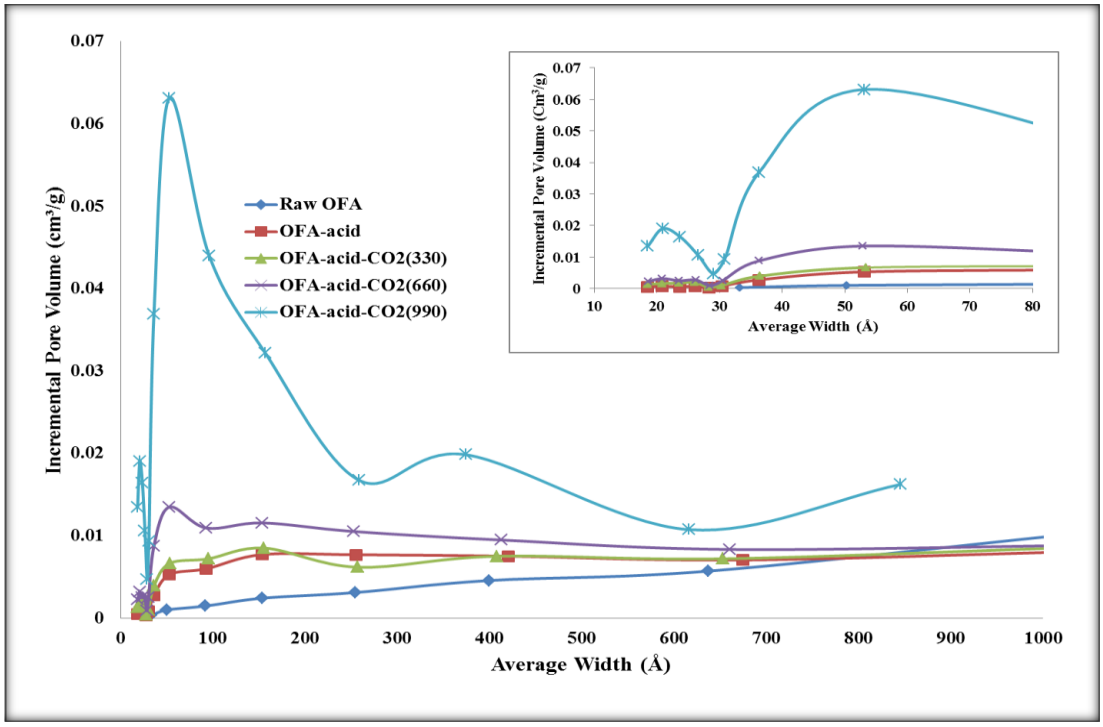

Figure 6-1: Pore Size Distribution of Raw and Treated OFA

6.3.2 FTIR (Fourier Transform infra-red) Spectroscopy

FTIR spectrums of the different ash samples are shown in Figure 6.2. A broad band appears between 3100-3550 cm^{-1} for raw fly ash with a minimum at 3400 cm^{-1}. This is due to stretching vibration of free and associated hydroxyl groups (-OH) on the virgin ash. Two peaks (1625 cm^{-1} and 1115 cm^{-1}) between 1100-1650 cm^{-1} are indicative of C=C symmetrical stretching and C-O stretching, respectively. The acid treatment of OFA has introduced oxygenated acidic surface groups which mainly include phenolic hydroxyl, carboxylic and lactones. A broad peak at 3400 cm^{-1} corresponds to OH functional group. Acid treatment has produced new peaks at 1715 cm^{-1} and 1605 cm^{-1} that represent the presence of C=O stretching of carboxylic acid and C=C stretching vibrations. A broad peak at 1230 cm^{-1} corresponds to C-O stretching vibrations was also observed.

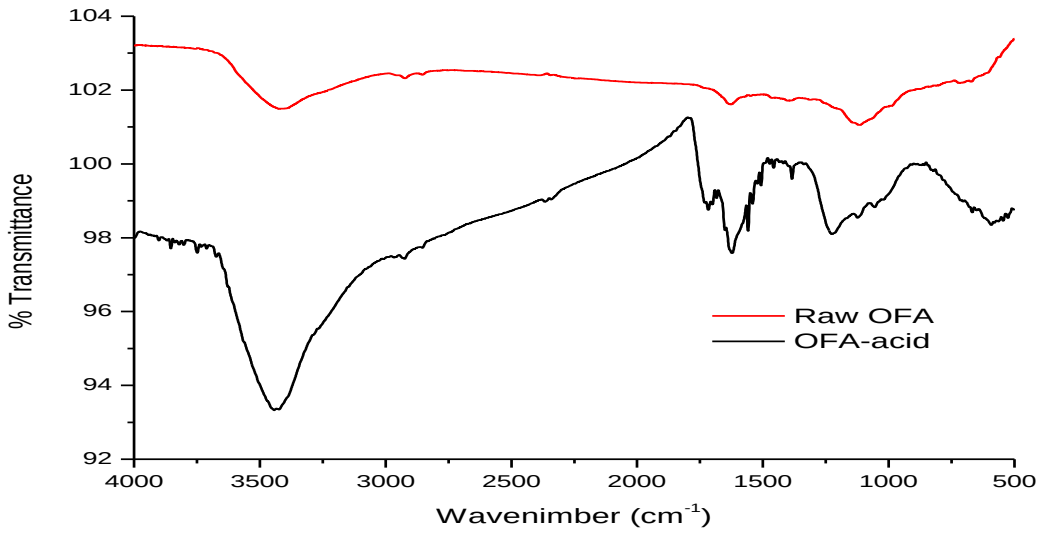

Figure 6-2: FTIR spectrum of raw and acid treated OFA

6.3.3 SEM (Scanning Electron Microscopy) Analysis

SEM analysis shows that fly ash particles are of spherical shapes. The porous texture can be seen in Fig.6.3 (a) where the pores of raw OFA range from few microns to larger pores. After acid treatment the fly ash surface is clearer and most of the pores are now in the range of macropores as shown in Fig.6.3 (b). All the foreign material has been removed by the acid. When the acid treated ash was subjected to CO_2 activation, more micro pores are produced and the surface area has increased (see Fig.6.3(c)).

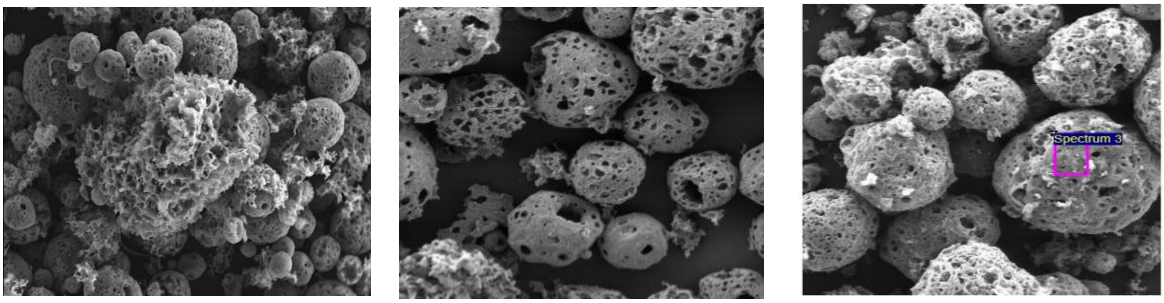

(a) Raw OFA (b)OFA-acid (c) OFA-acid-CO_2 (900°C)

Figure 6-3: SEM images of raw and activated ash

6.3.4 Breakthrough curves for H2S removal

Figures 6.4-6.6 show the behavior of raw and treated OFA. Adsorption capacity of ash has increased after acid treatment. But the adsorption capacity of acid treated ash is far less than the adsorption capacity of acid-CO_2 treated OFA. This is mainly due to two reasons. Firstly, the large number of micropores which were produced with CO_2 activation. Secondly, and the exposure of OFA-acid to high temperature under CO_2 atmosphere removes the acidic functional groups from the surface of ash and hence makes it more favorable for the adsorption of acidic gas. The wider gap between adsorption and desorption curves represents the chemisorption. Different models were

also being tested to fit the experimental data as shown in Table 6.3. BET isotherm data is found to be more accurate which suggests multilayer adsorption of H_2S on the surface of activated ash.

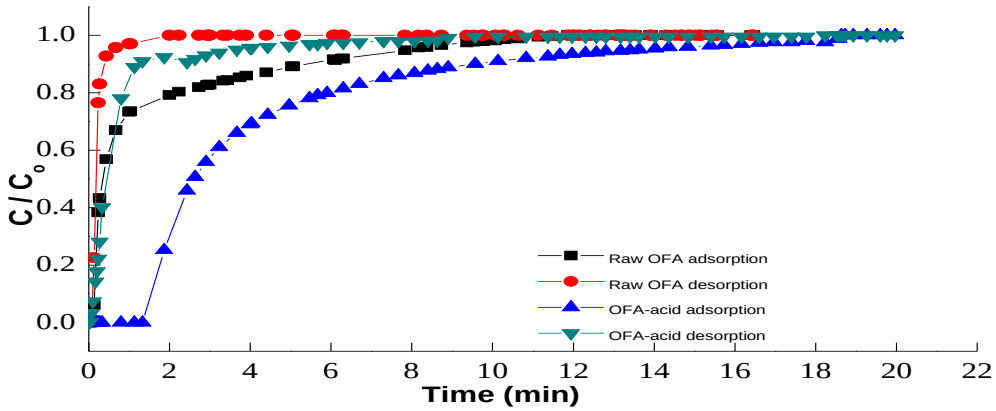

Figure 6-4: Breakthrough curve for raw and acid treated OFA

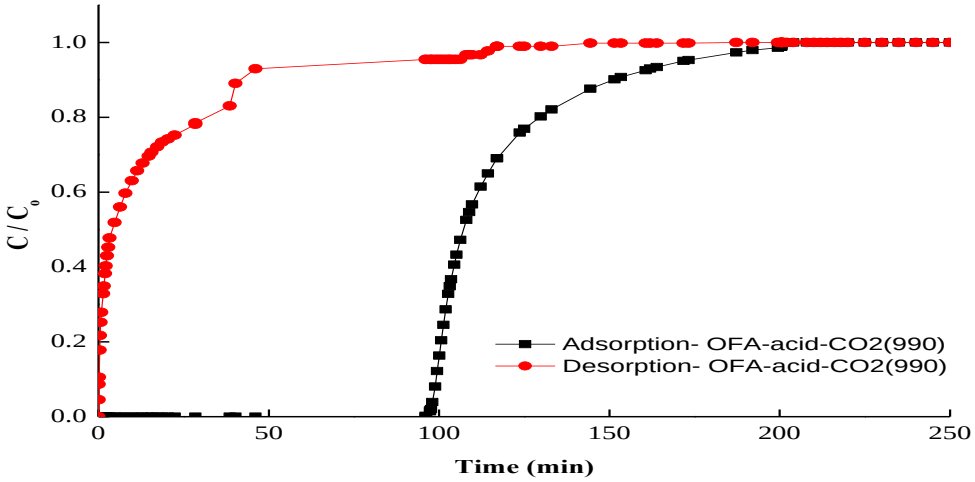

Figure 6-5: H_2S Break through Curve for OFA-acid-CO_2 (990)

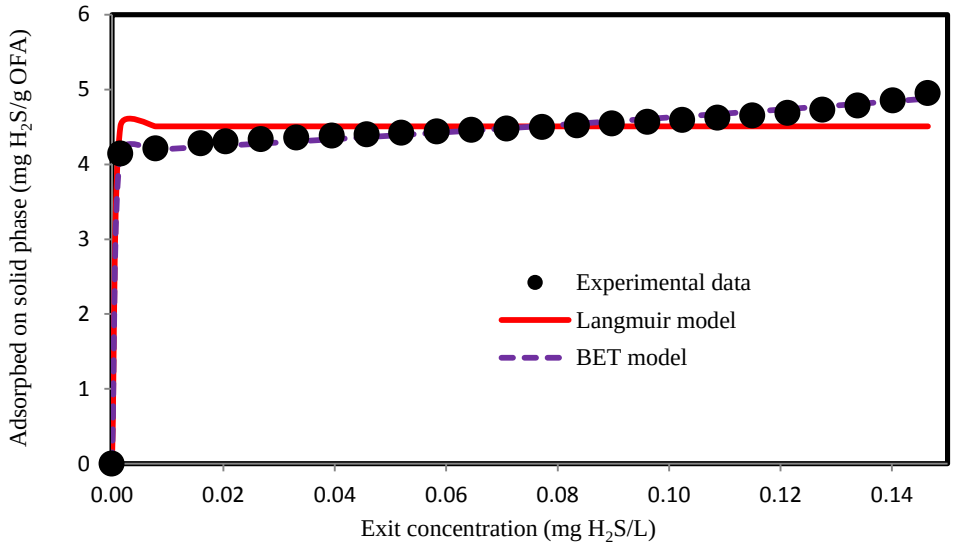

Figure 6-6: Modeling parameters of OFA-acid-CO_2(990).

Table 6–3: Regression parameters of OFA-acid-CO_2(990).

Langmuir Isotherm Parameters	**$q_{m\ (mg/g)}$**	4.508642
	K	804.3752
	R^2	0.95456
BET Isotherm Parameters	**$q_{m\ (mg/g)}$**	4.164059
	K	244620.4
	R^2	0.998179

6.4 Conclusions

Oil fly ash (OFA) is chemically treated using different acid mixtures as oxidizing agents followed by either steam or CO_2 activation. The oven temperature is maintained at three different temperatures namely 330, 660, and 990^{o}C. Characterization for surface area, pore size distribution and morphology is performed. The treatment with 40 wt.% (16M) HNO_3, 40 wt.% (18 M) H_3PO_4 and 20 wt.% (18 M) H_2SO_4 followed by CO_2 activation at 990 ^{o}C resulted in the highest surface area of 375 m^2/g. SEM images have shown more micro-pores and well developed particle size and porous structure resulting from steam activation at high temperature. The maximum adsorption capacity for H_2S from natural

gas, obtained at ambient conditions and a flow rate of 0.4 L/min, is found to be 4.9 mg/g. Chemisorption of H_2S on the surface is suggested by the sorption kinetics. The sorption isotherm shows a multilayer adsorption which fits BET equation.

6.5 References

[1] ECRA (Electricity & Cogeneration Regulatory Authority), 2012 Annual report 2012.

[2] M. A. Al-Gouti, Y. S. Al-Degs, A. Ghrair, H. Khoury, M. Ziedan, Chem. Eng. J., 173 (2011) 191– 197.

[3] Hsieh Y.-M., Tsai M.-S., Carbon, 41 (2003), 2317–2324.

[4] S.L. Tsai, M.S. Tsai, Mining. Metall., 41(2) (1997) 57–68.

[5] Mofarrah, T. Husain, C. Bottaro, Int. J. Environ. Sci. Technol., 2013.

[6] N. Jiang, K. L. Dreher, J. A. Dye, Y. Li,* J. H. Richards, L. D. Martin, K. B. Adler, Toxicol. Appl. Pharmacol. , 163(2000) 221–230.

[7] M. H. Al-Malack, A. A. Bukhari, O. S. Al-Amoudi, H. H. Al-Muhanna, T. H. Zaidi, Int. J. Environ. Res. , 7(2) (2013) 455-466.

[8] Fernandez, J. O.L. Wendt, N. Wolski, K. R.G. Hein, S. Wang, M. L. Witten, Chemosphere , 51 (2003) 1129–1137.

[9] A.L. Yaumi, I.A. Hussien, R.A. Shawabkeh, Surface modification of oil fly ash and its application in selective capturing of carbon dioxide. Appl. Surf. Sci., 2013; 266:118– 125.

[10] M.J. Khan, R.A. Shawabkeh, A.A. Al-Juhani, A. Ul-Hamid, I.A. Hussein, J. Polym. Res., 18 (6) (2011) 2275–2284.

[11] M. Ahmaruzzaman, Prog. Energy and Combust. Sci. , 36 (2010) 327–363.

[12] Rubio, M.T. Izquierdo, Waste Manag. , 30 (2010) 1341–1347.

[13] Wang, J. Li, L. Wang, X. Sun, J. Huang, Chin. J. Chem. Eng., 17(3) (2009)513-521.

[14] M. Visa, A. Duta, Chem. Eng. J., 223 (2013) 860–868.

[15] S. Guo, J. Peng, W. Li, K. Yang, L. Zhang, S. Zhang, H. Xia, Appl. Surf. Sci., 255 (2009) 8443–8449.

[16] M. Seggiania, S. Vitoloa, P. De Filippis, Fuel, 84 (2005) 1854–1857.

CHAPTER 7

Adsorption of Dyes on a waste oil fly ash based adsorbent from single and binary component aqueous Solution

(This paper is under preparation)

7.1 Introduction

Dye-bearing wastewater releases to aquatic biota from various industrial sources including textile, dye manufacturing, distillery, pharmaceutical, food, leather, cosmetics and paper industries. 7x 10^5 tones of dyes and pigments are produced each year and out of which 2% are directly discharged during manufacturing process and 10% are lost in dyeing operations[1]–[3]. Colored waste water poses a serious threat to aquatic living species by inhibiting light penetration and photosynthesis process and also blemishes the aesthetics of the environment. Being toxic in nature, dyes are also carcinogenic, mutagenic and can cause skin allergy to human beings[4], [5]. High volume of aqueous effluent discharged from various industries and stringent standards levied by government agencies calls for proper removal of dyes from the waste streams to the acceptable level[6]. Primarily, the constituting element of all the synthetic dyes are the complex aromatic and heterocyclic structure which render them as physio-chemically and thermally stable entity because of this structural stability , it is difficult to biodegrade[7].

These are various chemical, physical and biological methods to treat the dye-laden waste water. These include oxidative methods by either Fenton reagent (H_2O_2 – Fe(II) salt) or by ozone but both have some limitation due to the formation of sludge in oxidation with Fenton's reagent and short half-life of ozone in ozonation method . Degradation of dye molecules either photo chemically or by NaOCl and using cucurbituril have their own limitations and benefits[8]. On the other hand, biological degradation of dyes is a slow process which needs a favorable environment with proper maintenance and nutritional value[9], [10]. Physical treatment processes include membrane filtration[11], ion exchange[12] and numerous solid adsorbents. Among all the methods, adsorption with

re-generable sorbent is most attractive if the source of adsorbent is cheap and material is available abundantly. Large variety of solid adsorbents, ranging from clay minerals, agricultural waste, wood chips, peat, fly ash to industrial by-products, have been tested to check their efficiency for the treatment of dye-containing aqueous streams as shown in the table 7.1.

Table 7–1: Adsorbents used for the treatment of dye-containing aqueous solutions

Dye Stuff	Type of Adsorbent	Capacity (mg/g)	Reference
Basic blue 3 Basic yellow 21 Basic Red 22	Peat	390 300 240	[13]
Basic Red18 Acid Blue 9	Activated Clay	157 57.8	[14]
Rmazol red Ramazol Black B	Wood Chips	150 175	[15]
Orange-G	Baggase Fly ash	0.018	[7]
Methylene Blue	Coal Fly ash	15	[16]
Basic Blue Reactive Orange 16	Rice Hull	14 60	[17]
Ethyl Orange Metanil Yellow Acid Blue 13	Carbon Slurry of Fertilizer plant	198 211 219	[18]

It is concluded that the adsorption may be adopted as treatment process in industry for the dye removal and could be viable option if the source of adsorbent is cheap like oil fly ash. Huge amount of fly ash has been released from utility industries every year but only 30% is being utilized of total amount (700million per year) generated worldwide [19]. In US out of 150million ton fly ash per year only 27% is reused in different application while remaining is disposed of as landfill or surface impounded[20]. Depending upon the fuel

(i.e. solid or liquid) being burned, the constituents of fly ash vary considerably, but all the fly ash comprises of Aluminum oxide (Al_2O_3) and Silicon dioxide (SiO_2) with the traces of heavy metals. Exploiting the use of fly ash as a precursor of activated carbon is advantageous due to its cheap source, availability, and one step activation procedure as compared to conventional production of activated carbon by two step activation.

The objective of this work is to study the simultaneous removal of combination of different combinations of Methylene blue, Methyl orange and Rhodamine 6G from synthetic aqueous solution using amine treated fly ash. The study includes the effect of concentration of one dye on the removal of competing dye in the binary solution. Effect of pH was aslo examined. Kinetic data were collected by running different combination of dyes at different temperatures.

7.2 Experimental

7.2.1 Materials

The Methylene Blue (molecular formula: $C_{16}H_{18}CINSxH_20$, MW: 319.85 g/mol, Dye content: 82%, λ_{max} = 660nm) and Methyl orange (Molecular formula: $C_{14}H_{14}N_3NaO_3S$, MW: 327.34g/mol, λ_{max} = 460nm) were provided by LOBA Chemie and BDH Chemicals respectively and were used without prior purification. The Rhodium 6G (Molecular formula: $C_{28}H_{31}N_2O_3Cl$, MW: 479.01 g/mol, Dye content: 95%, λ_{max} = 523.5nm) from by Sigma Aldrich. Analytical grades Nitric and Phosphoric acids were delivered by Panearac Company, Spain. Ammonia solution (32% w/w) of density 0.9g/cm^3 was obtained from Scharlau Company, Spain. A separate stock solution of 500ppm of each dye was prepared by dissolving appropriate amount of dyes in double distilled water. Working concentrations

had been prepared by successive dilutions of stock solution. The oil fly ash used in the experiments was obtained from Rabigh power plant located in Jeddah, Saudi Arabia. All the glassware were washed with distilled water and dried in an oven at 105^{o}C before use.

7.2.2 Preparation of an Adsorbent

First of all, the received fly ash was sieved through BSS Taylor Sieve of 45-mesh and collect the under size ash. 15 g of ash was treated with 300mL of acidic solution (comprises of 10%HNO_3, 40% H_3PO_4, 50% water) in a round bottom flask and boiled under total reflux conditions for 4hrs. Then activated ash was filtered and the filter cake was washed with distilled water three times to remove the acid contents from the filter cake. The filter cake was put into the oven and dried at 105^{0}C. After getting enough amount of acid treated fly ash by repeated experiments, 80g of acid activated fly ash was mixed with 600mL of aqueous ammonia in a beaker and stirred for 6hr. 1500mL of water was further added into the beaker after 6hr and left it overnight. Fly ash was settled down at the bottom and filtered. Now the amine functionalized ash was dried in an oven at 105^{0}C. Dried amine functionalized ash was saved in a closed cap bottle for further use.

7.2.3 Batch Adsorption Experiments

All the adsorption experiments were carried out on a Thermo scientific shaker at 150rpm using Erlenmeyer flasks of 125ml capacity at 20^{0}C. Based on the preliminary tests to find out the adsorbent dose and equilibrium time, the experimental run time was fixed to 8hrs with 0.5g adsorbent ash. 100mL of dyes solution of various concentrations (as in the following table) have been prepared and contacted them with 0.5g of adsorbent. The solutions were shaking at 150rpm for 8hr and then left them overnight to settle down the ash particles. Then the solution was filtered to find out the subsequent concentration of

dye in aqueous solution. At time t = 0 and after equilibrium the methylene blue, methyl orange and Rhodamine 6G concentration was determined using UV-Spectrophotometer. The uptake of adsorbent, q_e (mg/g), was calculated by the following equation

$$q_e = \frac{(C_o - C_e)V}{W} \ldots\ldots\ldots\ldots\ldots \quad (7.1)$$

Where C_o (ppm) and C_e (ppm) are the initial and equilibrium concentration of dyes in solution respectively. V (mL) is the volume of dyes solution and W (g) is the weight of dried adsorbent. For pH experiments the equi concentration solution of different combination of dyes (Methylene blue& Methyl orange, Methylene blue & Rhodamine 6G, Methyl Orange & Rhdamine 6G) were tested by varying the pH from 2 to 11 and recorded the Concentration of dyes after adjusting the pH and after finishing the adsorption test. For Kinetic, the experiments were started with equi concentration of different combination of dyes and running the adsorption test at four different temperatures from 10˚C to 40˚C.the samples were collected at different times to record the concentration drop of dyes with time.

7.3 Characterization of an adsorbent

7.3.1 BET analysis of Adsorbent

Figure 7.1 shows the hysteresis in the N_2 adsorption test. The Hysteresis is associated with capillary condensation in mesoporous structure. The adsorption isotherm is closer to Type H3 adsorption isotherm in IUPAC system. This may be associated with slit shaped pores of adsorbent. Maximum amount of N_2 adsorbed is 0.78mmol/g and the hysteresis ends in the middle of relative pressure range of about 0.4. The table 7.2 summarizes the other physisorption characteristics.

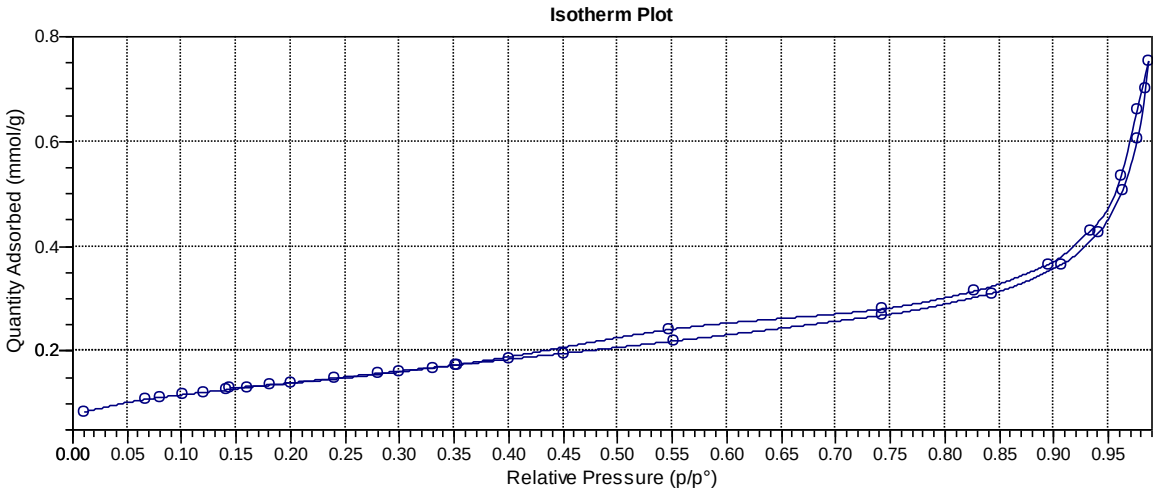

Figure 7-1: N_2 adsorption isotherm of fly ash activated carbon

Table 7–2: Physical adsorptive Characteristics of Activated carbon

BET Surface area	11.0656	m^2/g
Micropore Area	0.0173	m^2/g
BJH Cumulative adsorption pore volume	0.025527	Cm^3/g
BJH Cumulative desorption pore volume	0.022603	Cm^3/g

7.3.2 Scanning Electron Microscopy of Adsorbent

The figure 7.2 shows the scanned images of fly ash carbons before and after activation process. The fly ash carbon comprises of small spherical particles with some foreign materials adhere to its surface. Most of the surface is opaque and have very minute pores. After achieving it with acid and subsequent amine treatment, all the foreign materials have been removed and more clear pores with some mesopores can be seen from the figure 7.2(b).

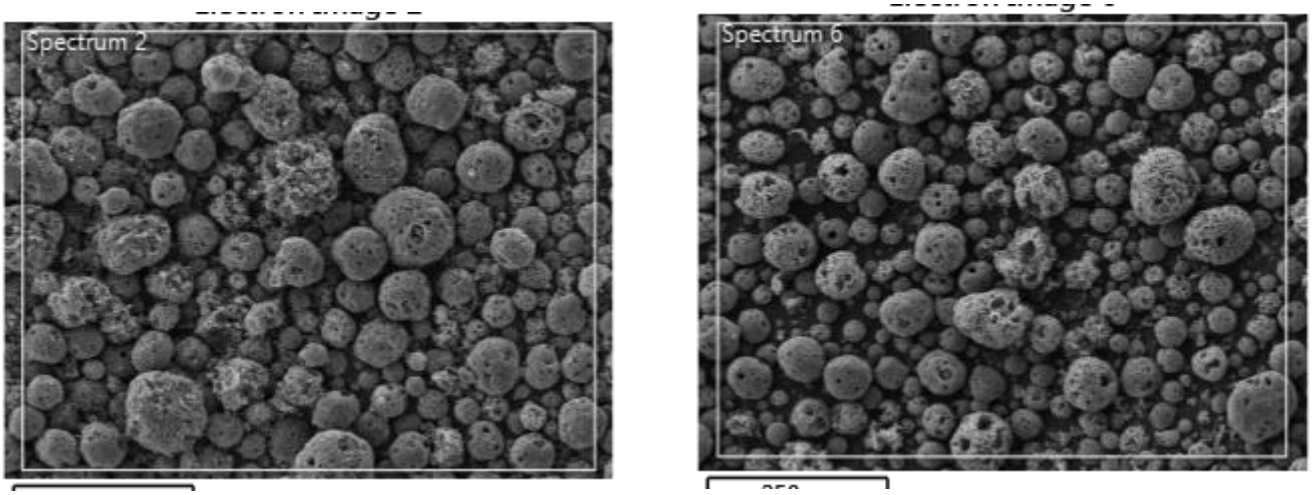

Figure 7-2: SEM images of Raw and activated fly ash carbons

7.3.3 Fourier Transform Infra-red Spectroscopy

In order to observe the various functional groups on the surface of raw and activated fly ash, Fourier Transform spectroscopy was done by scanning the sample from 400cm^{-1} to 4000cm^{-1} wavenumber and percent transmittance was recorded. Figure7.3 shows the IR spectrums of raw and modified ash. The spectrum of raw ash gives a peak at 3433cm^{-1} representing the presence of OH stretching vibrations of surface hydroxyl groups and chemisorbed water.Two small peaks between 2920cm^{-1} to 2850cm^{-1} are associated with symmetric and asymmetric stretching vibrations of aliphatic C-H groups. In the triple bond zone (2400-2100cm^{-1}), week peaks at 2361cm^{-1} and 2338cm^{-1} can be assigned to internal alkyne (C≡C) stretches. Two main peaks i.e. 1635cm^{-1} and 1123cm^{-1} appears in the lower wavenumber region, these may be regarded as the stretching of conjugated carbonyl (C=O) and C-O groups respectively. A small peak at 1384cm^{-1} is arising due to symmetrical bending vibrations of methyl C-H bond. It is noted that raw fly ash contains oxygenated functional groups including hydroxyl and carbonyl along with other unsaturated and saturated hydrocarbons. Activation of fly ash carbon not only produces

some new peaks but also increases or decreases the intensity of already existing peaks. Comparison of spectrum between 3000cm^{-1} to 3700 cm^{-1} demonstrates the clear change in the peak intensity. The resulting peak after chemical activation of raw ash is broadened with center at 3431cm^{-1}. This is associated with the overlapping bands of hydroxyl and amine stretching vibrations, which might be the result of hydrogen bonding between them and cannot conclusively divided into individual vibrations. The high intensity strong peaks at 2360cm^{-1} and 2340cm^{-1} can be assigned to -C≡N which could be formed during the reaction of raw ash with acid mixture. The stronger peak of nitrile in the activated fly ash spectrum as compared to alkyne peak in the raw ash is because of high polarity of -C≡N functional group.

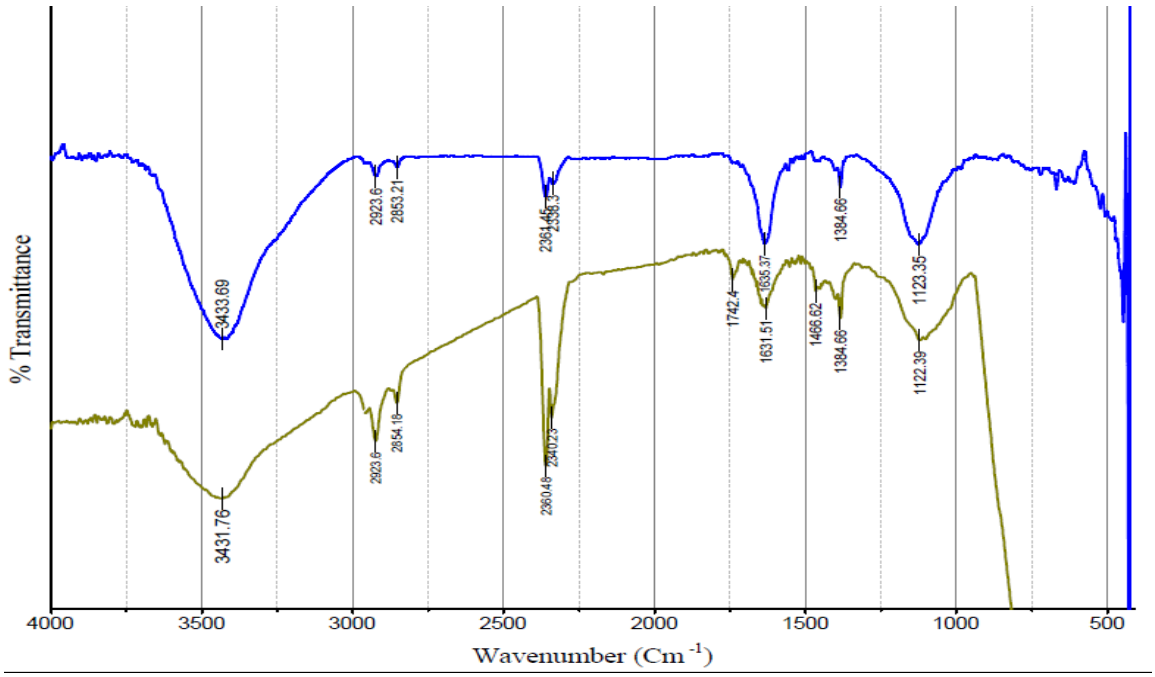

Figure 7-3: FTIR spectrum of raw and activated dye adsorbent

7.4 Results and Discussion

7.4.1 Effect of Concentration of Methylene Blue on Methyl Orange Removal

Binary component experiments were carried out with thirty six samples with same adsorbent concentration, Initial pH and solution temperature. The only difference was initial concentration of participant dyes. The table 7.3 summarizes the Effect of concentration of methylene blue on the removal of Methyl orange. It can be seen that the removal of methylene orange decreases as the concentration of methylene blue increases due to competition of two dyes for adsorption onto the adsorbent surface. But after the initial concentration of methylene blue goes beyond 60ppm the methyl orange uptake increases due to electrostatic interactions of two opposite dyes.

Table 7–3: Effect of concentration of Methylene blue(MB) on the removal of methyl orange (MO) (adsorbent dose = 0.5g, volume of solution = 100mL stirring speed = 150rpm)

$C_{o,MO}$	$C_{o,MB}$	$C_{eq,MO}$	$C_{eq,MB}$	$C_{eq,total}$	$q_{eq,MO}$	$q_{eq,MB}$	$q_{eq,total}$
(mg/L)	(mg/L)	(mg/L)	(mg/L)	(mg/L)	(mg/g)	(mg/g)	(mg/g)
1E-15	1E-15	0.0	0.0	0.0	0.0	0.0	0.0
20	1E-15	5.6	0.0	5.6	2.9	0.0	2.9
40	1E-15	9.5	0.0	9.5	6.1	0.0	6.1
60	1E-15	21.8	0.0	21.8	7.6	0.0	7.6
80	1E-15	31.4	0.0	31.4	9.7	0.0	9.7
100	1E-15	40.2	0.0	40.2	12.0	0.0	12.0
1E-15	20	0.0	0.0	0.0	0.0	4.0	4.0
20	20	4.9	0.4	5.3	3.0	3.9	6.9

40	20	13.0	0.3	13.3	5.4	3.9	9.3
60	20	31.2	0.2	31.4	5.8	4.0	9.7
80	20	44.4	0.3	44.7	7.1	3.9	11.1
100	20	53.0	0.6	53.6	9.4	3.9	13.3
1E-15	40	0.0	0.3	0.3	0.0	7.9	7.9
20	40	5.6	0.3	5.9	2.9	7.9	10.8
40	40	11.2	0.3	11.5	5.8	7.9	13.7
60	40	31.8	0.3	32.1	5.6	7.9	13.6
80	40	39.2	0.2	39.4	8.2	8.0	16.1
100	40	59.6	0.4	60.0	8.1	7.9	16.0
1E-15	60	0.0	0.4	0.4	0.0	11.9	11.9
20	60	6.5	0.3	6.8	2.7	11.9	14.6
40	60	16.7	0.3	17.0	4.7	11.9	16.6
60	60	32.5	0.4	32.9	5.5	11.9	17.4
80	60	45.2	0.5	45.6	7.0	11.9	18.9
100	60	59.6	0.4	60.0	8.1	11.9	20.0
1E-15	80	0.0	0.3	0.3	0.0	15.9	15.9
20	80	7.5	0.3	7.8	2.5	15.9	18.4
40	80	18.2	0.3	18.4	4.4	15.9	20.3
60	80	30.9	0.5	31.4	5.8	15.9	21.7
80	80	37.8	0.9	38.7	8.4	15.8	24.3
100	80	52.3	0.5	52.9	9.5	15.9	25.4
1E-15	100	0.0	0.3	0.3	0.0	19.9	19.9
20	100	6.9	0.3	7.2	2.6	19.9	22.6
40	100	17.1	0.4	17.5	4.6	19.9	24.5
60	100	27.0	0.5	27.5	6.6	19.9	26.5
80	100	34.5	0.5	35.0	9.1	19.9	29.0
100	100	49.2	0.5	49.7	10.2	19.9	30.1

7.4.2 Effect of Concentration of Rhodamine 6G on Methyl Orange Removal

The following table 7.4 summarizes the results of combination of Rhodamine 6G and Methyl Orang. The overall uptake of methyl orange is higher in this case as compared to methylene blue and methyl orange combination. The electrostatic interactions between cationic and anionic dyes were operative after the initial concentration of Rhodamine 6G (cationic dye) goes beyond 60ppm.

Table 7–4: Effect of concentration of Rhodamine 6G (Rh) on the removal of methyl orange (MO) (adsorbent dose = 0.5g, volume of solution = 100mL stirring speed = 150rpm)

$C_{o,MO}$	$C_{o,Rh}$	$C_{eq,MO}$	$C_{eq,Rh}$	$C_{eq,total}$	$q_{eq,MO}$	$q_{eq,Rh}$	$q_{eq,total}$
(mg/L)	(mg/L)	(mg/L)	(mg/L)	(mg/L)	(mg/g)	(mg/g)	(mg/g)
1E-15	1E-15	0.0	0.0	0.0	0.0	0.0	0.0
20	1E-15	5.1	0.0	5.1	3.0	0.0	3.0
40	1E-15	8.7	0.0	8.7	6.3	0.0	6.3
60	1E-15	19.8	0.0	19.8	8.0	0.0	8.0
80	1E-15	28.5	0.0	28.5	10.3	0.0	10.3
100	1E-15	36.4	0.0	36.4	12.7	0.0	12.7
1E-15	20	0.0	0.4	0.4	0.0	3.9	3.9
20	20	5.5	0.8	6.3	2.9	3.8	6.7
40	20	16.7	1.9	18.6	4.7	3.6	8.3
60	20	30.6	3.3	33.9	5.9	3.3	9.2
80	20	41.6	4.5	46.2	7.7	3.1	10.8
100	20	50.0	6.0	55.9	10.0	2.8	12.8
1E-15	40	0.0	0.5	0.5	0.0	7.9	7.9

20	40	7.5	1.0	8.4	2.5	7.8	10.3
40	40	17.3	2.0	19.4	4.5	7.6	12.1
60	40	31.1	3.4	34.4	5.8	7.3	13.1
80	40	43.4	4.7	48.1	7.3	7.1	14.4
100	40	50.0	6.1	56.0	10.0	6.8	16.8
1E-15	60	0.0	0.6	0.6	0.0	11.9	11.9
20	60	5.3	0.9	6.1	2.9	11.8	14.8
40	60	12.8	1.6	14.3	5.4	11.7	17.1
60	60	26.8	3.1	29.9	6.6	11.4	18.0
80	60	40.9	4.4	45.3	7.8	11.1	18.9
100	60	50.0	5.7	55.7	10.0	10.9	20.9
1E-15	80	0.0	0.5	0.5	0.0	15.9	15.9
20	80	1.7	1.8	3.5	3.7	15.6	19.3
40	80	10.7	1.4	12.0	5.9	15.7	21.6
60	80	19.3	2.2	21.5	8.1	15.6	23.7
80	80	36.4	4.0	40.4	8.7	15.2	23.9
100	80	37.5	4.0	41.4	12.5	15.2	27.7
1E-15	100	0.0	0.6	0.6	0.0	19.9	19.9
20	100	2.0	6.5	8.5	3.6	18.7	22.3
40	100	4.7	0.8	5.6	7.1	19.8	26.9
60	100	13.1	1.6	14.7	9.4	19.7	29.1
80	100	28.0	3.1	31.0	10.4	19.4	29.8
100	100	28.4	3.0	31.4	14.3	19.4	33.7

7.4.3 Effect of Concentration of Methylene Blue on Rhodamine 6G Removal

The table 7.5 shows that the decreases in uptake of Rhodamine 6G as the concentration of methylene blue increase. It seems that the adsorbent surface is more attractive for methylene blue.

Table 7–5: Effect of concentration of Methylene Blue (MB) on the removal of Rhodamine 6G (Rh) (adsorbent dose = 0.5g, volume of solution = 100mL stirring speed = 150rpm)

$C_{o,\ Rh}$	$C_{o,MB}$	$C_{eq,\ Rh}$	$C_{eq,MB}$	$C_{eq,total}$	$q_{eq,Rh}$	$q_{eq,MB}$	$q_{eq,total}$
(mg/L)	(mg/L)	(mg/L)	(mg/L)	(mg/L)	(mg/g)	(mg/g)	(mg/g)
1E-15	1E-15	0.0	0.0	0.0	0.0	0.0	0.0
20	1E-15	0.4	0.0	0.4	3.9	0.0	3.9
40	1E-15	0.5	0.0	0.5	7.9	0.0	7.9
60	1E-15	0.6	0.0	0.6	11.9	0.0	11.9
80	1E-15	0.5	0.0	0.5	15.9	0.0	15.9
100	1E-15	0.6	0.0	0.6	19.9	0.0	19.9
1E-15	20	0.0	0.4	0.4	0.0	3.9	3.9
20	20	0.5	0.4	0.8	3.9	3.9	7.8
40	20	0.5	0.4	0.9	7.9	3.9	11.8
60	20	0.8	0.3	1.1	11.8	3.9	15.8
80	20	1.7	0.2	2.0	15.7	4.0	19.6
100	20	3.2	0.2	3.4	19.4	4.0	23.3
1E-15	40	0.0	0.4	0.4	0.0	7.9	7.9
20	40	0.4	0.3	0.7	3.9	7.9	11.9

40	40	0.5	0.3	0.8	7.9	7.9	15.8
60	40	0.9	0.3	1.2	11.8	7.9	19.8
80	40	2.9	0.3	3.2	15.4	7.9	23.4
100	40	8.4	0.3	8.7	18.3	7.9	26.3
1E-15	60	0.0	0.3	0.3	0.0	11.9	11.9
20	60	0.4	0.3	0.7	3.9	11.9	15.9
40	60	17.9	1.8	19.8	4.4	11.6	16.0
60	60	3.9	0.3	4.2	11.2	11.9	23.2
80	60	6.5	0.3	6.8	14.7	11.9	26.6
100	60	12.6	0.3	12.9	17.5	11.9	29.4
1E-15	80	0.0	0.3	0.3	0.0	15.9	15.9
20	80	0.5	0.3	0.8	3.9	15.9	19.8
40	80	8.6	0.9	9.4	6.3	15.8	22.1
60	80	5.3	0.3	5.6	10.9	15.9	26.9
80	80	17.9	2.2	20.2	12.4	15.6	28.0
100	80	17.6	1.1	18.7	16.5	15.8	32.3
1E-15	100	0.0	0.3	0.3	0.0	19.9	19.9
20	100	1.1	0.3	1.4	3.8	19.9	23.7
40	100	5.8	1.3	7.1	6.8	19.7	26.6
60	100	15.1	1.7	16.9	9.0	19.7	28.6
80	100	17.9	2.8	20.7	12.4	19.4	31.9
100	100	20.1	6.0	26.1	16.0	18.8	34.8

7.4.4 Effect of pH on adsorption of dyes with binary solution

As can be seen from the figure 7.4 for all examined pH range the methylene blue was completely removed in the combination of methylene blue and methyl orange. As compared to methylene blue the methyl orange was only removed 90%. As can be seen in the graph the concentrations of both dyes were reduced during pH adjustment. This could be due to some structural changes and possible reaction between two dyes.

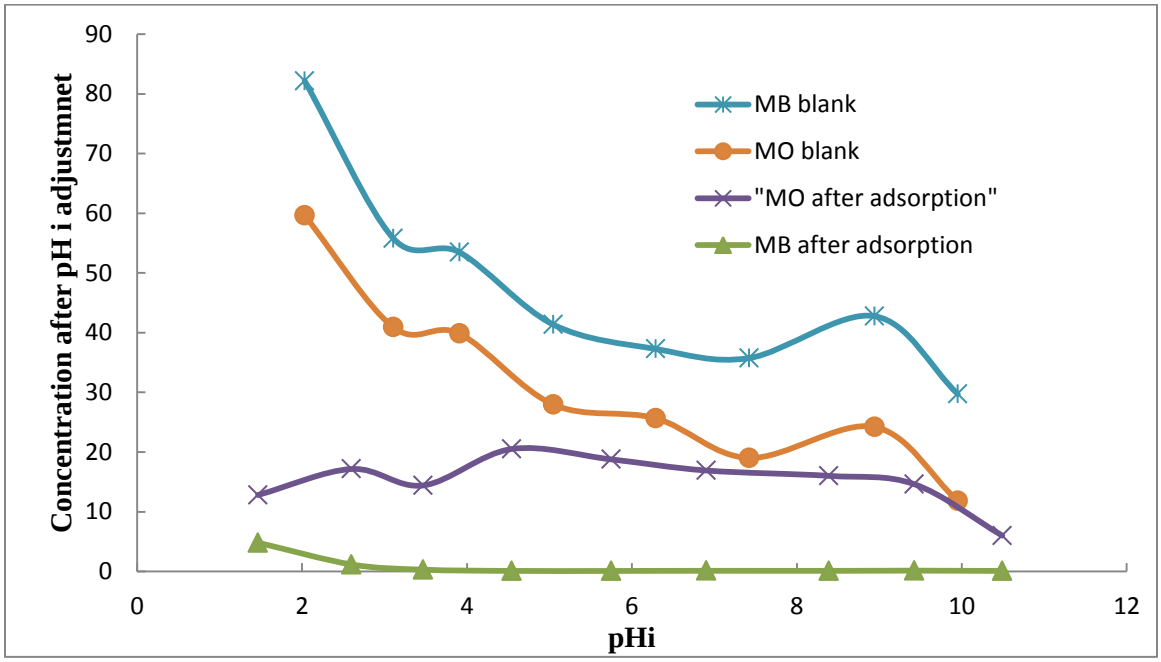

Figure 7-4: Effect of pH on the Binary (MB-MO) dye solution

Figure 7.5 shows the effect of pH on the adsorption of Methylene blue and Rhodamine 6G combination. The initial concentration of both dyes seems to be ineffective with tested pH range but after the solution is contacted with adsorbent there is a clear difference between the final concentrations of each dye. Methylene blue was 100% removed for all pH range but the Rhodamine concentration is slightly deviated from its initial concentrations

For Methyl orange and Rhodamine combinations (Figure 7.6), the Rhodamine is more likely to adsorb on the surface as compared to methyl orange. This may be due to surface characteristics of solid adsorbent of due to molecular size of dyes. The initial concentration of methyl orange passes through the maximum during pH adjustment of binary solution. This shows the structure changes of Methyl orange at lower pH and solubility effects at higher pH.

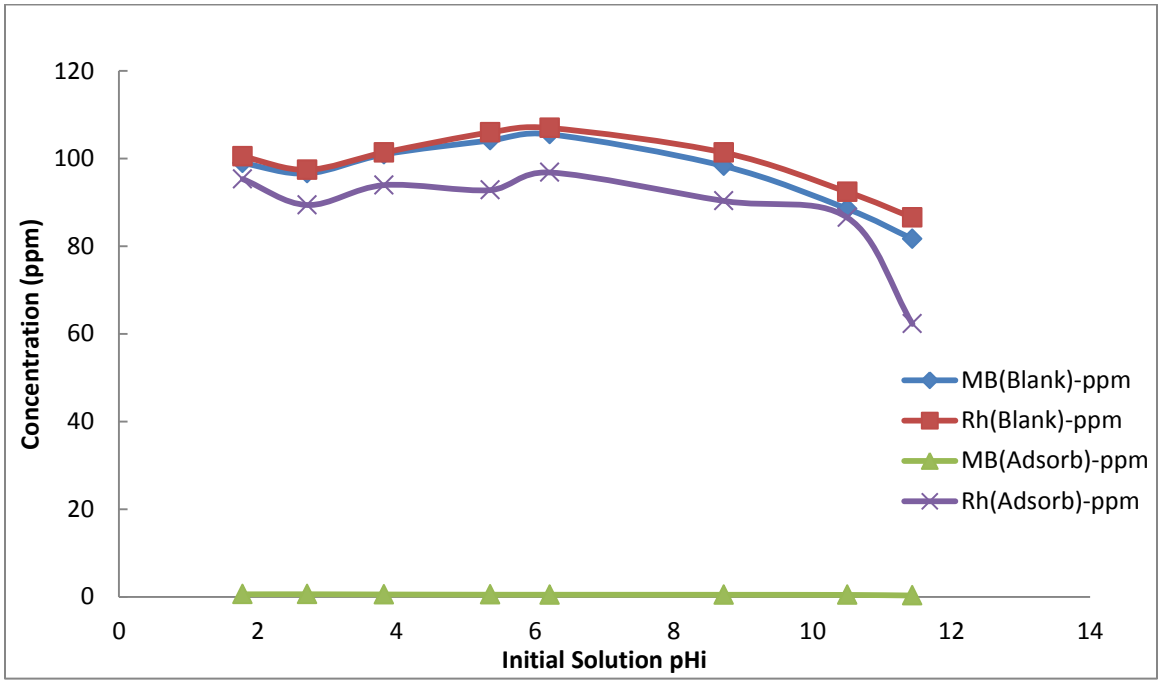

Figure 7-5: Effect of pH on the Binary (MB-Rh) dye solution

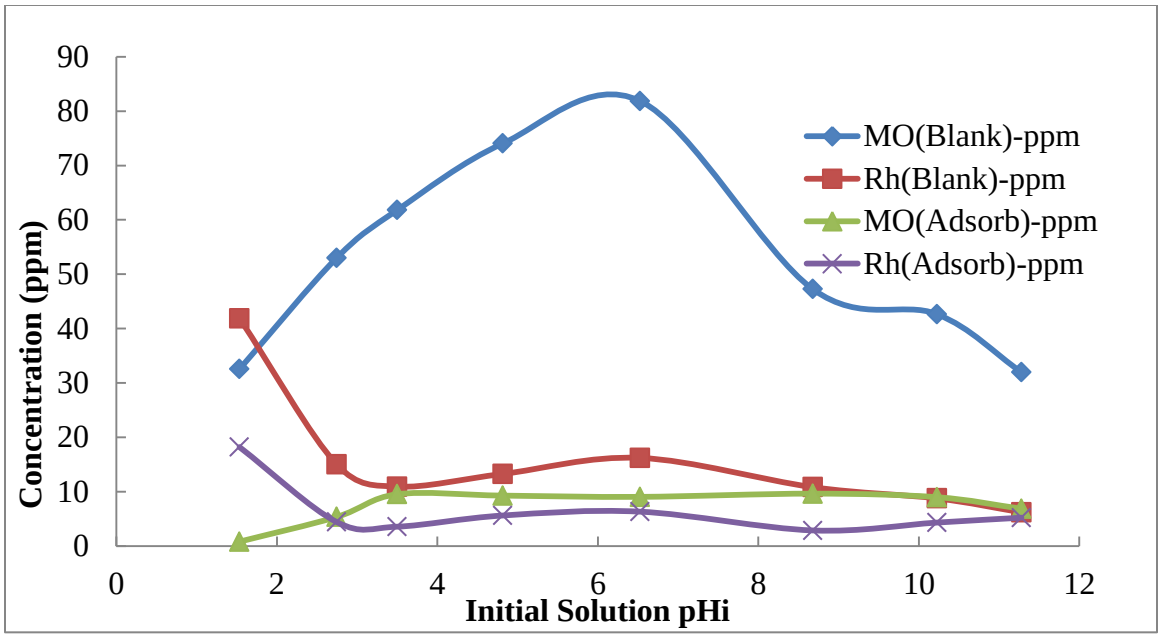

Figure 7-6: Effect of pH on the Binary (MO-Rh) dye solution

7.4.5 Effect of Temperature on the adsorption of Dyes

As a single dye solution all three dyes show the endothermic nature of adsorption. This is because of greater movement of solute molecules and there would be a greater probability of interaction of and collisions of solute molecules to adsorbent surface. And as a result the adsorption uptake increases with rise in temperature. But for the case of adsorption in binary solution the two combinations like Methylene blue with methyl orange and Rhodamine 6G with methylene blue revert the thermodynamics and shows exothermic adsorption as shown in the figure 7.7 and 7.8

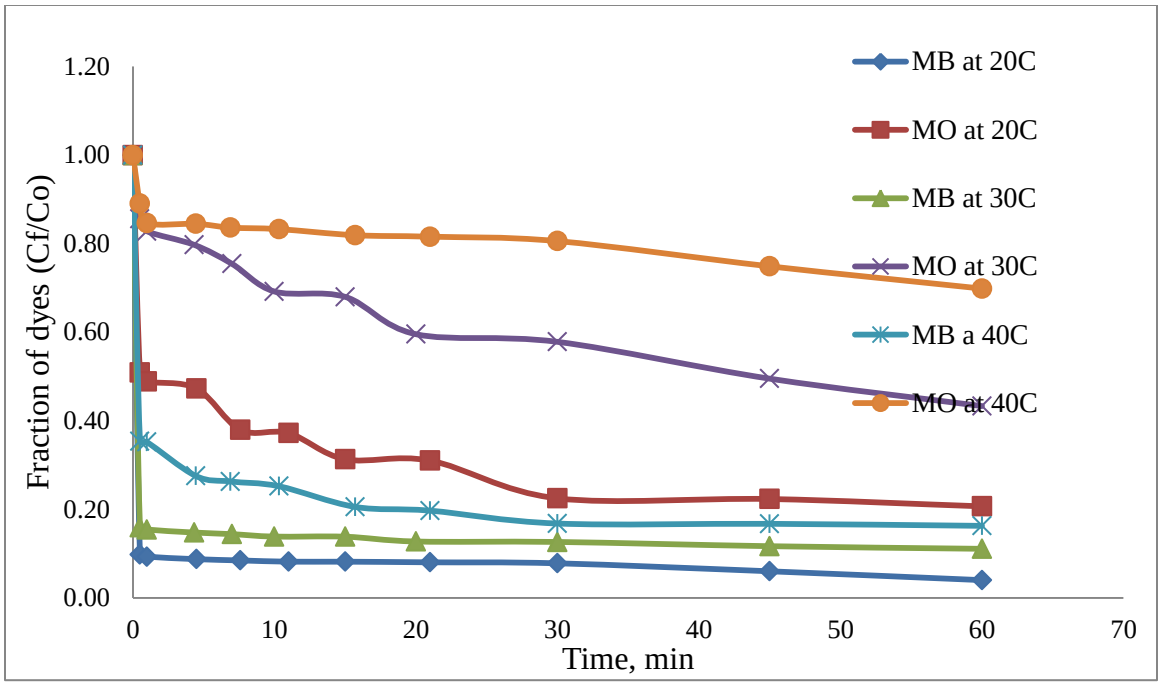

Figure 7-7: Kinetic data at different temperatures for MB and MO combination.

For the combination of Methyl orange and Rhodamine (figure 7.9) the system follows the endothermic behavior of adsorption of both dyes. But the concentration reduction of Rhodamine 6G is higher than its concentration reduction as single component it means there is possible reaction between methyl orange and Rhodamine 6G. The Methyl orange concentration at 40C isotherm is lower as compared to its concentration as single dye adsorption. This strength the point that the reaction between Rhodamine and methyl orange dyes or there possible structures combinations.

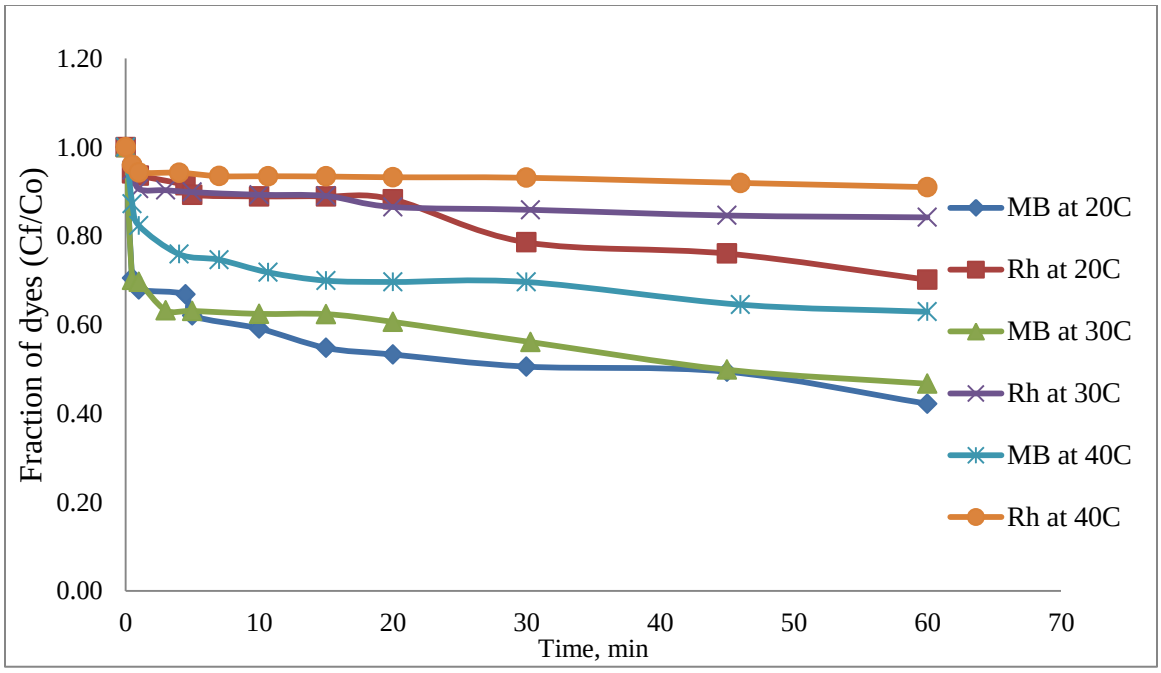

Figure 7-8: Kinetic data for MB and Rh combination at different temperatures

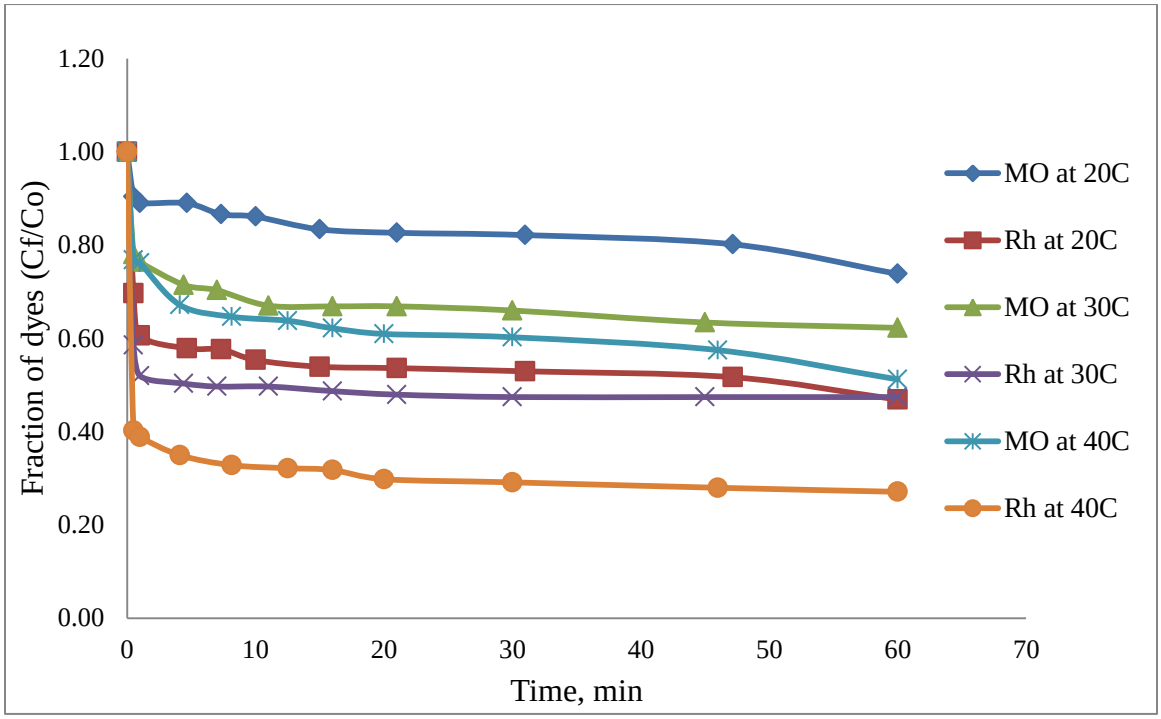

Figure 7-9: Kinetic data at different temperatures for MB and Rh combination

7.5 Conclusion

It can be concluded that the fly ash adsorbent can be a cheap source for the removal of dyes from waste water. The overall adsorption capacity of Cationic dyes (Methylene Blue and Rhodamine 6G) is higher (~19.9mg/g) than anionic dyes (~ 12mg/g). Adsorption an experiment with binary solution comprises of cationic and anionic combinations of dyes shows synergistic effect. Solution comprises of only cationic dyes (Methylene Blue and Rhodamine 6G) exhibits a constant uptake for all concentration tested. Kinetic data shows the endothermic adsorption of all three dyes as single component adsorption. During binary component adsorption some combination (like methylene blue / methyl orange and methylene blue / Rhodamine 6G) exhibits exothermic adsorption while the solution comprises of Rhodamine 6G and Methyl orange presents endothermic adsorption.

7.6 References

[1] A. Asghar, A. A. Abdul Raman, and W. M. A. W. Daud, "Advanced Oxidation Processes for In-situ production of Hydrogen peroxide/Hydroxyl radical for Textile Wastewater Treatment: A Review," *J. Clean. Prod.*, Sep. 2014.

[2] Z. Zhang, I. M. O'Hara, G. a. Kent, and W. O. S. Doherty, "Comparative study on adsorption of two cationic dyes by milled sugarcane bagasse," *Ind. Crops Prod.*, vol. 42, no. March, pp. 41–49, Mar. 2013.

[3] Z. Eren, "Ultrasound as a basic and auxiliary process for dye remediation: a review.," *J. Environ. Manage.*, vol. 104, pp. 127–41, Aug. 2012.

[4] K. H. Gonawala and M. J. Mehta, "Removal of Color from Different Dye Wastewater by Using Ferric Oxide as an Adsorbent," vol. 4, no. 5, pp. 102–109, 2014.

[5] D. Sun, X. Zhang, Y. Wu, and X. Liu, "Adsorption of anionic dyes from aqueous solution on fly ash.," *J. Hazard. Mater.*, vol. 181, no. 1–3, pp. 335–42, Sep. 2010.

[6] X.-C. Jin, G.-Q. Liu, Z.-H. Xu, and W.-Y. Tao, "Decolorization of a dye industry effluent by Aspergillus fumigatus XC6.," *Appl. Microbiol. Biotechnol.*, vol. 74, no. 1, pp. 239–43, Feb. 2007.

[7] I. D. Mall, V. C. Srivastava, N. K. Agarwal, and I. M. Mishra, "Removal of congo red from aqueous solution by bagasse fly ash and activated carbon: kinetic study and equilibrium isotherm analyses.," *Chemosphere*, vol. 61, no. 4, pp. 492–501, Oct. 2005.

[8] T. Robinson, G. Mcmullan, R. Marchant, and P. Nigam, "Remediation of dyes in textile e uent : a critical review on current treatment technologies with a proposed alternative," vol. 77, pp. 247–255, 2001.

[9] I. M. Banat, P. Nigam, D. Singh, and R. Marchant, “MICROBIAL DECOLORIZATION OF TEXTILE-DYE- CONTAINING EFFLUENTS : A REVIEW,” vol. 58, no. 1996, pp. 217–227, 1997.
[10] G. Crini, “Non-conventional low-cost adsorbents for dye removal: a review.,” *Bioresour. Technol.*, vol. 97, no. 9, pp. 1061–85, Jun. 2006.
[11] Y. Xu, R. E. Lebrun, P.-J. Gallo, and P. Blond, “Treatment of Textile Dye Plant Effluent by Nanofiltration Membrane,” *Sep. Sci. Technol.*, vol. 34, no. 13, pp. 2501–2519, Sep. 1999.
[12] Y. M. Slokar and A. M. Le Marechal, “Methods of Decoloration of Textile Wastewaters,” vol. 37, no. 4, pp. 335–356, 1998.
[13] S. J. Allen, “Multi-component Sorption Isotherms of Basic Dyes onto Peat,” vol. 52, pp. 39–53, 1988.
[14] Y. Ho and C. Chiang, “REMOVAL FROM AQUEOUS SOLUTION INTRODUCTION,” vol. 36, no. 11, pp. 2473–2488, 2001.
[15] P. Nigam, G. Armour, I. M. Banat, D. Singh, and R. Marchant, “Physical removal of textile dyes from e , uents and solid-state fermentation of dye-adsorbed agricultural residues,” vol. 72, pp. 219–226, 2000.
[16] T. Viraraghavan and K. R. Ramakrishna, “Fly ash for colour removal from synthetic dye solutions,” no. March, p. 1999, 1999.
[17] S. T. Ong, C. K. Lee, and Z. Zainal, “Removal of basic and reactive dyes using ethylenediamine modified rice hull.,” *Bioresour. Technol.*, vol. 98, no. 15, pp. 2792–9, Nov. 2007.
[18] a. . Jain, V. . Gupta, and a Bhatnagar, “Utilization of industrial waste products as adsorbents for the removal of dyes,” *J. Hazard. Mater.*, vol. 101, no. 1, pp. 31–42, Jul. 2003.
[19] J.-H. Wee, “A review on carbon dioxide capture and storage technology using coal fly ash,” *Appl. Energy*, vol. 106, pp. 143–151, Jun. 2013.
[20] H. Rostami and W. Brendley, “Alkali ash material: a novel fly ash-based cement.,” *Environ. Sci. Technol.*, vol. 37, no. 15, pp. 3454–7, Aug. 2003.
[21] J. D. S. Macedo, N. B. da Costa Júnior, L. E. Almeida, E. F. D. S. Vieira, A. R. Cestari, I. D. F. Gimenez, N. L. Villarreal Carreño, and L. S. Barreto, “Kinetic and calorimetric study of the adsorption of dyes on mesoporous activated carbon prepared from coconut coir dust.,” *J. Colloid Interface Sci.*, vol. 298, no. 2, pp. 515–22, Jun. 2006.
[22] M. O. Dye, M. Danish, R. Hashim, and M. N. M. Ibrahim, “com Characterization of Physically Activated Acacia mangium Wood-Based Carbon for the Removal of Methyl Orange Dye,” vol. 8, no. Tsyganova, pp. 4323–4339, 2013.
[23] R. Gong, J. Ye, W. Dai, X. Yan, J. Hu, X. Hu, S. Li, and H. Huang, “Adsorptive Removal of Methyl Orange and Methylene Blue from Aqueous Solution with Finger-Citron-Residue-Based Activated Carbon,” 2013.
[24] M. Turabik, “Adsorption of basic dyes from single and binary component systems onto bentonite: simultaneous analysis of Basic Red 46 and Basic Yellow 28 by first order derivative spectrophotometric analysis method.,” *J. Hazard. Mater.*, vol. 158, no. 1, pp. 52–64, Oct. 2008.

[25] O. S. Chan, W. H. Cheung, and G. McKay, “Single and multicomponent acid dye adsorption equilibrium studies on tyre demineralised activated carbon,” *Chem. Eng. J.*, vol. 191, pp. 162–170, May 2012.

Vitae

Name	HAFIZ MUHAMMAD ZAHEER ASLAM
Nationality	Pakistani
Date of Birth	12/25/1984
Email	zaheer202@hotmail.com
Address	Lahore, Pakistan
Academic Background	M.Sc. Chemical Engineering from UET, Lahore
	B.Sc. Chemical Engineering from UET, Lahore

JOURNAL PUBLICATIONS

1. Zaheer M.,Ramzan N.,Naveed S.,Feroz N,"Nickel(II) removal by biosorption using Ficus Religiosa (peepal) leaves" ,J.chil.chem.soc.,54, N05(2010).
2. Zaheer Aslam, Reyad A. Shawabkeh, Ibnelwaleed A. Hussein, Nadhir Al-Baghli, Mladen Eic, "Synthesis of activated carbon from oil fly ash for removal of H_2S from gas stream" Applied Surface Science, Volume 327, 1 February 2015, Pages 107–115
3. Zaheer Aslam, Reyad A. Shawabkeh, Ibnelwaleed A. Hussien, "Thermochemical Treatment of Fly Ash for Synthesis of Mesoporous Activated Carbon" submitted to "Journal of thermal analysis and Calorimetry
4. Zaheer Aslam, M. Anwar Parvez, Ibnelwaleed A. Hussein, Reyad A. Shawabkeh, Adsorption of H2S onto activated oil fly ash: Kinetics and Modeling (Ready to submit)
5. Zaheer Aslam, Reyad Shaeabkeh, "Removal of Methylene blue and Methylene orange from a binary solution by fly ash based activated carbon" (under process)

CONFERENCE PAPERS

1. Reyad Shawabkeh, Hafiz Muhammad Zaheer Aslam, Ibnelwaleed Hussein and Nadhir Al-Baghli, Sorption of Hydrogen Sulfide from Natural Gas using Physicochemical Treated Fly Ash, 2013AIChE Annual Meeting, Nov 3-8, Hilton San-Francisco Union Square, San Francisco, CA.

2. Reyad Shawabkeh, Hafiz Muhammad Zaheer Aslam, Ibnelwaleed Hussein and Nadhir Al-Baghli, Adsorption of CO_2 and H_2S from Natural Gas by Activated Fly Ash, AIChE 2014 Spring Meeting & 10th Global Congress on Process Safety.

3. Reyad Shawabkeh, Zaheer Aslam, Thermochemical Treatment of Fly Ash for Synthesis of Mesoporous Activated Carbon, 42nd Annual Conference of NATAS, September 15-17, Santa Fe, New Mexico.

4. Zaheer Aslam, Reyad A. Shawabkeh, Ibnelwaleed A. Hussien, Adsorption of H_2S from Natural Gas using treated Oil Fly Ash, Proceedings of the 4th International Gas Processing Symposium, October 26–27, 2014, Doha, Qatar.